UNIVERSIDADE D
COIMBRA

Mafalda de Carvalho Nogueira Amaro

# Modeling and Control of pH in Tubular Photobioreactors on Microalgae Plant

**Dissertation under the Master of Science Degree in Electrical and Computer Engineering supervised by Professor Doctor Jérôme Amaro Pires Mendes, and Professor Doctor Rui Alexandre de Matos Araújo, and presented to the Department of Electrical and Computer Engineering, Faculty of Science and Technology, University of Coimbra.**

February 2024

University of Coimbra
Faculty of Sciences and Technology
Department of Electrical and Computer Engineering

# Modeling and Control of pH in Tubular Photobioreactors on Microalgae Plant

Mafalda de Carvalho Nogueira Amaro

Dissertation under the Master of Science Degree in Electrical and Computer Engineering supervised by Professor Doctor Jérôme Amaro Pires Mendes, and Professor Doctor Rui Alexandre de Matos Araújo, and presented to the Departement of Eletrical and Computer Engineering, Faculty of Science and Technology, University of Coimbra.

February 2024

# Acknowledgment

I would like to thank the following people, without whom I would not have been able to complete this work, and without whom I would not have made it through my master's degree.

To the project "InGestAlgae - Plataforma Inteligente de Gestão da Produção de Microalgas", with reference CENTRO-01-0247-FEDER-046983, co-financed by Fundo Europeu de Desenvolvimento Regional (FEDER), through the Programa Operacional da Região Centro (CENTRO 2020), which my project was a part of. To the Institute of Systems and Robotics (ISR-UC), Oncontrol Technologies, and Buggypower.

To Professor Doutor Jérôme Amaro Pires Mendes and to Professor Doutor Rui Alexandre de Matos Araújo, my dissertation supervisor and co-supervisor, for all the provided guidance, support, and patience throughout this work.

To my friends, I want to express my gratitude for always being there for me and for the good times we've shared. Their support and motivation made this last stage possible.

For last, I will write my last acknowledgment in Portuguese: *Aos meus avós e à minha tia, agradeço todo o apoio e as palavras reconfortantes. Aos meus pais e irmãs, quero expressar o meu agradecimento por todo o suporte, motivação, palavras de encorajamento e muita paciência. Obrigado por tudo, sem vocês esta jornada não teria sido possível.*

# Abstract

Microalgae are microscopic organisms, they are unicellular and typically habit marine systems or freshwater. Differently from other plants, microalgae don't possess roots, stems or leaves. Nevertheless, they have the ability to perform photosynthesis. Photosynthesis is a biological process that converts light energy into chemical energy, where oxygen is produced as a byproduct. Additionally, these organisms' biodiversity is very extensive, being only a small part studied. These organisms have been used for centuries by humans as a food source. Nonetheless, through the years they have been associated with other activities, such as, cosmetics, pharmaceuticals and biofuels. Furthermore, in order to produce higher quantities of microalgae, these organisms are typically produced in appropriate infrastructures, named photobioreactors.

Photobioreactors encompass multiple structures, classified according to their production characteristics. Microalgae essentially require three major components in their production process including sunlight, water, and nutrients. Additionally, culture conditions in a photobioreactor, on a microalgae plant production, are essential for production rates, and the pH value is one of the critical variables for an harmonizing process. However, the biological nature of microalgae growth represents a complex reaction that is difficult to model and control.

The work presented in this dissertation proposes an approach for the application of adaptive identification and predictive control to regulate the pH in a photobioreactor in a microalgae production system. The proposed approach is composed of two main stages: identification and control. The identification is performed by a Takagi-Sugeno (T-S) fuzzy model, which will be learned with an offline strategy, by the fuzzy c-means method for the antecedent part, and by the Least Squares Method for the consequent part. Then, the model is updated with an online method, the Recursive Least Squares with Adaptive Directional Forgetting factor algorithm. The control scheme is based on a Generalized Predictive Control approach, which is a Model Predictive Controller, with the adaptive T-S fuzzy model designed in the identification stage. In this way, the model parameters from Generalized Predictive Control are online adapted by Recursive Least Squares with Adaptive Directional Forgetting. To validate the control structure, the proposed approach was tested by using a model estimated from real data of a microalgae production process.

**Keywords:** Microalgae, Photobioreactor, Generalized Predictive Control, Fuzzy Model.

# Resumo

As microalgas são organismos microscópicos unicelulares, que tipicamente habitam sistemas marinhos ou águas doces. Estes seres, ao contrário das plantas comuns, têm a particularidade de não possuírem raízes, caules ou folhas. No entanto, são seres fotossintéticos. A fotossíntese é um processo biológico, que permite a conversão de energia solar em energia química, do qual resulta a produção de oxigénio. Como tal, este processo é essencial para a vida na Terra. É estimado que as algas contribuam para grande parte da produção do oxigénio terrestre, e que existe um extensivo número de espécies, grande parte ainda por identificar e estudar. Estes organismos têm sido usados pelos seres humanos como fonte de alimento ao longo dos últimos séculos. Contudo, nos últimos anos têm sido associados a outras atividades, como a cosmética, a industria farmacêutica e aos biocombustíveis. Consequentemente, de forma a produzir maiores quantidades destes micro-organismos, estes são normalmente produzidos em infraestruturas adequadas, denominadas de fotobiorreatores.

O termo fotobiorreator abrange múltiplas estruturas, classificadas de acordo com as suas características de produção. Quanto ao processo de produção de microalgas, são considerados três requisitos essenciais, nomeadamente, luz solar, água e nutrientes. Além disso, as condições da cultura dentro dos fotobiorreatores, na produção de microalgas, são essenciais para as taxas de produção, sendo o valor do pH uma das variáveis críticas para um processo harmonioso. No entanto, as reações biológicas associadas ao crescimento das microalgas, representam uma reação complexa, difícil de modelar e controlar.

Como tal, este trabalho propõe uma abordagem baseada na aplicação de identificação adaptativa e em controlo preditivo, para regular o pH num fotobiorreator, para um sistema de produção de microalgas. A abordagem proposta é composta por duas etapas principais: identificação e controlo. A identificação é realizada por um modelo difuso, Takagi-Sugeno, que será aprendido através de uma estratégia "offline". Primeiramente é usado o algoritmo "fuzzy c-means", para a parte antecedente do modelo, e implementando o "Least Squares Method", para obter a parte consequente do modelo. Em seguida, o modelo é atualizado com um método "online", com recurso ao algoritmo "Recursive Least Squares with Adaptive Directional Forgetting". Por sua vez, a estrutura do controlador é baseada numa abordagem de Controlo Preditivo, com o modelo difuso adaptativo T-S, projetado na etapa de identificação. Desta forma, os parâmetros do modelo de Controlo Preditivo são adaptados de forma iterativa pelo método "Recursive Least Squares with Adaptive Directional Forgetting". Para validar a estrutura do controlador, a abordagem proposta foi testada utilizando um modelo estimado a partir de dados reais de um processo de produção de microalgas.

**Palavras-chave:** Microalgas, Fotobiorreator, Controlo Preditivo, Modelo Difuso.

# Contents

# Acronyms

**ADF** Adaptive Directional Forgetting.

**AFGPC** Adaptive Fuzzy Generalized Predictive Control.

**ARX** Autoregression with Exogenous Input.

**DO** Dissolved Oxygen.

**FCM** Fuzzy c-Means.

**FIS** Fuzzy Inference System.

**FL** Fuzzy Logic.

**FLC** Fuzzy Logic Control.

**FLS** Fuzzy Logic Systems.

**GPC** Generalized Predictive Control.

**LSM** Least Squares Method.

**MPC** Model Predictive Control.

**MSE** Mean Squared Error.

**PBR** Photobioreactor.

**PI** Proportional Integral.

**PID** Proportional-Integral-Derivative.

**RLS** Recursive Least Squares.

**RLS-ADF** Recursive Least Squares with Adaptive Directional Forgetting.

**T-S** Takagi-Sugeno.

# List of Figures

# List of Tables

# Chapter 1

# Introduction

## Contents



## 1.1 Motivation

For a few years now, there has been a new chapter in industrial processes, Industry 4.0 [1]. This movement intends to revolutionize the industrial process, both improving its flexibility and agility, integrating new technologies. However, these systems can be highly complex and their development may represent a challenge [2, 3].

Microalgae are microscopic eukaryotic[1] organisms, and they are phytoplankton that can be found in seawater and freshwater. These microorganisms have a high biotechnological potential to produce a diversity of substances present in many valuable industries, such as pharmaceutical, animal nutrition and human supplements, cosmetics production, wastewater treatment processes, and, as a new approach, in clean energy sources, called "third generation biofuels" [4, 5, 6]. Back in 1972, a technical book was published that inferred Earth's physical limits and its influence in policies in the first half of the 21st century [7]. These conclusions have been lost or pushed to future actions. Nevertheless, as Earth's finite resources become more evident and studied [8], more strategies emerge to counterbalance a climate crisis. Facing an increasing energy demand, along with fossil fuel environmental effects, some challenges have emerged, such as the ones related to economic, social and environmental factors. Three important strategies to respond to these challenges are the adoption of renewable energies, carbon capturing techniques, and increase energy efficiency, all aiming to reduce the greenhouse effect [9]. Among different carbon capturing techniques, direct $CO_2$ capturing, using third generation biomass - microalgae, is one of the options. These microorganisms perform the photosynthesis process to grow, requiring sunlight and carbon dioxide, and producing oxygen, at higher rates than other plants. Therefore, producing microalgae has the potential to reduce global warming and also to

[1] Eukaryotes are organisms whose cells contain a nucleus and other membrane-bound organelles. They may be either single-celled or multicellular

be a source of bioenergy or other economically valuable products. An example of a recent industry application for microalgae is an air filter named "Biosmotrap", which is intended to reduce outdoor and indoor air pollution [10]. However, for a biofuel application to be viable as a clean and renewable energy source, the cost and production levels must, respectively, decrease and increase. As a consequence, in the past few years, there has been a new interest in the microalgae industry due to its recent applications. This renewed interest triggered investment in the existing high-value microalgae production structures to transform the microalgae cultivation process into a more productive one, by minimizing costs and maximizing microalgae harvesting.

Microalgae plants have the capacity to grow in several aquatic environments with low requirements, allowing a great range of infrastructures for these micro-organisms production. Hence, these organisms can be produced in very simple infrastructures with very little control. However, the production purpose determines the type of infrastructure, and the necessary control. In a functional bioreactor, for photosynthetic microorganism's production, there are some core requirements for a quality end product. The most important factor, for an operating photobioreactor, is light availability, since light is the motor of the photosynthetic growth. The most common light source is sun radiation, however, there are already modern alternatives with a combination, or full use, of an artificial light source, provided that the radiated light is between 400 to 700 nm range (Photosynthetically Active Radiation), since microorganisms only use that light interval. Examples of artificial light sources used are lamps and LEDs to optimize culture growth. Moreover, the nutrients supply is also one of the main components in a photobioreactor and indispensable for microalgae development. For productivity maximization, the medium culture nutrients should be approximately, carbon (30%-50% dry weight (d.wt.)), oxygen (30%-50% d.wt.), hydrogen (3%-7% d.wt.), nitrogen (4%-9% d.wt.), phosphorus (1%-3% d.wt.) and other elements in small percentages [11]. The introduction method of the nutrients is also relevant, since only the liquid phase components are actually available for cell utilization. Another important component for microalgae production are the culture conditions, that encompass the culture pH and temperature. The culture pH can have an optimal range value of 7.0 to 10.0, being required an adaptation to the specific microalgae species in production. The control of this variable is frequently done by managing pure carbon dioxide gas injections in the culture, and is one of the most critical variables to control, since this gas injection can constitute up to 30% of production costs [12]. As for the temperature, the range of optimal degrees can vary from 20°C up to 35°C, also depending on the cultivated species. This variable is highly dependent on the absorbed radiation, and must be specifically adjusted to the production location. Some methods to help maintain the culture temperature at an equilibrium already exist, such as using water masses as a thermostat. The last significant factor of a photobioreactor is the mixing mechanism, used to minimize the gradient of nutrients in the culture, avoid cell sedimentation and allow the cells to circulate between dark and light zones. Some common mixing techniques are air bubbling, usually in closed photobioreactors, stirring and liquid circulation by pumps. Furthermore, when considering control approaches, it is essential to consider the type of industry application. Where a more demanding end product implies a more demanding production process. This means that the type of implemented control method must meet the desired compliance regarding culture conditions. Moreover, most control applications to this industry's high value facilities started with a Proportional Integral (PI) controller or a Proportional-Integral-Derivative (PID) controller incorporation into the system. However, some facilities have integrated classic Model Predictive Control (MPC)

or Fuzzy Logic (FL) controllers. Nevertheless, none of the studied approaches considered condition variations associated with the different seasons. So, applying adaptive control to these systems may be beneficial.

Considering all the above factors, it is clear that producing microalgae in a photobioreactor can be a complex process, even more so when considering high-value microalgae production processes. Additionally, in order for this industry to economically compete in the biofuels market, it must improve production efficiency. Implementing an adequate control method is crucial to improve the microalgae production process, in order to obtain a refined operation, by achieving cheaper photobioreactor performances and a higher yield percentage.

## 1.2 Dissertation Objective

This work aims at developing a pH control process for a photobioreactor environment, producing microalgae plants, with the aim of transforming these systems into more productive facilities. The microalgae plant infrastructures have highly complex nonlinear and time-varying dynamics and require "ideal" characteristics to achieve maximum growth. When greatly diverging from those conditions, the growth rate decreases or these microorganisms don't survive. Nevertheless, to maintain these conditions close to optimal values, an adequate type of control is required. Furthermore, as already mentioned, microalgae have the potential to become a competitor for fossil fuels, as the third generation biofuel, however, this target is still far from viable, due to their expensive production process [12]. So, it is crucial to increase yield quantities and decrease production costs. In [12] multiple changes necessary in this industry to achieve these purposes are presented, ranging from equipment to labor cost reductions. This document focuses on improving microalgae growth rate by controlling the culture pH, and a consequent improved carbon dioxide injection management, that may reduce operational costs. For this purpose, it is proposed to develop a predictive controller with an online adaptive model procedure. This method, due to its adaptive characteristics, permits an iterative update of both the controller and the model. The adaptive controller was contemplated due to the process to control irregular behavior throughout distinct seasons and multiple operational points, caused by the effect of process disturbances.

## 1.3 Dissertation Contributions

This dissertation's contributions and developments encompass the following points:

- Acquisition of real raw dataset on a microalgae plant, including dataset filtration, organization and division.

- Development of a discrete-time Autoregression with Exogenous Input (ARX) model for control simulation purposes.

- Development from scratch of the design of a Takagi-Sugeno fuzzy model and the respective identification process. The identification was performed in an offline way, using the Fuzzy c-Means clustering algorithm to design the antecedent part, and the Least Squares Method to design the consequent part.

- A new alternative to control a photobioreactor pH levels, was developed from scratch. Due to the uncertainty of the process and time-varying behavior through the seasons, the designed offline model is updated using Recursive Least Squares with Adaptive Directional Forgetting (RLS-ADF) factor algorithm and it is used as the predictive model on the model predictive controller, a Generalized Predictive Control (GPC). In this way, the GPC parameters, which depend on the model, are updated online.

- Validations of the proposed approach by using a model estimated from real data of a microalgae production process.

- Throughout the development of this work, an article was published in the second edition of IEEE Industrial Electronics Society Annual Online Conference (IES ONCON 2023). See Appendix A.

## 1.4 Dissertation Organization

The remainder of this document is organized as follows.

In Chapter 2, the state of the art is presented. First, is put forward an overview of the microalgae production structures, the photobioreactors, for a better notion and understanding of the following sections. From different types of infrastructures, their important characteristics and their most suited applications. Afterwards, some examples of distinct approaches on photobioreactors control are described, encompassing Proportional-Integral-Derivative Control, Model Predictive Control and Fuzzy Logic Control. In Chapter 3, some base concepts of Model Predictive Control and Fuzzy Logic Control are presented, that are important notions within the framework developed in this dissertation. In Chapter 4, the fuzzy system identification process and the controller's adjustments to process the model's parameters update are described. The fuzzy system identification process description is presented in the second section of the chapter. This section firstly presents the fuzzy model concepts and main equations, and its first subsection details the implementation of the Fuzzy c-Means clustering algorithm. The following subsection delineates the Least Squares Method, and the third subsection presents the Recursive Least Squares with Adaptive Directional Forgetting. With the last three methods implemented for the model parameters identification. The controller adjustment process is presented in the third section. In Chapter 5, the dataset organization is presented, followed by a description of the fuzzy model and predictive control implementation. Moreover, this chapter presents the simulation control results performed to test the selected approach. Lastly, in Chapter 6 the conclusions and future assignments of the developed work are presented.

# Chapter 2

# Overview on Photobioreactors and their Control

## Contents



## 2.1 Introduction

Algaes have been used for centuries by humans, as a food source, particularly important during food shortage periods [4]. An example of a known algae species, used for food in the last thousands of years, and popular in the modern times, is *Arthrospira (Spirulina)* species. However, the microalgae cultivation process is relatively new [13], dated back to 1890. Nevertheless, the cultivation of microalgae for commercial purposes only started in the early sixties, in Japan [14], for the *Chlorella* algae species. This process was motivated by the world's population increase, and the consequent predictions on insufficient food supplies. By 1980, there were 46 factories for microalgae production, producing about 1000 kg of dry matter per month in Asia, that were promptly followed by Israel and USA factories [4]. In 2004, the microalgae biomass market produced around 5000 t of dry matter per year [15]. Therefore, in a small interval of a few years, the microalgae production industry development occurred at an increasing rate, and diversified into other industry applications, such as pharmaceuticals and cosmetics industries [4]. Another consequence of the world's population increase, is the increasing energy demand, that has a direct influence on the rise of fossil fuel use; Which causes an increase in greenhouse gas emissions into the atmosphere. So, it is fundamental to adopt renewable energy technologies, carbon dioxide capture technologies, and increase energy efficiency equipment. As a photosynthetic process, microalgae production has a beneficial impact on carbon dioxide mitigation, and

has higher rates of photosynthesis than other plants. As a result, microalgae production positively affects $CO_2$ atmospheric levels, potentially reducing global warming, and represents a source of bioenergy, as a biofuel. Microalgae production requires specialized infrastructures, the photobioreactors, that should be adequately designed, built, and operated to achieve the selected microalgae necessities. Some important conditions to consider in this process are the light source and nutrients (carbon, nitrogen, phosphorous, etc) supply, the culture conditions (pH, temperature, etc), and mixing mechanisms, to avoid culture medium gradients, that would reduce production [16]. On a small scale, for example, in a laboratory setup, these conditions are not so difficult to implement, however, when considering large-scale production, these requirements can be difficult to implement, especially considering cost limitations. This chapter presents an introduction of important notions on photobioreactors and their operation. Afterwards, an overview of some control approaches on how to control and improve microalgae production is also presented. All studied approaches encompass the process pH control.

## 2.2 Photobioreactors Description

There are two major categories of photobioreactors structures to be considered in the microalgae production industry [11]: open and closed. The first occurrence and most elementary type of structures are the open photobioreactors, due to their operation simplicity. As the name suggests, these systems are open, meaning that the culture has a direct contact with the environment. These systems are considerably cheaper and more practical than closed systems [17], being associated with certain operation advantages, such as direct sunlight exposure, simple cleaning procedure, self-cooling by evaporation, and lower oxygen accumulation, consequence of the direct exposure to the atmosphere. However, a direct contact with the atmosphere results in a major dependence on natural climate variations, to its contaminating agents, and to high carbon dioxide losses. And, although this system's construction cost is lower than that of closed systems, due to their limitations in controlling the culture conditions and contamination, they are only suited to the most robust species. The most frequent types of these systems are artificial ponds, raceways, illustrated in Figure 2.1, tanks, and thin-layer (inclined surface systems), illustrated in Figure 2.2a. Conversely, closed system photobioreactors are characterized by the absence of contact between the culture and the environment, being the most frequently implemented infrastructures the tubular loop, illustrated in Figures 2.4 and 2.3, and the flat-panels, illustrated in Figure 2.2b. In this type of systems, it is possible to produce mono-cultures of a selected microalgae. It is also possible to grow more sensitive strains, due to their controlled environment and higher contamination protection. In these structures, the culture control is more efficient and allows better production results. For example, pH control implementation enables production maximization and cost reductions.

When considering microalgae production photobioreactors there are a set of indispensable requirements. The first to consider is light availability, since microalgae plants are photosynthetic organisms, and light source works as a power input. Nevertheless, excess light exposure can cause problems in microalgae's growth [22]. So, the microalgae growth is determined by the photosynthesis rate, which depends on the amount of irradiance exposure in the culture. Irradiance is the quantity of radiation reaching a certain point from all directions. Nonetheless, because of culture depth and biomass concentration, the

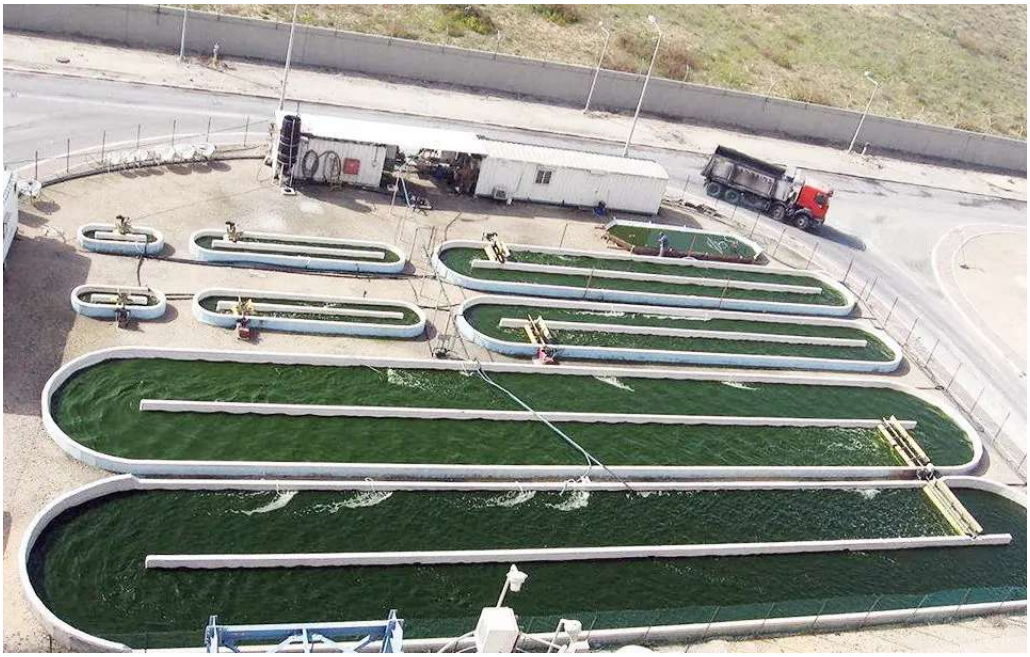

Figure 2.1: Open raceway culture pond, from [18].

irradiance in the microalgae culture is not homogeneous. Another important factor to consider in microalgae production is the nutrient supply. Nutrients mostly encompass carbon, oxygen, hydrogen, nitrogen, phosphorus, potassium, magnesium and calcium [11]. Generally, providing an excess of nutrients allows maximizing productivity, however, this can represent an economic disadvantage, if a re-circulation of culture medium is not implemented. Moreover, it has to be considered that only the dissolved nutrients can be used in the microalgae growth process. Assuming a gas carbon dioxide supply, only the part transferred to the liquid phase is really accessible for the cells. To sustain microalgae activities, a carbon dioxide shortage supply must be avoided, as the oxygen amount should not rise above saturation levels. Additional requirements for photobioreactors operation are the culture conditions, that encompass the pH and the temperature of the culture. These conditions affect the process rate production, and optimal values enable maximum production rate [23]. The culture pH suffers variations due to the photosynthesis reaction, which results in carbon consumption and increasing pH levels. To control these variations, it is usually injected $CO_2$, which simultaneously supplies carbon dioxide for the photosynthesis process, and decreases the culture pH. A last requirement to consider is the mixing mechanism, that allows the minimization of medium gradients, cell sedimentation and cells circulation between dark and light zones. However, too much mixing actions can damage microalgae growth. Some examples of usually used methods are air bubbling, stirring or liquid circulation.

The first photobioreactor design to appear was an open system type, the raceway ponds, illustrated in Figure 2.1, and has been pointed as the most frequently implemented photobioreactor model in the industry, going up to 95% of worldwide implementation by 2017 [11]. This model is characterized by its low cultivation costs in commercial production of microalgae, and by its flexibility in scaling up, which explains this model's vast utilization. Nevertheless, this system also has some drawbacks, related to the low light utilization efficiency, majorly due to the tank depth, and an insufficient mixing, which leads to a poor gas/liquid transformation. Resulting from its advantages and limitations,

(a) (b)

Figure 2.2: (a) Open photobioreactor - thin layer system, from [19], and (b) close photobioreactor - flat-plate system, from [20].

Figure 2.3: Tubular photobioreactor, for microalgae cultivation. From Buggy Power.

these types of systems are associated with less demanding and more flexible industries, like wastewater treatments or human consumption production processes.

The thin-layer or inclined platforms systems, illustrated in Figure 2.2a, are an open type of system, characterized by the low-depth cultures, in order to maximize light utilization, which leads to an increase in biomass concentration. Consequently, this system has the highest growth rates and microalgae productivity and, therefore, has been attracting some attention. This model is also known for its advantages, combining open system characteristics, direct sunlight exposure, easy heat dissipation, easy cleaning and maintenance, and some closed systems characteristics, such as high biomass concentration production and elevated productivity. Nevertheless, it continues to exhibit a lack of the system variables control and high contamination probability.

For more demanding cultures, with higher production standards, the most frequent design is the tubular photobioreactor, which is a type of closed system. A tubular system can have distinct designs, depending on the tube's organization. For example, in a "Serpentine photobioreactor", illustrated in Figure 2.4, a set of tubes is connected by a set of U-shaped bridges to form a flat loop, that can be arranged vertically or horizontally. In a "Manifold photobioreactor" the tubes are organized in parallel, connected at the ends by two manifolds, one for distribution and one for culture collection purposes. Moreover, these models are usually used to produce high-quality biomass for high-value applications.

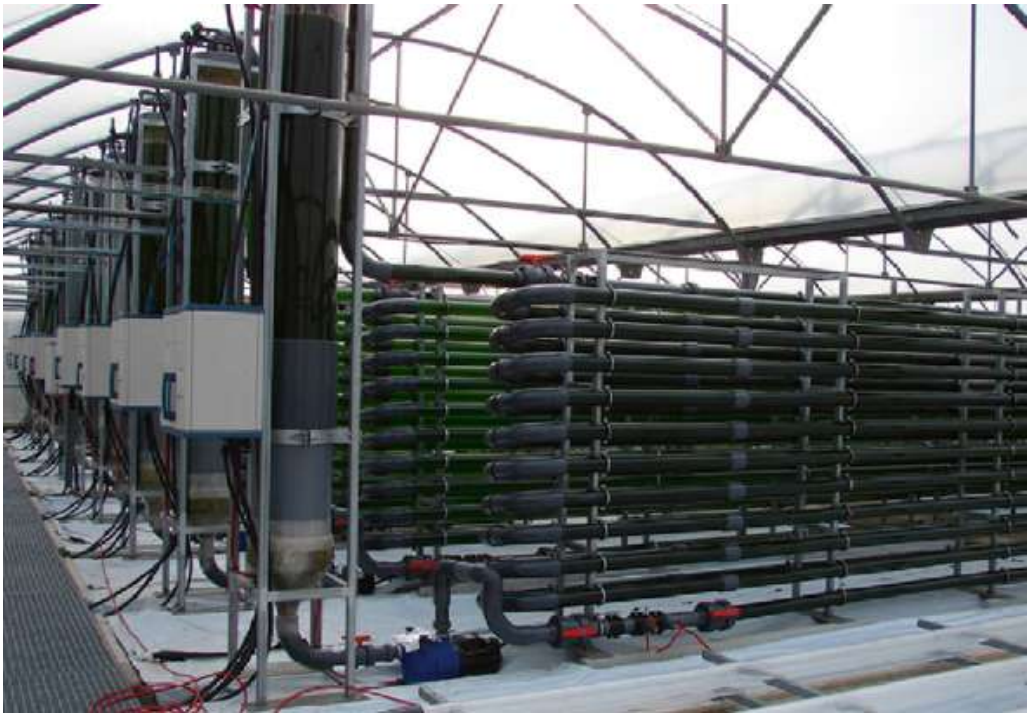

Figure 2.4: Vertical tubular serpentine photobioreactor, from [21].

However, their productivity depends on multiple factors, such as the algae species being produced, the production location, the tube's diameter, the biomass concentration, the distance between the tubes, etc. Being a closed type of photobioreactor, this model has the corresponding advantages, but its structures imply a significant drawback. The tubular structures have shown a fouling behavior of microalgae, that can only be stopped with a regular photobioreactor clean-up, that implies periodical pauses in the cultural production.

The flat-plate photobioreactor, illustrated in Figure 2.2b, is another type of a closed system, with a basic design, that consists of two parallel transparent panels with a thin layer of microalgae culture suspension flowing between them. One of this model's advantages is its efficiency of the culture sun exposure. However, as a consequence, the temperature fluctuations are difficult to control and the culture overheating is a regular problem. Nevertheless, there are already two mainly used solutions for this problem [11]. One of them is using a water spray method on the panel surface to promote heat dissipation, and the other option involves a double layered system, on which one of the spaces has the growing culture and the other a water sheet to produce heat dissipation from the overheated culture.

There has been some investment in this industry caused by the market demand. In the future, the main improvements are focused on three key details, motivated by cost minimization and production maximization [11]. The first aspect involves the development of new technologies for phototropic cultures production, in order to achieve better performances. The second aspect focuses on scaling-up the production facilities, and the third one involves the industrialization of the microalgae biomass production process. Ultimately, to choose the most fitted photobioreactor infrastructure design to implement, it is crucial to develop a study to find the most suited model that coincides with the project specifications and budget.

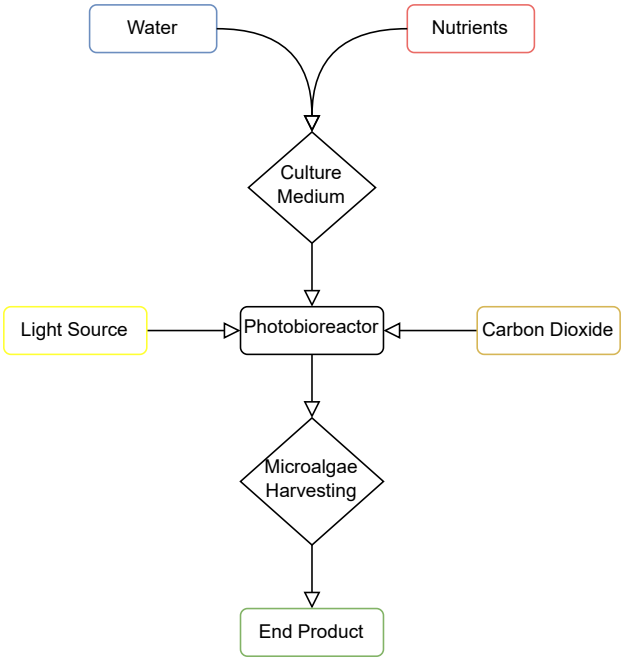


Figure 2.5: Photobioreactor Operation Scheme.

## 2.3 Tubular Photobioreactors Operation

The most frequent closed photobioreactor design, implemented at industrial scale, for phototrophic microorganism's production, is the tubular model [24], which is the photobioreactor type studied in this work. These structures are normally made of transparent glass or plastic hollow tubes, with 0.1 meters in diameter, where the culture circulates. The tubes can be arranged in a vertical or horizontal formation and are generally connected to a pump that circulates the culture medium and microalgae through the system. Normally, there are two segments in tubular reactors [11], the photostage loop, where the biomass growth occurs, and the retention tank, where the oxygen is removed and culture variables are controlled. Illustrated in Figure 2.5, there is a schematic of simplified steps for a photobioreactor continuous operation. Starting with the culture medium production, essentially constituted by water and nutrients. Depending on water origin, it may or may not be necessary to perform filtration/sterilization of the medium, to remove possible contamination particles. Then, the culture medium is continuously circulated through the tubes, while light is supplied from artificial sources or natural sunlight. As described in [12], to reduce production costs, it should be used seawater and natural sunlight. Throughout the operation, the main variables, such as temperature, pH, nutrient levels, and light intensity (when in a laboratory setup) are usually controlled and monitored, to optimize microalgae growth and productivity. These variables optimal values depend on the microalgae species cultivated, however, the usual range for temperature is 20-30°C, while the pH is between 7-10 [11]. The nutrient levels are adjusted according to the specific needs of the selected microalgae cycle, and the light intensity is adjusted to ensure that the microalgae receive enough light to carry out photosynthesis. The culture medium must be regularly reinforced with fresh nutrients to ensure that the culture

medium contains an adequate level of the essential nutrients. This is typically done by adding fresh culture medium to the system at regular intervals or in a continuous rate. The microalgae harvesting is typically done periodically, either by manual or automated methods. Overall, the operation of a tubular photobioreactor requires continuous and careful motorization and control of various parameters to ensure an optimal microalgae productivity. Furthermore, the system must be cleaned at regular intervals to prevent contamination and ensure a high quality operation.

## 2.4 Photobioreactors pH Control

When considering the culture pH control, the frequent approach is the manipulation of carbon dioxide gas injections into the culture medium. This is usual because the continuous biological reaction, occurring inside the photobioreactor, causes the medium acidity to decrease, by $CO_2$ consumption, which is explained through the photosynthesis process transformation, normally represented by Equation (2.1) [25]. Nevertheless, $CO_2$ injections into the culture medium can lead up to 67% losses in open photobioreactors and up to 50% losses in closed photobioreactors [11]. In open photobioreactors, most of $CO_2$ losses occur due to direct contact with the atmosphere, however, in closed photobioreactors, most $CO_2$ losses can occur due to the gas-liquid phase transformation or loss in the exhaust gas, when supplied in excess. When considering tubular photobioreactors, $CO_2$ losses can be reduced to less then 30% through proper control methods implementation [25]. Additionally, the work presented in [26] correlates the reduction of $CO_2$ injections, and consequent $CO_2$ injection time, to lower $CO_2$ losses.

$$6CO_2 + 6H_2O \xrightarrow{\text{light}} C_6H_{12}O_6 + 6O_2, \tag{2.1}$$

where $CO_2$ represents the carbon dioxide chemical compound, $H_2O$ represents a water molecule, $C_6H_{12}O_6$ represents the glucose chemical compound, and $O_2$ represents the oxygen molecule.

Microalgae production involves a biological process and, therefore, it is very complicated to describe in a mathematical formula. This results in a lack of developed control systems for this process. The existing ones are based on an on-off type of control, that leads to large $CO_2$ losses and constant pH variations from the set value. Although this technique allowed some improvements, it has been proven that, in order to achieve higher performances, a more complex control alternative must be implemented, such as a Model Predictive Control (MPC) or Fuzzy Control [27, 25]. The pH control is a nonlinear problem, viewed from a theoretical approach, that can only become linear under specific conditions [28].

To maximize the culture yield, it is essential to maintain some conditions at optimal values, such as temperature levels, oxygen values, the medium pH levels, etc. Being the medium pH one of the most critical variables to control, that is also the main focus of this work. Phototrophic reactions transform carbon dioxide molecules and water molecules into oxygen molecules and sugar molecules. This reaction causes a decrease in the organic carbon in the culture medium, leading to an increasing culture pH value. Therefore, the $CO_2$ regular injections into the culture medium serve two purposes: balance the acidity levels and provide the necessary carbon dioxide molecules to the photosynthetic process. This process has to be carefully controlled, since an excess of carbon dioxide in the culture may reduce the pH value into damaging values whereas a scarcity of $CO_2$ limits the

microalgae's growth, reducing its production levels. Furthermore, carbon dioxide injection can also represent an increasing production cost factor[12].

Through the last couple of years, multiple pH control approaches have been studied for photobioreactors. In the following sections, some of those approaches are summarized. Nevertheless, it is important to keep in mind that every approach has to be carefully studied and multiple factors have to be considered, such as, the cultivated species, the photobioreactor model and technology, culture end product application, the local weather and its usual variations, mixing method implemented, etc.

### 2.4.1 Proportional-Integral-Derivative Control

Proportional-Integral-Derivative (PID) control is potentially the most widely used control strategy, and is often applied with the derivative gain equal to zero turning it into a Proportional Integral (PI) control [29, 30]. In a simple way, PID control continuously calculates an error value, and uses it to apply a correction in further applications, resulting in a relatively simple and efficient control method. This control method is divided into three segments [31], the proportional term, that provides a correction value related to the all-pass gain factor. The integral term, that offers a low-frequency compensation, by decreasing the steady state errors, and the derivative term, that refines the transient response, using high frequency term. This control method has some positive characteristics that contribute to its popularity. For example, their constituent members are intuitive and easily implemented, since they do not require a deep mathematical knowledge. Furthermore, PID control has already been used for a couple of years, therefore, has a great extent of documentation, example implementations, and detain a good versatility and adaptation.

In a photobioreactor control context, the PID approach is also viable and studied. From the studied approaches, there were two similar methods, based on PID. One with a complete PID [32] and one only with a PI control [26]. In [32], it is studied a conventional linear feedback PID and a PID with a feed-forward compensation, for the photobioreactor culture pH levels and Dissolved Oxygen (DO) control. The subject of this article is a pilot scale photobioreactor, designed for laboratory experiments on a torus model photobioreactor, with a high culture conditions control. Being one of its most interesting characteristics, its potential for gas-liquid mass transfer efficiency. The objective optimal value for the cultivated species pH is 7.5, which can be manipulated using a combination of two approaches: using pure $CO_2$ injections and nitrogen injections. However, for the DO variable, nitrogen injections are also used, to maintain its concentration below inhibition levels (25 mg/L). These two inputs, carbon dioxide and nitrogen, form a multi-variable system with a strong interaction between them. In order to describe the pH progression, the model used in this approach encompasses all the chemical reagent molecules of the solute systems $NH_3$ - $CO_2$ - $H_2O$ and results in a high-order differential-algebraic system of equations. The global description of the microalgae growth was obtained by combining a radiative model, a biological model and a thermodynamic model. The global photoautotroph organisms growth is finally represented by a state space with seventeen variables. Being the pH influence described by Equation (2.2) and the DO by Equation (2.3), where $pH_{min}$ and $pH_{max}$ are the top and low reference values for the photosynthesis operation, and $c_{O_2}$ is the dissolved oxygen.

$$f_{pH} = \frac{pH - pH_{min}}{pH_{max} - pH}\left(1 - \frac{pH - pH_{min}}{pH_{max} - pH}\right) \tag{2.2}$$

$$f_{DO} = \frac{1}{1 + 10^{-23}{c_{O_2}}^{14}} \tag{2.3}$$

In this control approach, the pH variable has a PID control, since the system behaves as a second order system, and the DO has a PI control, due to its first-order system behavior. Finally, the study concludes that the individual use of PID control may not be a successful approach, and proposes an alternative to improve the control results with feed-forward compensation. Moreover, the simulation and real experiments presented promising results for the proposed approach. Nevertheless, in a reference for future work, the work indicates an inclination for a model predictive control approach implementation, in order to further reduce $CO_2$ losses.

In [26], the pH is the only regulated variable, with a $CO_2$ losses minimization goal, in a tubular photobioreactor. This work compares the results of a controller with on-off valves to those of a PI control system with a feed-forward term to compensate for the radiance influence on the system. Considering the culture pH as the system output, the carbon dioxide valve aperture as the manipulated variable, and the solar radiation as the system main disturbance, it considers the photobioreactor pH levels represented by Equation (2.4). The pH reference considered in this work is set to 8.

$$pH = \frac{k_1}{1 + \tau s} \frac{k_2 \omega_n^2}{s^2 + 2\delta\omega_n s + \omega_n^2} e^{-t_r} CO_2 + \frac{k_r}{1 + \tau_r s} I, \tag{2.4}$$

where $pH$ is the culture medium pH, $CO_2$ is the valve aperture percentage, $I$ is the global radiation, $t_r$ is a time delay, $\omega_n$ and $\delta$ are two variables related with the system mass transfer capacity, $\tau$ are parameters dependent on the culture state and $k_1$, $k_2$ and $k_r$ are estimated variables.

Furthermore, the control strategy implemented in this article describes a PI control and a feed-forward compensator. This approach's ultimate goal is to reduce the number of times necessary to inject carbon dioxide into the photobioreactor and reduce its percentage of $CO_2$ losses. In contrast, an implemented simple on-off switching control strategy is presented, that is based on a selected set pH value. In particular, when the controlled variable (pH) is below or higher than the set value, the controlled output is turned Off or On, respectively. Moreover, this work presents simulation results and real results performed in a tubular photobioreactor. Between the On-Off controller, the PI controller and the PI+feed-forward controller, the experiments showed that the last two alternatives allowed a decrease in the $CO_2$ time injection, directly correlated with the decrease of $CO_2$ losses and, therefore, beneficial for cost reduction. Considering only the PI and PI+feed-forward controllers, the PI+feed-forward controller obtained better results, mostly resulting in less carbon dioxide injections.

### 2.4.2 Model Predictive Control

Model Predictive Control (MPC) encompasses some advanced control methods based on a cost function minimization, the satisfaction of a set of constraints, and the prediction of the future behavior of the controlled systems [33]. MPC has been widely applied in multiple fields with satisfying results. This control approach has become increasingly popular due to advances in the optimization algorithms, which have made it possible to solve large-scale optimization problems, required for many industrial applications. Furthermore, some positive points of this type of control are its flexibility to handle changing operations conditions, its ability to manage complex systems with multiple input and output variables,

its predictive strategy, and its performance improvement compared to traditional control methods. In a microalgae production photobioreactor control context, there are also some documented approaches with different MPC methodologies. Some of the studied documents will be discussed.

In 2004, it was published an article on a branch-and-bound on–off model-based predictive control implementation strategy, aiming to control the pH and minimizing $CO_2$ losses in a photobioreactor [34]. Being its overall objective to improve the production of high-value algal products. In this controller, the command signal variable represents the pure carbon dioxide injections, by manipulating the $CO_2$ valve aperture. The pH reference value was set to 7.7, and the used sampling time was of $20s$. In this method, the model used is similar to Equation (2.4), a linear approach model, relating the pH output to the $CO_2$ injection input and the solar radiance influence. Addressing the control scheme, the motivation that led to the selection of this controller, involves its good performance in a variety of processes, from a simple dynamic processes to complex processes. Validating the selected approach, this article describes positive results from the performed simulations and real-experiments. In these tests, the implemented control method is compared with a classical on-off controller, which presents a reduction of carbon dioxide losses up to 75%, during day time. During night time, these results are even higher, due to the culture's biological reactions. Additionally, the results also evidence a low pH variance, which creates a healthier environment for microalgae's growth.

Ten years later, in 2014, an interesting event-based model predictive control algorithm application to regulate the pH of a photobioreactor was published in [27]. The control process objective is to maintain a more stable pH culture value, in order to improve microalgae production, and to minimize the $CO_2$ losses. The selected control strategy is based on a Generalized Predictive Control (GPC) with an event detector, which serves as an enabler for the control signal, that represents the $CO_2$ valve aperture. As a result, with the event detector, it is possible to control the action execution frequency of the controller, allowing a frequency adaptation to the culture environment. For instance, if the pH readings are proximate to the established optimal value and inside an established interval, the event frequency is low. However, if the controlled variable diverges from the optimal value, and is outside the defined interval, the event frequency increases. The goal is to accelerate the convergence process between the culture pH value and the reference value. The reference value point was defined to $8 \pm \beta$, with $\beta = 0.075$. Moreover, the number of control actions directly determines the number of carbon dioxide injections performed, which reflects on the $CO_2$ losses. As a consequence, it is possible to identify two sampling times, the process output constant sampling time set to 1 min and the control action sampling time variable taken from (1,2,3,4,5). Furthermore, the model used in the controller is similar to Equation (2.4), where $k_2$ is fixed to one. To test the theory of the described event-based GPC, a number of tests were conducted in simulation and, afterwards, in the physical photobioreactor. The experimental results confirm this approach's potential when compared to classical on-off controllers. In particular, in this comparison, the control accuracy highly improves, and the carbon dioxide losses reduce more than two times. Additionally, it is also performed a comparison to the controller described in [34], with this new approach presenting better results.

### 2.4.3 Fuzzy Logic Control

Fuzzy Logic Control (FLC) is an intuitive controller using fuzzy logic, which consists of a knowledge-based system composed of a set of fuzzy control rules that can represent control actions based on knowledge obtained from human experts [35, 36]. In the real world, not every decision is of yes and no, and may be open to interpretation and require some flexibility and uncertainty. In [37], it is proposed to apply a fuzzy controller to simultaneously control the algal biomass concentration, the culture pH, and the average irradiance inside the photobioreactor (laboratory setup). The described control strategy considers three requisites, in the microalgae growth process: 1) achieve the algal biomass set-point concentration (0.85-0.95 g/L), controlled through the dilution rate, 2) reach a pH value that enables maximum culture growth (6.5-7), controlled through $CO_2$ flow, and 3) control the average light flux provided to the photobioreactor (80-85 $\mu$mol photon/$m^2/s$). The type of fuzzy controller used in this application was a Mamdani FLC, since it is relatively affordable to implement, possible to personalize, imitates human thinking, and it is efficient. The proposed FLC system was validated in simulation and in experimental processes. In these two types of validations, the results were promising, proving the potential of a fuzzy logic controller implementation in a photobioreactor control. Furthermore, in the documented laboratory experiments only the biomass concentration control was performed with a fuzzy controller, being the pH and average irradiance controlled by conventional PI controllers. The PI controller replacement for fuzzy controller is one of the indicated future work points mentioned in [37].

## 2.5 Conclusion

In conclusion, the control of microalgae production systems is still an active investigation area, with a great potential to evolve. However, in order for these systems to become competitive in the biofuel market, as much as to improve in other industries, the photobioreactors operational costs must decrease. With this purpose, there are a few central actions to consider, which are analyzed with detail in [12]. For example, it is important to increase culture yield by controlling the system conditions, namely the pH levels. Nevertheless, this variable can be complex to control, considering the biological reactions that influence its behavior. For this reason, from the presented scenarios of the studied documents (Subsections 2.4.1, 2.4.2 and 2.4.3), the application of a control method, such as PID control, MPC control or fuzzy control, can become very beneficial.

Considering all the examined approaches, the methodology selected to be studied in this dissertation involves a GPC algorithm combined with a fuzzy model. This fuzzy model allows an iterative parameters update, resulting in both model and controller adaptation throughout the photobioreactor operation. Additionally, as contemplated in the state of the art Section 2.4, none of the presented studied approaches applied an adaptive methodology. However, an adaptive approach can be considered an advantage taking into account the process to control distinct behavior through the seasons. Therefore, the selected approach permits an iterative adaptation to the irregular behavior caused by the ambient natural conditions, that may also be adapted to multiple facilities, even if situated in different locations.

# Chapter 3

# Concepts of Model Predictive Control and Fuzzy Control

## Contents



## 3.1 Model Predictive Control

Model Predictive Control (MPC) was firstly introduced in the late seventies, and its methodology has evolved since then. This term, MPC, doesn't designate a specific type of control, instead, it encompasses a span of control methods. These methods are characterized for using a model of the process to acquire the control signal, by minimizing an objective function. Consequently, the controller's success highly depends on the accuracy of the process model. Over the years, predictive control methods have proven to be quite successful, with some of their advantages including the variety of possible process applications, the compensation of dead times, and the feed-forward control introduced when compensating measurable disturbances, among others [38]. However, this type of controller is normally more complex than classical PID controllers. Nevertheless, they frequently achieve better results. As mentioned earlier, the beginning of the MPC methods was in the end of the 1970s, particularly with Richalet et al. (1978) [39] and Cutler and Ramaker (1980) [40]. In Richalet et al. (1978), a Model Predictive Heuristic Control technique, also known as Model Algorithmic Control, is presented. A couple of years later, in Cutler and Ramaker (1980), the Dynamic Matrix Control is introduced.

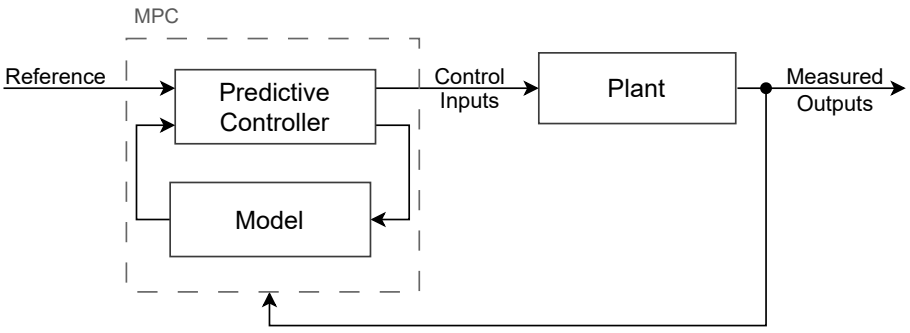


Figure 3.1: MPC control block diagram.

Both of these algorithms use a dynamic process of the model, with impulse and step response, respectively, to predict future process reactions to the computed control actions. The control actions are calculated by minimizing the predicted error at every iteration (sampling time). The following years were centered on these approaches, or similar implementations to the industry [41], due to its good control performance compared to classical methods. Later, the research focus shifted, and efforts were directed towards improving the robustness and stability of Model Predictive Control (MPC) [42, 43, 44, 45, 46]. During these years, Model Predictive Control (MPC) gained popularity in chemical processes, and a new perspective emerged with work on adaptive control [47, 48]. From this concept, the famous Generalized Predictive Control (GPC) was developed [38].

In Figure 3.1, a generic MPC control scheme is represented, composed of two main blocks: 1) the MPC block, which encompasses the predictive controller and the model of the plant to be controlled, and 2) the plant block, that is the system to be controlled. The MPC block considers the reference value and the measured output to obtain the control actions. The plant, utilizing the control action as input values, generates the measured outputs. Regarding the MPC control strategy, Figure 3.2 presents a diagram of the control strategy at instant $t$. In this figure, with $N_p$ as the prediction horizon, the following principles are observed:

- By minimizing an objective function, the future control signals (light blue) are obtained from instant $t$ to $t + N_p$, and the first computed control action is then applied.
- The reference trajectory (red line), describing the desired process behavior, is considered from instant $t$ until instant $t + N_p$.
- At every instant $t$, the future $N_p$ outputs (light green) are obtained, based on the process model predictions, using the system inputs and outputs until instant $t$ (dark green and dark blue) and calculated future control signals (light blue).

These principles are repeated at every instant to adapt the control action to the current situation and achieve the intended output. Prediction and optimization are the two main differences from classical approaches. Additionally, the prediction horizon, $N_p$, should be large enough to encompass the resulting variations in the controlled variable, a consequence of the calculated values of the manipulated variable.

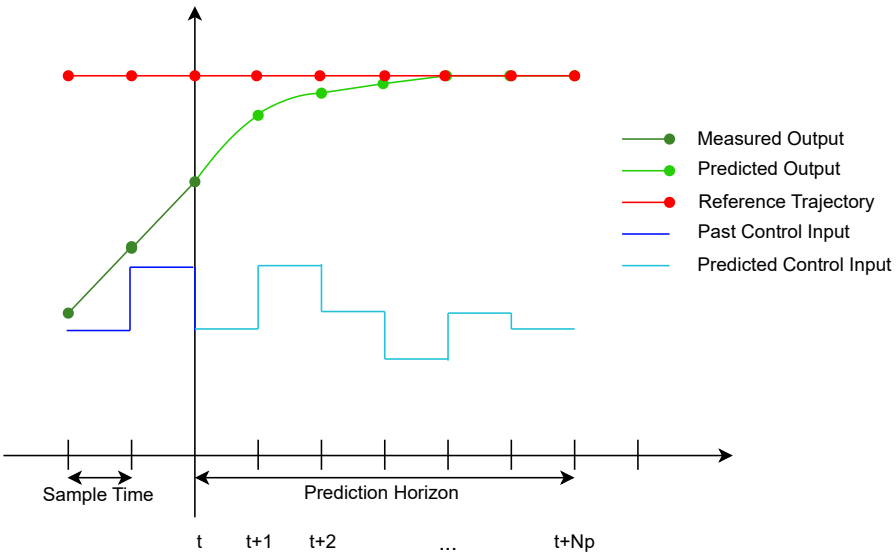


Figure 3.2: MPC strategy diagram.

### 3.1.1 Generalized Predictive Control

Generalized Predictive Control (GPC) was proposed by Clarke et al. (1987) [49] and has become the most popular predictive control algorithm, both in industry and academic fields [38]. This algorithm has been successfully implemented in multiple industries with various applications [50, 51, 52, 33], and has exhibited good performance and robustness. This method, being an MPC method, is also based on the calculation of future control signals, minimizing a cost function, defined over a prediction horizon. In addition, future optimizations depend on a quadratic function measuring the distance between the predicted output and the future reference sequence, plus a quadratic function measuring the control effort, over the prediction horizon. Distinctively, this method allows more variety in control objectives and comprises the notion of weighting control considerations in the cost function. Furthermore, this work considers a process affected by external disturbances, produced by measurable variables. The following Equation (3.1) describes the considered system to be controlled:

$$A(z^{-1})y(t) = B(z^{-1})u(t-1) + D(z^{-1})v(t), \tag{3.1}$$

where $u(t)$ is the plant control signal, $y(t)$ is the plant output signal, and $v(t)$ is the measured disturbance. $A(z^{-1})$, $B(z^{-1})$ and $D(z^{-1})$ are polynomials described by:

$$A(z^{-1}) = 1 + a_1 z^{-1} + a_2 z^{-2} + \cdots + a_{n_a} z^{-n_a},$$
$$B(z^{-1}) = b_0 + b_1 z^{-1} + b_2 z^{-2} + \cdots + b_{n_b} z^{-n_b},$$
$$D(z^{-1}) = d_0 + d_1 z^{-1} + d_2 z^{-2} + \cdots + d_{n_d} z^{-n_d},$$

where $n_a$, $n_b$ and $n_d$ are the orders of polynomials $A(z^{-1})$, $B(z^{-1})$ and $D(z^{-1})$, respectively. The GPC algorithm main component is based on a control sequence that is defined by the minimization of a cost function with the following structure:

$$J(N_1, N_2, N_u) = \sum_{j=N_1}^{N_2} \delta(j)[\hat{y}(t+j|t) - r(t+j)]^2 + \sum_{j=1}^{N_u} \lambda(j)[\Delta u(t+j-1)]^2, \tag{3.2}$$

where $\hat{y}(t+j|t)$, for $j \geq N_1$ and $j \leq N_2$, is an optimal $j$ step ahead prediction output up to time $t$, $N_1$ and $N_2$ are minimum and maximum prediction horizons, $N_u$ is the control horizon, $\Delta u(t+j-1)$ is variation of the future control command, $\delta(j)$ and $\lambda(j)$ are weighting sequences, and $r(t+j)$ represents the future reference values. In this work it is considered $\delta(j) = 1$ and $\lambda(j) = \lambda$. The purpose of this method is to compute a future control sequence, $u(t), u(t+1), \ldots, u(t+j-1)$, that influences the future plant output, $y(t+j)$, to be similar to the future reference trajectory, $r(t+j)$.

By applying the Diophantine Equations described in [38] it is possible to obtain the following Equations. Being the respective polynomials described in [38], and briefly described in the following equations. When considering the Diophantine Equation (3.3),

$$1 = E_j(z^{-1})\tilde{A}(z^{-1}) + z^{-j}F_j(z^{-1}), \tag{3.3}$$

where $\tilde{A}(z^{-1}) = \Delta A(z^{-1})$, the polynomials $E_j(z^{-1})$ and $F_j(z^{-1})$ can be obtained by dividing 1 by $\Delta\tilde{A}(z^{-1})$ until the remainder can be factorized as $z^{-j}F_j(z^{-1})$. Furthermore, in [38] it is described a method to obtain $E_j(z^{-1})$ and $F_j(z^{-1})$ using recursive Diophantine Equations. With $E_j(z^{-1})$ and $F_j(z^{-1})$ defined by:

$$E_j(z^{-1}) = e_{j,0} + e_{j,1}z^{-1} + \cdots + e_{j,j-1}z^{-(j-1)}, \tag{3.4}$$

$$F_j(z^{-1}) = f_{j,0} + f_{j,1}z^{-1} + \cdots + f_{j,n_a}z^{-n_a}, \tag{3.5}$$

and $E_{j+1}(z^{-1})$ and $F_{j+1}(z^{-1})$ are calculated recursively using the same procedure, respectively defined by:

$$E_{j+1}(z^{-1}) = E_j(z^{-1}) + e_{j+1,j}z^{-j}, \tag{3.6}$$

$$F_{j+1}(z^{-1}) = f_{j+1,0} + f_{j+1,1}z^{-j} + \cdots + f_{j+1,n_a}z^{-n_a}, \tag{3.7}$$

where $e_{j+1,j} = f_{j,0}$ and $f_{j+1,i} = f_{j,i+1} - f_{j,0}\,\tilde{a}_{i+1}$ with $i = 0, \ldots, n_a - 1$. Additionally, polynomial $G_{j+1}$ can be recursively obtained by:

$$G_{j+1} = E_{j+1}B = (E_j + f_{j,0}z^{-j})B = G_j + f_{j,0}z^{-j}B, \tag{3.8}$$

where its coefficients are given by $g_{j+1,j+i} = g_{j,j+i} + f_{j,0}b_i$ with $i = 0, \ldots, n_b$. And polynomial $H_j$ can similarly be obtained by:

$$H_j = E_jD. \tag{3.9}$$

Considering $j \geq N_1$ and $j \leq N_2$, the optimal output sequence $y(t+j)$ is computed to optimize the cost function, applying Equation (3.10).

$$\mathbf{y} = \mathbf{G}\mathbf{u} + \mathbf{H}\mathbf{v} + \mathbf{F}(z^{-1})y(t) + \mathbf{G}'(z^{-1}) + \mathbf{H}'(z^{-1}), \tag{3.10}$$

where

$$\mathbf{y} = \begin{bmatrix} \hat{y}(t+N_1|t) \\ \hat{y}(t+N_1+1|t) \\ \vdots \\ \hat{y}(t+N_2|t) \end{bmatrix}, \qquad \mathbf{u} = \begin{bmatrix} \Delta u(t) \\ \Delta u(t+1) \\ \vdots \\ \Delta u(t+N_u-1) \end{bmatrix},$$

$$\mathbf{G} = \begin{bmatrix} g_0 & 0 & \ldots & 0 \\ g_1 & g_0 & \ldots & 0 \\ \vdots & \vdots & \vdots & \vdots \\ g_{N_u-1} & g_{N_u-2} & \ldots & g_0 \end{bmatrix}, \qquad \mathbf{F}(z^{-1}) = \begin{bmatrix} F_{N_1}(z^{-1}) \\ F_{N_1+1}(z^{-1}) \\ \vdots \\ F_{N_2}(z^{-1}) \end{bmatrix},$$

$$\mathbf{H} = \begin{bmatrix} h_0 & 0 & \dots & 0 \\ h_1 & h_0 & \dots & 0 \\ \vdots & \vdots & \vdots & \vdots \\ h_{N_u-1} & h_{N_u-2} & \dots & h_0 \end{bmatrix}, \qquad \mathbf{v} = \begin{bmatrix} \Delta v(t+1) \\ \Delta v(t+2) \\ \vdots \\ \Delta v(t+N_u) \end{bmatrix},$$

$$\mathbf{G}'(z^{-1}) = \begin{bmatrix} (G_{N_1}(z^{-1}) - g_0)z\Delta u(t-1) \\ (G_{N_1+1}(z^{-1}) - g_0 - g_1 z^{-1})z^2\Delta u(t-1) \\ \vdots \\ (G_{N_2}(z^{-1}) - g_0 - g_1 z^{-1} - \dots - g_{N_u-1}z^{-(N_u-1)})z^{N_u}\Delta u(t-1) \end{bmatrix},$$

$$\mathbf{H}'(z^{-1}) = \begin{bmatrix} (H_{N_1}(z^{-1}) - h_0)z\Delta v(t-1) \\ (H_{N_1+1}(z^{-1}) - h_0 - h_1 z^{-1})z^2\Delta v(t-1) \\ \vdots \\ (H_{N_2}(z^{-1}) - h_0 - h_1 z^{-1} - \dots - h_{N_u-1}z^{-(N_u-1)})z^{N_u}\Delta v(t-1) \end{bmatrix},$$

being that $N_1$ and $N_2$ already consider the system dead time $d$.

However, considering the future disturbances to be equal to the last measured value ($v(t+j) = v(t)$ with $j$ being future instants, then $\Delta v(t+j) = 0$), the second term of Equation (3.10) vanishes:

$$\mathbf{y} = \mathbf{G}\mathbf{u} + \mathbf{F}(z^{-1})y(t) + \mathbf{G}'(z^{-1}) + \mathbf{H}'(z^{-1}). \tag{3.11}$$

To solve the GPC optimization Equation (3.11), the control signal sequence is obtained with the following Equation:

$$\Delta u(t) = \mathbf{K}[\mathbf{R} - \mathbf{F}y(t) - \mathbf{G}' - \mathbf{H}'], \tag{3.12}$$

where $\mathbf{K}$ is a gain factor obtained with:

$$\mathbf{K} = [1\,0\dots0]_{1\times N_u}(\mathbf{G}^\intercal\mathbf{G} + \lambda\mathbf{I})^{-1}\mathbf{G}^\intercal, \tag{3.13}$$

$\mathbf{R}$ is a vector with the future reference values,

$$\mathbf{R} = [r(t+N_1)\;\; r(t+N_1+1)\;\; \dots\;\; r(t+N_2)]^\intercal, \tag{3.14}$$

and $\lambda$ is considered to be a positive constant ($\lambda > 0$) [53].

Analyzing Equation (3.12) it is possible to verify that if there is no future prediction error ($\mathbf{R} - (\mathbf{F}y(t) - \mathbf{G}' - \mathbf{H}') = 0$), the control signal is zero, since the objective is achieved with the natural process evolution. However, when $\mathbf{R} - (\mathbf{F}y(t) - \mathbf{G}' - \mathbf{H}') \neq 0$, the control action increment is the result of the future error multiplied by a $\mathbf{K}$ factor.

## 3.2 Fuzzy Logic Systems

Fuzzy Logic (FL) was initially introduced as Fuzzy Sets, in 1965 by Lotfi A. Zadeh [54], describing a group of information that can be characterized by a membership function, which represents each group level of belonging to a correspondent characteristic. In the following years, Zadeh proposed several complementary concepts to the Fuzzy logic notion, such as Fuzzy Algorithms in 1968 [55], Decision-Making in a FL environment in 1970 [56], Fuzzy Ordering in 1971 [57] and the notion of linguistic variables and IF-THEN rules to describe human decision in 1973 [58]. In these years, fuzzy logic theory was constructed

and consolidated, which allowed the first implementations. One of the earlier known applications was an experiment on the "linguistic" synthesis of a controller, for a model industrial plant - a small steam engine. This laboratory project was developed in the early 70s, by Mamdani and Assilian, with the experiment results presented in [59]. With this step, it was possible to prove the good performance of FL in systems control, and understand its promising applications. In the proceeding years the FL field of application increased mainly due to Japanese engineers, with implementations ranging from a self-parking car, by Sugeno and Nashida, in 1985 [60], to a control system for the Sandai subway, by Yasunobu and Miyamoto [61], finished in 1987. In Europe and in the United States, it was only in the 90s that Fuzzy systems implementation and investigation became more popular. Consequently, since Fuzzy Logic Systems (FLS) are relatively new, with less than sixty years since their appearance, it is still a fairly active investigation field. The Fuzzy Logic process is constructed similarly to the human reasoning process, since it is based on defined rules to make a decision. Furthermore, this type of logic has been applied in nonlinear systems control, which are frequently hard to model and control. As a result, when the model process is mathematically inaccurate, human knowledge based logic helps to describe the plant control with empirical knowledge. However, this process still presents a few challenges, namely determining the most fitting fuzzy rules and membership functions. More recently, a great part of fuzzy systems applications has been in nonlinear processes, due to its positive results. Moreover, FLS has been vastly used in the industry, such as in power plants and systems, telecommunications, transportation systems, decision-making support systems, in chemical processes, in Natural language processing, etc [62]. And, an example of a day-to-day system, that may use FLS, are washing machines.

### 3.2.1 Fuzzy Systems

Fuzzy Systems are based on fuzzy logic rules, to define the approach that is desired to implement. These rules are quite similar to the ones humans use in their everyday decisions. For example, when driving, the chosen course to arrive at the final destination is usually selected by a set of rules, defined in the driver's mind, and which may depend on distance, traffic, road preferences, etc. Fuzzy identification and control approaches have been used in numerous systems, such as aircraft flight control and navigation, automatic braking systems, etc. Additionally, these systems have proven to be able to resolve complex problems.

Fuzzy Systems have a defined structure in the form of IF-THEN rules that articulate the input-output relation of the system. The output of these systems is of a fuzzy set form, which expresses the membership degree of each output. The fundamental part of fuzzy logic is the membership function, which defines the belonging ratio of each input to the stipulated categories, or fuzzy sets. This value may range from 0 to 1, where 0 represents a total mismatch from a specific group, and 1 represents a full match to one category. These sort of systems are normally characterized by an architecture containing four blocks [63], represented in Figure 3.3. In Figure 3.3, the input and output are real numbers. The fuzzifier block converts the input value into fuzzy sets. The inference engine utilizes the knowledge-base rules to transform the fuzzy sets into other fuzzy sets, that represent those rules information. And the defuzzifier block transforms them into output values. These four blocks are detailed in the next subsections: the fuzzifier (Subsection 3.2.2), the knowledge-base (Subsection 3.2.3), the inference engine (Subsection 3.2.4), and

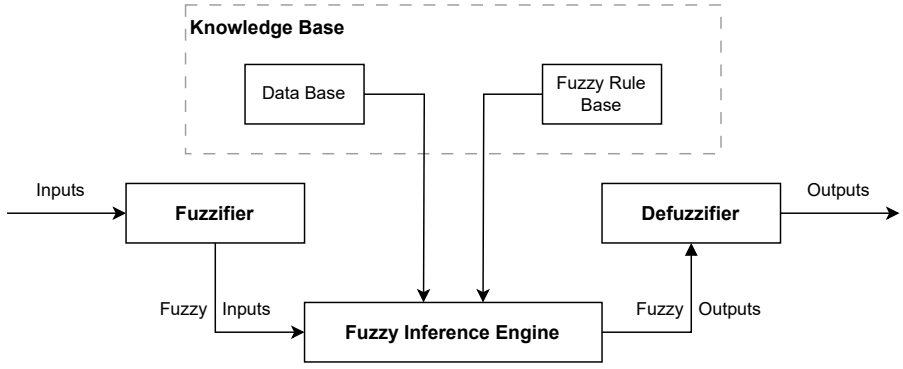


Figure 3.3: Fuzzy system block diagram.

the defuzzifier (Subsection 3.2.5).

### 3.2.2 Fuzzifier

The fuzzifier implements a mapping process between real values, $x^* \in U$, and the corresponding fuzzy sets, $A'$ in $U$. There are multiple fuzzifier methods, such as the singleton fuzzifier, the Gaussian fuzzifier, and the triangular fuzzifier.

The simpler method and the most used is the singleton fuzzifier, that is represented by the following membership function:

$$\mu_{A'}(x) = \begin{cases} 1 & \text{if } x = x^* \\ 0 & \text{otherwise} \end{cases}, \tag{3.15}$$

which is one at $x^*$ and zero at all other points.

### 3.2.3 Knowledge-Base

The knowledge-base, is the core of a fuzzy system. This component comprises $N$ fuzzy IF-THEN rules ($R_i$), that the other three fuzzy logic blocks apply. The mentioned IF-THEN fuzzy rules, are characterized by two important fragments, the antecedent parcel (IF) and the consequent parcel (THEN). In Equation (3.16), a representation of these rules is presented.

$$R_i : \text{IF } x_1(t) \text{ is } A_1^j, \text{ and } \ldots \text{ and } x_n(t) \text{ is } A_n^i, \text{ THEN } u(t) \text{ is } B_i, \tag{3.16}$$

where $i$ ($i = 1, \ldots, N$) represents the rule number, $x_j$ ($j = 1, \ldots, n$) represent the fuzzy system input variables, and $u$ is the fuzzy system output. $A_j^i$ and $B_i$ are fuzzy sets characterized by the following fuzzy membership functions: $\mu_{A_j^i}(x_j)$ and $\mu_{B_i}(u)$. Let us consider the following example.

**Example:** Consider a simple fuzzy controller used to control a closed Photobioreactor (PBR) culture levels of pH, using a $CO_2$ valve aperture percentage. The human knowledge

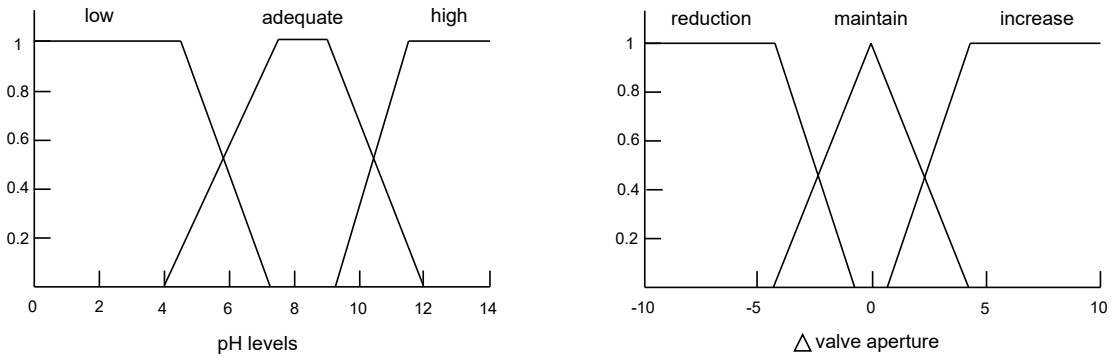


(a) (b)

Figure 3.4: Fuzzy controller example membership functions: (a) *pH levels* membership function, and (b) *valve aperture* membership function.

for controlling the pH can be simply represented in the following fuzzy rules.

$$\begin{aligned}
&\text{IF the } \textit{pH level} \text{ of the PBR is } \textit{adequate},\\
&\quad \text{THEN } \textit{maintain valve aperture} \text{ applied.}\\
&\text{IF the } \textit{pH level} \text{ of the PBR is } \textit{high},\\
&\quad \text{THEN apply an } \textit{increase} \text{ in } \textit{valve aperture}.\\
&\text{IF the } \textit{pH level} \text{ of the PBR is } \textit{low},\\
&\quad \text{THEN apply a } \textit{reduction} \text{ in } \textit{valve aperture}.
\end{aligned} \tag{3.17}$$

Where the key expressions “adequate”, “high”, “low”, “maintain”, “increase” and, “reduction” are specified by membership functions. The majority of membership functions used are trapezoidal, triangular, and Gaussian membership functions. For this example, the *pH levels* (the input variable) can be characterized by the membership function presented in Figure 3.4a, and the *valve aperture* (output variable) to apply can be characterized by the membership function presented in Figure 3.4b.

### 3.2.4 Fuzzy Inference Engine

In the fuzzy inference engine, the Knowledge-Base IF-THEN rules are used to map the $A'$ in $U$ fuzzy set to a $B'$ in $V$ fuzzy set. So, in this step, the matching degree of each fuzzy input to each rule is solved, in order to determine the rules that should be used. This element is responsible for simulating human decision operations, to produce fuzzy conclusions (output).

### 3.2.5 Defuzzifier

The defuzzifier is responsible for the transformation of the fuzzy inference engine output, $B'$, to a real value output, $y^* \in V$. In this process the best point representation of the fuzzy set $B'$ is defined. There are various defuzzifier methods, and there are three important criteria to consider when selecting one, being: 1) Plausibility, meaning that it should

be intuitive to attribute $y^*$ to set $B'$, 2) Computational simplicity, and 3) Continuity, meaning that a small alteration to the set should not result in big changes over the output. Two examples of defuzzifier are the center of gravity defuzzifier, and the center average defuzzifier.

The first defuzzifier example, the center of gravity, follows Equation (3.18).

$$y^* = \frac{\int_V y\mu_{B'}(y)dy}{\int_V \mu_{B'}dy} \tag{3.18}$$

This defuzzifier can be characterized for being intuitive, however, the computational power involved may represent a disadvantage. Considering the center average, that is one of the most used defuzzifier, since application resolves the complex computational problem, associated with the center of gravity diffuzifier. With this approach $y^*$ is determined with:

$$y^* = \frac{\sum_{l=1}^{M} \overline{y}^l w_l}{\sum_{l=1}^{M} w_l}, \tag{3.19}$$

where $N$ represented the total number of fuzzy sets, $\overline{y}^{-l}$ is the $l-th$ fuzzy set center, and $w_l$ is the $l-th$ fuzzy set height. Each fuzzy set corresponds to the output of one of $N$ rules.

### 3.2.6 Takagi-Sugeno Fuzzy Model

In a generic view, there are two types of fuzzy systems [64, 65], distinguished according to the output generation process and their distinct consequent IF-THEN rules component. Between these, the first system to appear was the Mamdani FIS [59], in 1975, while the Takagi-Sugeno FIS [66], was presented in 1985. In this work, only Takagi-Sugeno fuzzy systems are considered. Takagi-Sugeno fuzzy systems are less intuitive than Mamdani fuzzy systems, however, they are more versatile. Additionally, they are known to facilitate the fuzzy identification of dynamic systems and adaptive control. Besides, the T-S fuzzy systems have a distinct rule consequent formulation that does not entail fuzzy sets, as Mamdani fuzzy systems, but instead utilize mathematical expressions. These rules can be represented in the following form (3.20):

$$R_i: \text{ IF } x_1 \text{ is } A_1^i, \text{ and } \ldots \text{ and } x_n \text{ is } A_n^i \text{ THEN } y \text{ is } f^i(x_1, x_2, \ldots, x_n), \tag{3.20}$$

where $R_i$ denotes the $i$-th rule out of a total of $N$ rules. Variables $x_1(t), \ldots, x_n(t)$ stand for the selected T-S fuzzy system inputs, while $y$ represents the system output. $A_j^i$ represents fuzzy sets corresponding to the antecedent linguistic terms, and $f^i$ is a function of $x_1, x_2, \ldots, x_n$.

The identification process of a T-S fuzzy model aims to accurately construct a model to represent complex input-output relations of the system. This process involves the determination of its parameters based on available data. This model is a representation of a system that employs fuzzy logic and its applications encompass control, prediction, and analysis purposes. The following steps are an overview of the T-S fuzzy model identification process.

1. **Define input and output variables**: identify influencing factors in the system and the variable to be controlled;

2. **Collect a dataset:** assemble a dataset with input-output information that represents the system behavior;
3. **Fuzzification:** convert the inputs into fuzzy sets;
4. **Divide the input information:** divide the input information into fuzzy regions or clusters;
5. **Determine the fuzzy rules:** formulate fuzzy rules that relate the input variables to the output variable;
6. **Compute the rules consequent:** determine the consequent parts of each rule;
7. **Aggregate the fuzzy rules outputs:** combine the consequent fuzzy rules to obtain an output;
8. **Validate the model and parameter tuning:** evaluate the model performance and adjust parameters if necessary;
9. **Implement the model**.

Furthermore, it is frequent to further implement an algorithm to update the model parameters, in particular in systems presenting variations or evolving characteristics.

## 3.3 Overview

In this chapter, important notions for the following chapter were presented, as the selected approach involves an MPC controller with iterative parameter adaptation, using a T-S fuzzy model. From the set of MPC approaches, Generalized Predictive Control was selected due to its predictive characteristics, which are crucial in the controlled process, and its intuitive relation with a fuzzy T-S model. This combination of methods allows for an iterative update of the controller parameters. Furthermore, the following chapter describes the model identification process, including the implemented algorithms in each identification phase, as well as the process for updating the controller's parameters.

# Chapter 4

# Fuzzy System Identification and Predictive Control

## Contents



## 4.1 Introduction

This chapter describes the implemented fuzzy identification process to model the pH in tubular photobioreactors, and the controller's adjustments to process the model's parameters update. As mentioned in the previous chapter, the selected fuzzy model was a Takagi-Sugeno (T-S) fuzzy model, that is conceptually defined in this chapter. Therefore, the identification process is performed by a T-S fuzzy model, which is divided into two parts. As described in Section 3.2, the knowledge-base rules are composed of two parts, the antecedent and the consequent part. Accordingly, the identification process is divided into the corresponding methods of identification. Hence, the first part corresponds to the learning of the antecedent parameters, namely the membership function parameters, obtained by an offline strategy using the Fuzzy c-Means (FCM) algorithm. The second part executes the consequent parameters learning process, which is performed in two stages, offline and online. The offline stage is performed by applying the Least Squares Method (LSM), and the online stage is performed by an approach to recursively update the consequent parameter values, the Recursive Least Squares with Adaptive Directional Forgetting (RLS-ADF). RLS-ADF is a combination between the Recursive Least Squares (RLS) algorithm, centered in a constant forgetting factor, and an Adaptive Directional Forgetting (ADF) factor algorithm. An adaptive approach is relevant because, although computed with a large sample of data, the limited dataset may not provide an adequate

accuracy, considering the non-linearity and time-varying characteristics of the system. As such, an adaptive algorithm generally represents a favorable alternative to solve this limitation.

## 4.2 Takagi-Sugeno Fuzzy System Identification

The Takagi-Sugeno (T-S) fuzzy model is characterized by its consequent parameters, which are defined by mathematical expressions instead of fuzzy sets, as illustrated in Equation (3.20). This represents an advantage when performing a dynamic system identification [65]. Additionally, this model is also considered a universal approximator [67]. In this work, the T-S fuzzy model, to be used on the predictive controller, is defined by a set of $N$ rules with the following structure [68]:

$$\begin{aligned} R_i : \text{IF } & x_1(t) \text{ is } A_1^i, \text{ and } \ldots \text{ and } x_n(t) \text{ is } A_n^i \\ \text{THEN } & y_i(t) = a_i(z^{-1})y(t-1) + b_i(z^{-1})u(t-d-1) \\ & \quad + d_i(z^{-1})v(t-1) + \zeta(t), \end{aligned} \tag{4.1}$$

where $R_i$ represents the $i$-th rule, $\mathbf{x}(t) = [x_1(t), \ldots, x_n(t)]^\intercal$ and $x_j(t)$ $(j = 1, \ldots, n)$ represent the system inputs of instant $t$, $n$ is the total number of inputs of the fuzzy system, and $N$ is the total number of rules. $y(t)$, $v(t)$ and $\zeta(t)$ respectively represent the system output, the measured disturbance and noise of instant $t$. The $A_j^i$ is the respective symbol for the linguistic term, with $i = 1, \ldots, N$ and $j = 1, \ldots, n$, characterized by the fuzzy membership function, $\mu_{A_j^i}(x_j)$ [53]. The $u(t)$ represent the control output, $d$ is the delay of the system, and $a_i$ and $b_i$ are polynomials defined by:

$$\begin{aligned} a_i(z^{-1}) &= a_{1i} + a_{2i}z^{-1} + \ldots + a_{n_a i}z^{-(n_a-1)}, \\ b_i(z^{-1}) &= b_{1i} + b_{2i}z^{-1} + \ldots + b_{n_b i}z^{-(n_b-1)}, \\ d_i(z^{-1}) &= d_{1i} + d_{2i}z^{-1} + \ldots + d_{n_d i}z^{-(n_d-1)}, \end{aligned} \tag{4.2}$$

where $n_a$, $n_b$ and $n_d$ are the orders of polynomials $a_i$, $b_i$ and $d_i$, respectively. And $\boldsymbol{\theta}_i$ contains the model consequent parameters to be learned.

$$\boldsymbol{\theta}_i = [a_{1i}, \ldots, a_{n_a i}, b_{1i}, \ldots, b_{n_b i}, d_{1i}, \ldots, d_{n_d i}]^\intercal \tag{4.3}$$

Considering Gaussian membership functions, the antecedent fuzzy membership functions are given by:

$$\mu_{A_j^i}(x_j(t)) = \exp\left(\frac{(x_j(t) - v_{ij})^2}{\sigma_{ij}}\right), \tag{4.4}$$

where $v_{ij}$ and $\sigma_{ij}$ correspond, respectively, to the center and width of the defined membership functions. These two parameters are also defined as the antecedent parameters to be learned. The system output $y[\mathbf{x}(t)]$ of the T-S fuzzy model is calculated by the following equation [68]:

$$y[\mathbf{x}(t)] = \sum_{i=1}^{N} \bar{\omega}_i[\mathbf{x}(t)]\mathbf{x}^\intercal(t)\boldsymbol{\theta}_i, \tag{4.5}$$

where:

$$\bar{\omega}_i[\mathbf{x}(t)] = \frac{\prod_{j=1}^{n} \mu_{A_j^i}(x_j(t))}{\sum_{p=1}^{N} \prod_{j=1}^{n} \mu_{A_j^p}(x_j(t))}, \tag{4.6}$$

and $\mathbf{x}(t)$ is defined in this work as:

$$\begin{aligned}\mathbf{x}(t) = [&y(t-1), \ldots, y(t-n_a), u(t-d-1), \ldots, u(t-d-n_b),\\ &v(t-1), \ldots, v(t-n_d)]^\intercal.\end{aligned} \tag{4.7}$$

### 4.2.1 Fuzzy c-Means Clustering Algorithm

The Fuzzy c-Means (FCM) clustering method allows a multidimensional data organization into clusters and, in this case, it is used to obtain the antecedent parameters ($v_{ij}$ and $\sigma_{ij}$(4.4)) of the T-S fuzzy model (4.1). The learning process initializes with the dataset division into $N$ clusters, followed by the computation of their centers ($v_{ij}$) and widths ($\sigma_{ij}$). The following step encompasses the computation of each dataset point level of membership to the different clusters. To evaluate the corresponding membership degree of each point to the clusters, a calculation dependent on its distance to every cluster center is performed. For instance, a dataset point close to a cluster center will have a high membership value to that cluster, however, if the point is located far from the cluster center, the point will have a low level of membership related to that cluster.

Considering the dataset values,

$$\boldsymbol{X} = \begin{bmatrix} x_1(1) & x_2(1) & \ldots & x_n(1) \\ x_1(2) & x_2(2) & \ldots & x_n(2) \\ \vdots & \vdots & \vdots & \vdots \\ x_1(t) & x_2(t) & \ldots & x_n(t) \\ \vdots & \vdots & \vdots & \vdots \\ x_1(T) & x_2(T) & \ldots & x_n(T) \end{bmatrix}, \tag{4.8}$$

where $t$ is the row index, $i$ is the column index and $T$ is the total number of samples.

The fuzzy partition of the set $\boldsymbol{X}$ into $N$ clusters, is a group of fuzzy subsets defined as [69]:

$$\mu_i(t) = \mu_{A_j^i}(x_j(t)) \in [0, 1], \tag{4.9}$$

and the sum of all membership values of a sample is one, $\sum_{i=1}^{T} \mu_i(t) = 1$. Moreover, it is not possible for a cluster to encompass all the dataset samples, as it is also not possible for a cluster to be empty. The membership values originate a partition matrix $\mathbf{U}$, where the $i$-th row of this matrix corresponds to the membership values of the $i$-th fuzzy subset $A^i$. This matrix can be represented by:

$$\mathbf{U} = [\mu_i(t)] \in \mathbb{R}^{N \times T}. \tag{4.10}$$

The FCM objective function involves the clusters centers, the distance between a given sample and a cluster center, and a fuzziness parameter $\eta$, that controls the membership degree computation [69]. With a higher $\eta$, the clusters are more fuzzy and each point belongs to more clusters, with similar membership values. This function, that is to be minimized, is given by:

$$\mathbf{J}(\mathbf{X}, \mathbf{U}, \mathbf{V}) = \sum_{i=1}^{N} \sum_{t=1}^{T} \mu_i(t)^\eta l_i(t)^2, \tag{4.11}$$

where $l_i(t)$ represents the norm of the difference between $\mathbf{x}(t)$ and a cluster centers vector $\mathbf{v}_i$, given by the Euclidean distance:

$$l_i(t)^2 = (\mathbf{x}(t) - \mathbf{v}_i)^\intercal (\mathbf{x}(t) - \mathbf{v}_i), \tag{4.12}$$

where $\mathbf{v}_i = [v_{i1}, \ldots, v_{in}]^\intercal$ is the vector containing the center of the $i$-th cluster, and

$$\mathbf{V} = [\mathbf{v}_1, \ldots, \mathbf{v}_N]^\intercal \in \mathbb{R}^{N \times n}, \tag{4.13}$$

is a matrix composed of all the clusters centers, with

$$\mathbf{v}_i = \frac{\sum_{t=1}^{T} \mu_i(t)^\eta \mathbf{x}(t)}{\sum_{t=1}^{T} \mu_i^\eta(t)}, \tag{4.14}$$

or

$$v_{ij} = \frac{\sum_{t=1}^{T} \mu_i^\eta(t) x_j(t)}{\sum_{t=1}^{T} \mu_i^\eta(t)}. \tag{4.15}$$

Then, the second antecedent parameter, $\sigma_{ij}$, the width of Gaussian membership functions, is obtained using the $\mathbf{U}$ matrix values [69]:

$$\sigma_{ij} = \sqrt{\frac{2\sum_{t=1}^{T} \mu_i(t)(x_j(t) - v_{ij})^2}{\sum_{t=1}^{T} \mu_i(t)}}. \tag{4.16}$$

### 4.2.2 Least-Squares Method

The least squares method has been widely used to determine the rule consequent parameters ($\theta_{ij}$) [69, 70]. Transforming Equation (4.5),

$$\begin{aligned} y[\mathbf{x}(t)] &= \sum_{i=1}^{N} \bar{\omega}_i[\mathbf{x}(t)]\mathbf{x}^\intercal(t)\boldsymbol{\theta}_i \\ &= \boldsymbol{\psi}[\mathbf{x}(t)]^\intercal \boldsymbol{\Theta}, \end{aligned} \tag{4.17}$$

where $\boldsymbol{\Theta}$ contains the consequent parameters of all rules,

$$\boldsymbol{\Theta} = [\boldsymbol{\theta}_1^\intercal, \ldots, \boldsymbol{\theta}_N^\intercal]^\intercal, \tag{4.18}$$

and

$$\boldsymbol{\psi}[\mathbf{x}(t)] = [\bar{\omega}_1 \mathbf{x}^\intercal(t), \ldots, \bar{\omega}_N \mathbf{x}^\intercal(t)]^\intercal. \tag{4.19}$$

Considering $\mathbf{y}_d$ a vector containing the target output values:

$$\mathbf{y}_d = [y_d(\mathbf{x}(1)), \ldots, y_d(\mathbf{x}(T))]^\intercal, \tag{4.20}$$

it is possible to present the following Equation, according to (4.1):

$$\mathbf{y}_d = \boldsymbol{\Psi}\boldsymbol{\Theta}, \tag{4.21}$$

where

$$\boldsymbol{\Psi} \;=\; [\boldsymbol{\psi}(\mathbf{x}(1)), \ldots, \boldsymbol{\psi}(\mathbf{x}(T))]^{\intercal}. \tag{4.22}$$

Using the pseudo-inverse in (4.21), the optimal values of the consequent parameters, $\boldsymbol{\Theta}^*$, are obtained throughout the Equation:

$$\boldsymbol{\Theta}^* \;=\; (\boldsymbol{\Psi}^{\intercal}\boldsymbol{\Psi})^{-1}\boldsymbol{\Psi}^{\intercal}\mathbf{y}_d. \tag{4.23}$$

### 4.2.3 Recursive Least Squares Method With Adaptive Directional Forgetting

At this point of the process, an optimal set of Theta values $\boldsymbol{\Theta}^*$ were already calculated. The RLS-ADF is an interception between the RLS algorithm, centered in a constant forgetting factor, and an ADF factor algorithm. This approach is presented in [71] and [72], as a strategy to recursively update the consequent parameter values of a T-S fuzzy model. This algorithm (RLS-ADF), at each system iteration, performs the update of the Theta parameters based on the update of a covariance matrix ($\mathbf{C}_i(t)$) and in the forgetting factor ($\varphi_i(t)$).

The covariance matrix must be initialized to an identity matrix multiplied by a large number, for example $10^5$. For the iterative update of the covariance matrix corresponding to each rule, Equation (4.24) should be implemented.

$$\mathbf{C}_i(t) = \mathbf{C}_i(t-1) - \frac{\mathbf{C}_i(t-1)\boldsymbol{\psi}_i^{\intercal}(t)\mathbf{C}_i(t-1)}{\varepsilon_i^{-1} \;+\; \xi_i}, \tag{4.24}$$

with

$$\varepsilon_i \;=\; \varphi_i(t-1) - \frac{1-\varphi_i(t-1)}{\xi_i}, \tag{4.25}$$

where $\varphi_i(t-1)$ is the last iteration forgetting factor, for the $i$-th rule. Moreover, the forgetting factor iterative Equation is:

$$\varphi_i(t) \;=\; \frac{1}{1+(1+\rho)\left(\ln(1+\xi_i) + \left[\frac{(\nu_i(t)+1)\gamma_i}{1+\xi_i+\gamma} - 1\right]\frac{\xi_i}{1+\xi_i}\right)}, \tag{4.26}$$

with

$$\nu_i(t) = \varphi_i(t-1)(\nu_i(t-1)+1), \tag{4.27}$$

$$\gamma_i \;=\; \frac{(y_i(t) - \boldsymbol{\psi}_i\boldsymbol{\theta}_i(t-1))^2}{\tau_i(t)}, \tag{4.28}$$

$$\tau_i(t) \;=\; \varphi_i(t-1)\left[\tau_i(t-1) + \frac{(y_i(t) - \boldsymbol{\psi}_i\boldsymbol{\theta}_i(t-1))^2}{1+\xi_i}\right], \tag{4.29}$$

and $\rho$ is a positive constant. The initialization of these parameters, $\varphi$, $\tau$ and $v_i$, should be between zero and one.

Using the RLS-ADF, the consequent parameters are updated at each sample time $t$ by:

$$\boldsymbol{\theta}_i(t) = \boldsymbol{\theta}_i(t-1) \;+\; \frac{\mathbf{C}_i(t-1)\boldsymbol{\psi}_i^{\intercal}(t)}{1 \;+\; \xi_i}[y_i(t) \;- \boldsymbol{\psi}_i(t)\boldsymbol{\theta}_i(t-1)], \tag{4.30}$$

where

$$\boldsymbol{\psi}_i(t) = \bar{\omega}_i[\mathbf{x}(t)]\mathbf{x}^{\intercal}(t), \tag{4.31}$$

$$\xi_i = \boldsymbol{\psi}_i(t)\mathbf{C}_i(t-1)\boldsymbol{\psi}_i^{\intercal}(t). \tag{4.32}$$

## 4.3 Predictive Control

This section presents the overall control algorithm selected to control the pH levels in a photobioreactor. As previously mentioned, the selected approach is the Adaptive Fuzzy Generalized Predictive Control (AFGPC). This method is a combination of the estimated fuzzy model with adaptive parameters (described in Section 4.2) and the implemented GPC controller (discussed in Section 3.1.1). These two components were selected for their intuitive combination and the ease with which control parameters can be adapted by updating the model. For the controller implementation, the equations presented in subsection 3.1.1 were implemented in MATLAB, according to the recursive Diophantine equations described in [38]. Nevertheless, to do so the following equations were essential.

Considering the fuzzy rules presented in (4.1), and the fuzzy model of the form of Equation (4.17), the predictive model is given by:

$$\bar{a}(z^{-1})y(t-1) = \bar{b}(z^{-1})u(t-d-1) + \bar{d}(z^{-1})v(t-1) + \zeta(t), \tag{4.33}$$

where

$$\begin{aligned} \bar{a}(z^{-1}) &= 1 - \bar{a}_1 z^{-1} - \ldots - \bar{a}_{n_a} z^{-n_a}, \\ \bar{b}(z^{-1}) &= \bar{b}_1 + \bar{b}_2 z^{-1} + \ldots + \bar{b}_{n_b} z^{-(n_b-1)}, \\ \bar{d}(z^{-1}) &= \bar{d}_1 + \bar{d}_2 z^{-1} + \ldots + \bar{d}_{n_d} z^{-(n_d-1)}, \end{aligned} \tag{4.34}$$

where $n_a$, $n_b$ and $n_d$ are the orders of polynomials $\bar{a}$, $\bar{b}$ and $\bar{d}$, respectively. With its elements being computed through:

$$\begin{aligned} \bar{a}_l &= \sum_{i=1}^{c} \bar{\omega}_i[\mathbf{x}(t)] a_{mi}, \ l = 1, \ldots, n_a, \\ \bar{b}_l &= \sum_{i=1}^{c} \bar{\omega}_i[\mathbf{x}(t)] b_{mi}, \ l = 1, \ldots, n_b, \\ \bar{d}_l &= \sum_{i=1}^{c} \bar{\omega}_i[\mathbf{x}(t)] d_{mi}, \ l = 1, \ldots, n_d, \end{aligned} \tag{4.35}$$

where $a_{mi}$, $b_{mi}$ and $d_{mi}$ are corresponding to Equation (4.3) values, and $\bar{\omega}_i[\mathbf{x}(t)]$ are describes in Equation (4.6).

The structure of the AFGPC is illustrated in Figure 4.1, and is divided into three main blocks: the GPC controller (Subsection 3.1.1) using the predictive model defined in (4.33), the plant to be controlled, and the T-S fuzzy model (Section 4.2), which adapts the model's parameters of (4.33). The development steps are presented in Algorithm 1. In this algorithm, the first step includes the definition of several variables, encompassing dataset organization, the identification parameters definition ($d$, $N$, $\rho$, $\varphi_i$, $\tau_i$, $\nu_i$, $\mathbf{C}_i$, $n_a$, $n_b$ and $n_d$), and the selection of controller parameters ($N_1$, $N_2$, $N_u$, and $\lambda$). The second step comprises the offline fuzzy model identification, including the implementation of the Fuzzy C-Means (FCM) algorithm (Section 4.2.1) to obtain the antecedent parameters ($v_{ij}$ and $\sigma_{ij}$) and the implementation of the Least Squares Method (LSM) algorithm (Section 4.2.2) to obtain the consequent parameters ($\theta_{ij}$). The third step represents the controller computation cycle, which comprises the online parameters adaptation. This last step begins with the receiving of the fuzzy model inputs. It is followed by the computation of fuzzy model parameter adaptation using the Recursive Least Squares with Adaptive Forgetting (RLS-ADF) algorithm (Section 4.2.3) and subsequent calculation of

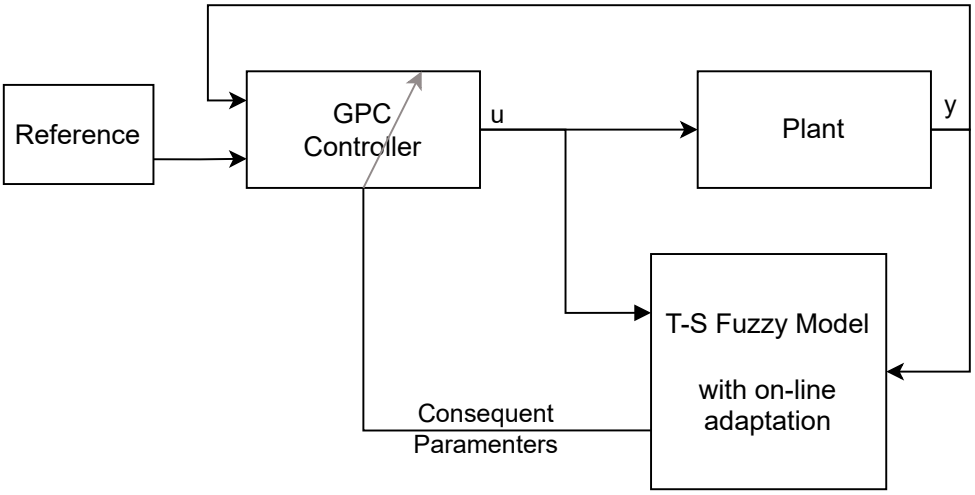


Figure 4.1: Adaptive Fuzzy Generalized Predictive Control.

**Algorithm 1** Control approach for pH control.

**Input**:
Dataset.
Identification parameters: the time delay $d$, the number of clusters/rules $N$, the polynomials order $n_a$, $n_b$, $n_d$, and the parameters for RLS-ADF: $\rho$, $\varphi_i$, $\tau_i$, $\nu_i$, $\mathbf{C}_i$.
Controller parameters: prediction horizons $N_1$, $N_2$ and $N_u$, and the control action weighting factor $\lambda$.
**Offline:**
Design the T-S fuzzy model (4.1).
Obtain the antecedent parameters using FCM (Subsection 4.2.1): $v_{ij}$ (4.14) and $\sigma_{ij}$ (4.16).
Obtain the consequent parameters using LSM (Subsection 4.2.2): $\theta_{ij}$ (4.23).
**Online:**
**while** Controller turned on **do**
    Read the input and output variables.
    Update the T-S fuzzy model, using RLS-ADF (4.30).
    Obtain the new values of model parameters $\bar{a}_l$, $\bar{b}_l$ and $\bar{d}_l$.
    Compute the control signal from GPC using (3.12).
**end while**

the predictive model parameters ($\bar{a}_l$, $\bar{b}_l$ and $\bar{d}_l$)), applying Equation (4.35). With the new parameters, the controller computes the new control signal, using Equation (3.12). This control command is then transmitted to the system plant, which consequently generates an output representing the new culture medium pH value.

## 4.4 Overview

In this chapter, the model identification process and the controller's iterative parameters adaptation were described. Firstly, a brief introduction to the chapter theme and

succeeding sections was presented. Then, in Section 4.2 the Takagi-Sugeno model used in the identification process constituted by three subsections was described. The first section presented the algorithm utilized for the antecedent parameters estimation, the fuzzy c-means clustering algorithm (Section 4.2.1). The second section presented the method used for the consequent parameters estimation, the least squares method (Section 4.2.2). The third section presented the method used for the recursive consequent parameters adaptation, the recursive least squares method with adaptive directional forgetting (Section 4.2.3). Afterwards, in Section 4.3, the controller's model adaptation and the overall control method structure were described.

# Chapter 5

# Experimental Results

## Contents



## 5.1 Introduction

This chapter presents the experimental results obtained from testing the developed approach to control the pH levels in a tubular photobioreactor for high-value microalgae production. To manage the control of this variable, the aperture percentage of the $CO_2$ valve is manipulated, directly managing the introduced carbon dioxide into the culture. This method, by aiming to maintain a more stable acidity level in the culture medium, intends to achieve a healthier culture environment, which translates to higher production rates. In the following sections some details of the system implementation are described. Firstly, the organization and processing stages of the dataset are described, followed by some implementation details on the fuzzy model and the predictive control. In the last section, simulation control results are presented, encompassing a variety of tests to demonstrate the effect of some variables on the controller's performance and the parameter adaptation rate. The tests were performed using the developed AFGPC approach and a version where the iterative RLS-ADF algorithm is omitted, resulting in fixed consequent parameters for the fuzzy model. In the next sections, the AFGPC approach is referred to as the adaptive parameters approach, and the version without the RLS-ADF algorithm is referred to as the fixed parameters approach. For each presented test, an analysis is performed, and with each group of tests, a comparison is presented, followed by further conclusions.

## 5.2 Dataset Organization

The dataset used in this work was constructed using data collected from a real operational photobioreactor. The provided data was in a raw form, obtained directly from the automation system, since it corresponded to all sensor readings without any type of filtering. Consequently, it was necessary to eliminate operational downtime, cleaning periods, reading errors, and construct continuous sequence data groups.

From the collected data, three variables were selected according to the state-of-the-art control approaches. The chosen variables for controlling the culture pH and constituting the dataset were the carbon dioxide valve aperture percentage, global irradiance, and the medium culture pH. These variables significantly influence the pH medium balance and are crucial to consider. Considering the natural evolution of the photobioreactor culture pH, exposure to a light source (irradiance) gradually increases it, driven by the biological reaction of photosynthetic organisms performing photosynthesis. When no acidic component is inserted into the closed photobioreactor, the culture pH increases until it becomes unsustainable for microorganisms to survive. Consequently, to counterbalance the natural behavior of the culture, $CO_2$ gas is injected into the photobioreactor. This gas reduces the culture pH levels due to its biological reaction with the culture ambient.

After the filtering procedures, the constructed dataset comprises approximately five months, including some spring and fall months and the entire summer period, with a five-minute sampling time, resulting in up to 288 sensor readings each day. Considering this span of information, the sampled data may already permit satisfactory parameter estimation. Furthermore, the dataset was segmented into several blocks based on the processed data intervals caused by the removed operational downtime and cleaning periods. Each block was assigned distinct purposes related to different estimation processes. For instance, one block was designated for estimating the model to test the controller, and another was dedicated to learning the T-S fuzzy model (the prediction model).

In Figures 5.1 and 5.2 three graphics are presented, corresponding to the same operational instants, one for each selected variable (irradiance $Wm^{-2}$, pH levels and $CO_2$ valve aperture percentage). Additionally, each figure represents two different parts of the dataset to demonstrate distinct operational points. The first scenario, illustrated in Figure 5.1, corresponds to a more stable behavior of the system, primarily identified by the pH levels curve in Figure 5.1b. The second scenario, illustrated in Figure 5.2, exemplifies a part of the data with high pH levels inconsistencies, indicating a less stable operation. Moreover, a difference between the irradiance curves is noticeable, represented in Figures 5.1a and 5.2a, explained through the correspondence to distinct data seasons. It is important to note that the presented examples do not represent the entire dataset. They serve only to illustrate two different behaviors, demonstrating the dataset's variety of operational points and providing the reader with a notion of its spectrum.

## 5.3 Fuzzy Model Design

The model identification process of the T-S fuzzy model has been theoretically described in Chapter 4. The T-S fuzzy model used in this work was conceptually described in Section 4.2, while its implementation is described in this section. This process can be divided in two segments, where the first is to find the antecedent parameters ($\mathbf{v}_i$ and $\boldsymbol{\sigma}_i$), and the second to find the consequent parameters ($\boldsymbol{\theta}_i$).

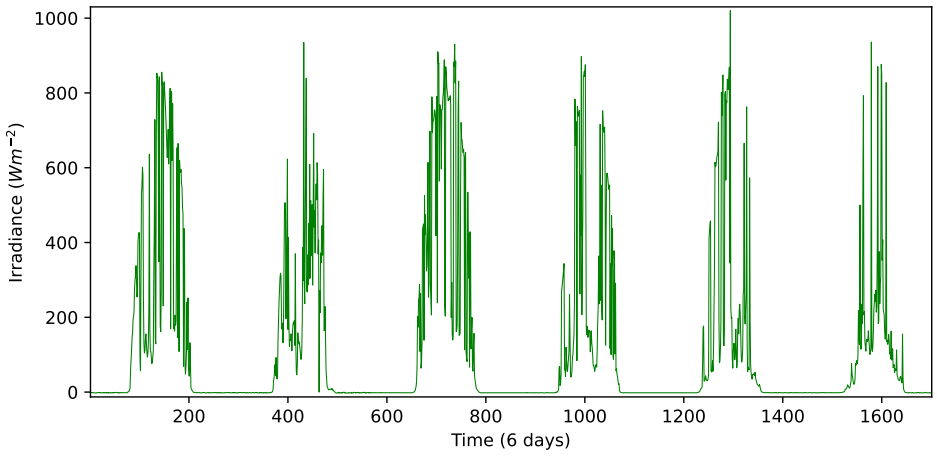


(a)

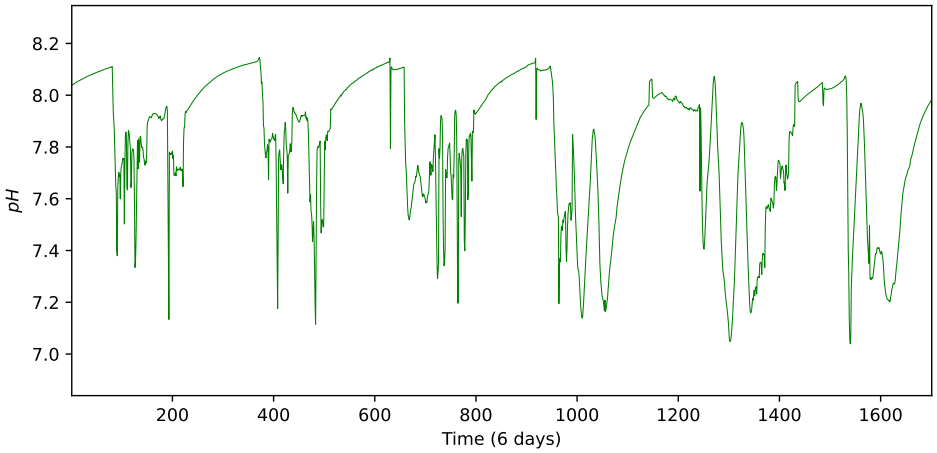


(b)

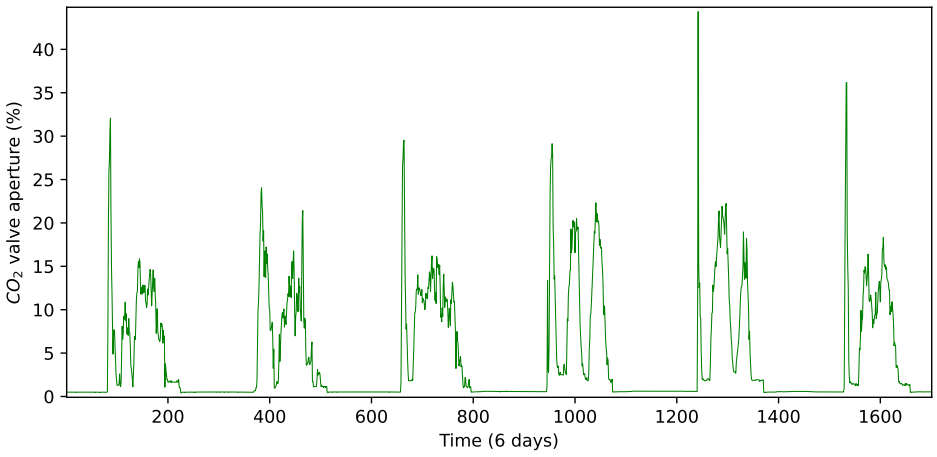


(c)

Figure 5.1: Dataset of the first scenario. Selected variables, (a) global irradiance, (b) pH and (c) carbon dioxide valve aperture (%), for the same operation time.

For $\mathbf{v}_i$ and $\boldsymbol{\sigma}_i$, the fuzzy c-means clustering algorithm was employed, as described in Subsection 4.2.1. This algorithm requires a dataset organized similarly to the matrix in

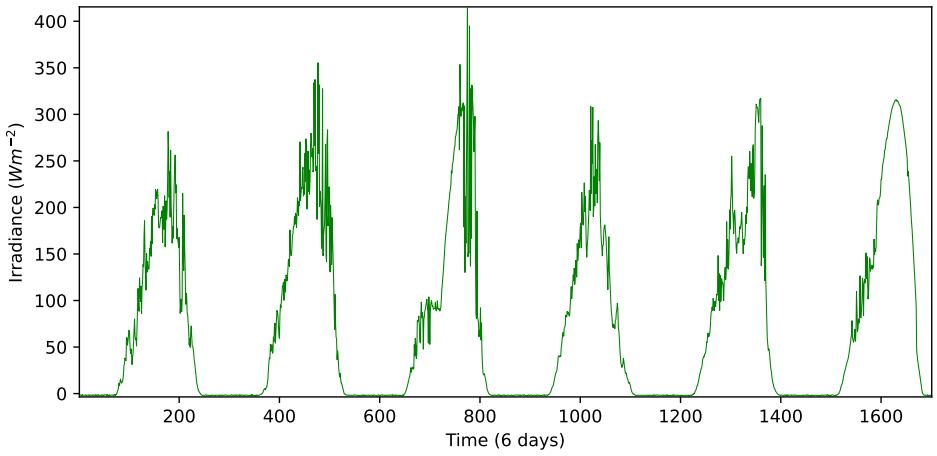


(a)

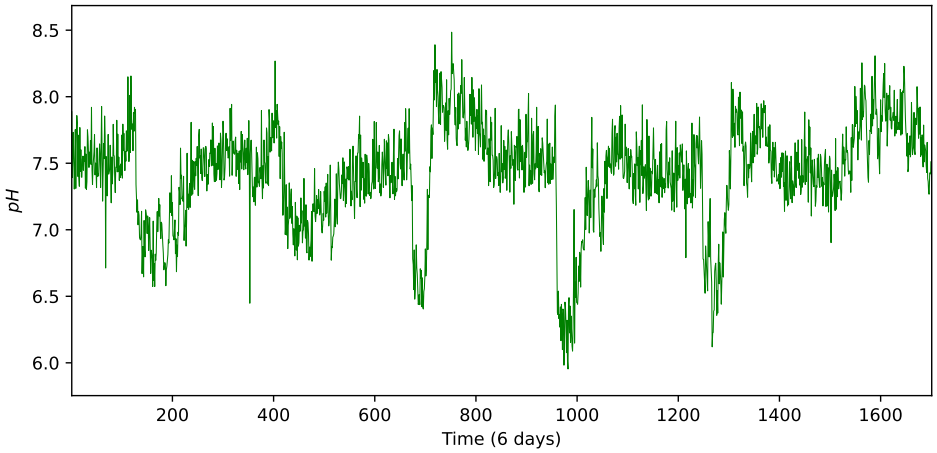


(b)

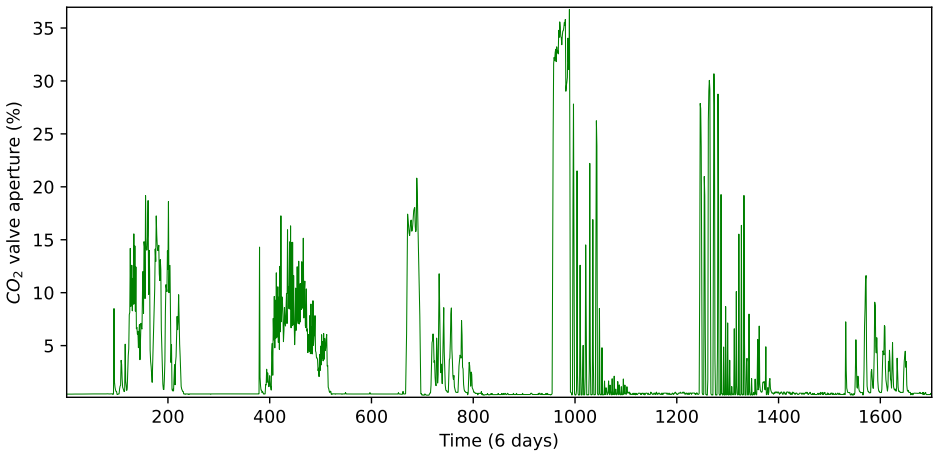


(c)

Figure 5.2: Dataset of the second scenario. Selected variables, (a) global irradiance, (b) pH and (c) carbon dioxide valve aperture (%), for the same operation time.

Equation (4.8). To meet this requirement, a portion of the available data was used to create a dataset. The input vector $\mathbf{x}(t)$ for the T-S fuzzy model system was defined as

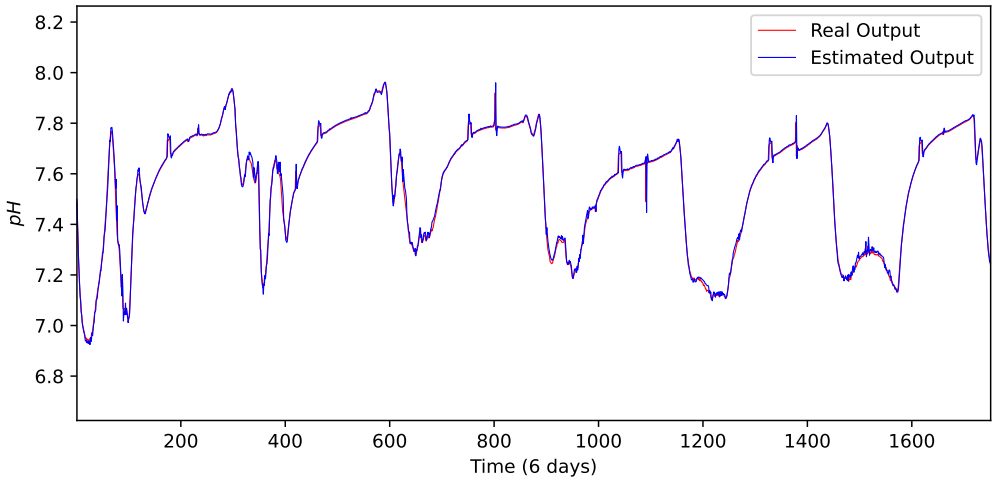


Figure 5.3: Fuzzy model training results.

follows:

$$\mathbf{x}(t) = [y(t-1)\, y(t-2)\, y(t-3)\, y(t-4)\, u(t-1)\, u(t-2)\, u(t-3)\, v(t-1)]^{\intercal}, \tag{5.1}$$

with eight inputs, where $u$ is the carbon dioxide valve aperture percentage, $v$ is the global irradiance and $y$ is the medium culture pH. Each row of matrix $\boldsymbol{X}$ (4.8) corresponds to a specific instant vector $\mathbf{x}(t)$. Once the dataset was organized and the number of inputs defined to be $n = 8$, the next step involved determining the number of clusters. This variable was studied according to the data space organization, and was adjusted to four clusters ($N = 4$). Subsequently, the cluster centers ($\mathbf{v}_i$) were computed using the *fcm* MATLAB function, with parameter $\eta$ set to 2. This function requires two input arguments: the organized dataset $\boldsymbol{X}$ and the number of clusters $N$. Moreover, the *fcm* MATLAB function offers three distinct clustering methods, as described in [73]. In this context, the option compatible with Equation (4.11), based on the Euclidean distance, was selected. As a result of executing the *fcm* function, the cluster centers ($\mathbf{v}_i$) and the fuzzy partition matrix were obtained. Thus, with both output arguments of this function, the clusters widths ($\boldsymbol{\sigma}_i$) were computed using Equation (4.16).

To compute the $\boldsymbol{\Theta}^*$ values, Equation (4.23) was applied. For that, some other values were calculated before, such as the $\Psi$ values. For this purpose, $\bar{\omega}_i[\mathbf{x}(t)]$ $(i = 1, \ldots, N)$ were computed using Equation (4.6). With all the parameters defined, several tests were conducted to validate the obtained values. In Figure 5.3, the results from the fuzzy model training phase are presented, showing two lines representing the real data (red line) and the estimated data (blue line) using the estimated fuzzy model. This graph illustrates the estimated fuzzy model's performance using the estimation dataset. Nevertheless, to demonstrate its effectiveness, a distinct part of the dataset was used. In Figure 5.4, two scenarios from the fuzzy model testing phase are presented, both showing favorable results.

After calculating all antecedent and consequent parameters and conducting all tests, it was possible to proceed to the construction of the RLS-ADF algorithm component. This component allows for the iterative update of the model parameters, and its algorithm is described in Subsection 4.2.3. Moreover, this component was developed in MATLAB from scratch.

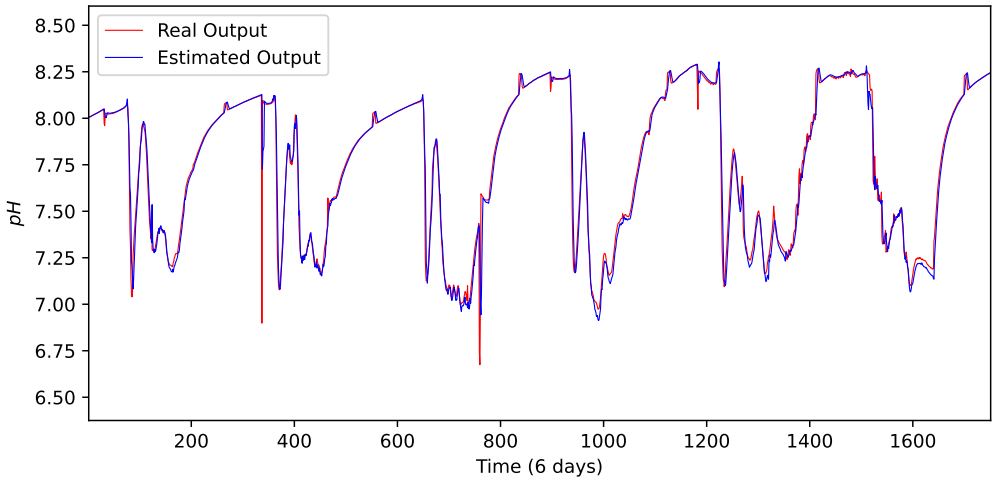


(a) Fuzzy model testing - scenario one.

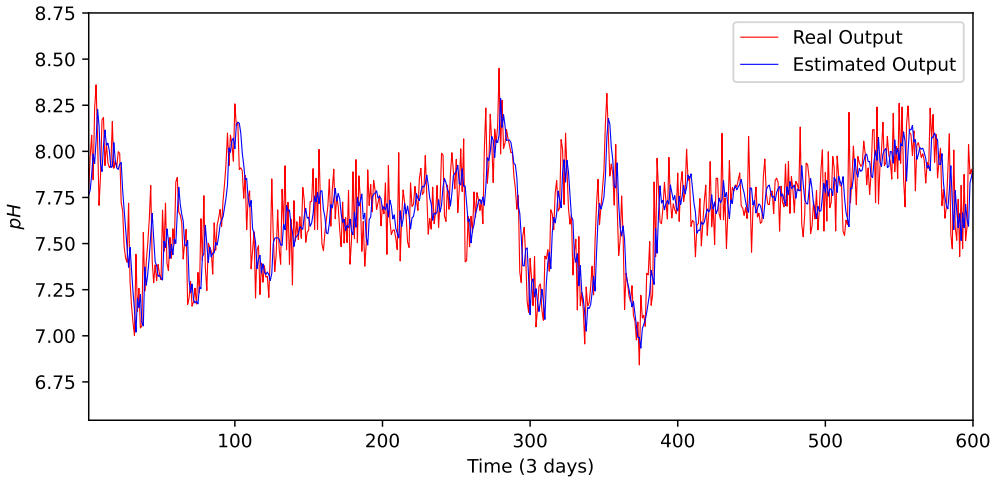


(b) Fuzzy model testing - scenario two.

Figure 5.4: Fuzzy model results in a (a) more stable operation point and in a (b) less stable operation region.

## 5.4 Model Designed to Validate the Predictive Controller

For control simulation purposes, the system pH level to be controlled is given by the following discrete-time model of Autoregression with Exogenous Input (ARX) model,

$$A(z^{-1})pH(t) = B_1(z^{-1})CO_2(t) + B_2(z^{-1})I_{rr}(t), \tag{5.2}$$

where $pH$ represents the acidity level in the photobioreactor, $CO_2$ represents the carbon dioxide valve aperture percentage, and $I_{rr}$ represents the measured irradiance. $A(z^{-1})$, $B_1(z^{-1})$ and $B_2(z^{-1})$ are the respective polynomials.

Using part of the collected data, the model (5.2) was learned by the *arx* MATLAB function. Moreover, as explained before, the selected data to estimate this model was different from the data used to estimate the fuzzy model. The estimated model (5.2) was $A(z) = 1 - 0.3707z^{-1} - 0.2609z^{-2} - 0.2008z^{-3} - 0.1684z^{-4}$, $B_1(z) = 0.00126 -$

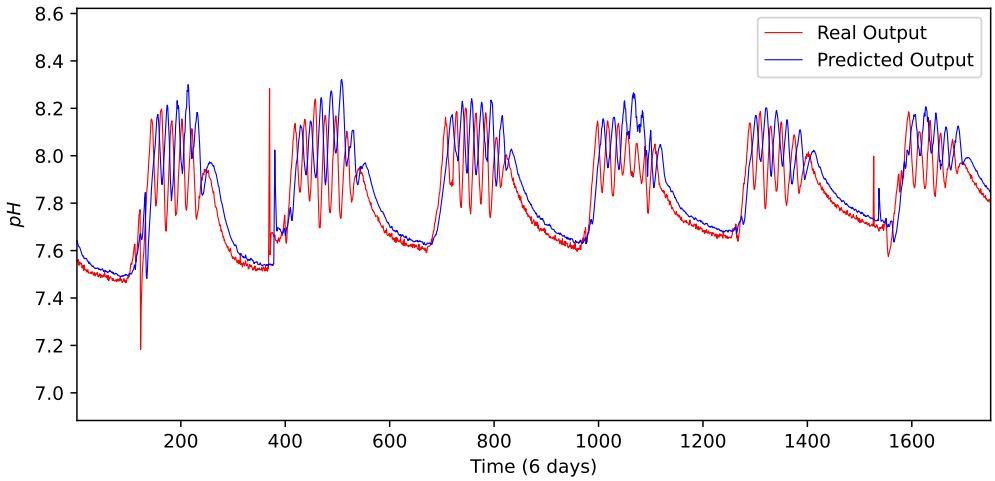


(a)

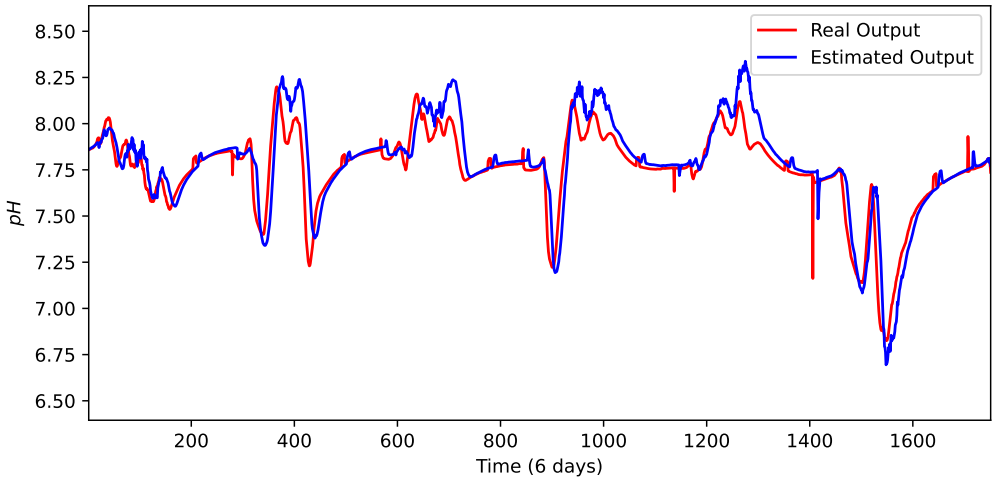


(b)

Figure 5.5: Results of the simulation model to test the controller, estimated and real outputs: (a) training results and (b) testing results.

$0.000909z^{-1} - 0.004927z^{-2}$ and $B_2(z) = 0.0001459$. The Mean Squared Error (MSE) of the learned model is 0.0259. In Figure 5.5 the estimated model behavior is presented and compared with the real output data, for training (Figure 5.5a) and testing (Figure 5.5b) scenarios.

## 5.5 Simulation Control Results

In this section, the obtained results from testing the developed AFGPC method are presented. To test the implemented approach, the MATLAB Simulink tool was used, and all the following results are the outcome of simulations performed on the developed MATLAB blocks and functions. The testing phase was divided into two parts. Firstly, the developed controller was tested with fixed model parameters, which means that the RLS-ADF algorithm was "turned off". In the second testing phase, the RLS-ADF algorithm was "turned on", to test the adaptive parameters approach. These two testing

phases are presented in Subsections 5.5.1 and 5.5.2, respectively. Afterward, in Subsection 5.5.3, the two methods are compared and further analyzed.

The MPC technique implemented in this work was a Generalized Predictive Control (GPC) controller, as theoretically described in Subsection 3.1.1. This predictive controller design encompasses the definition of the prediction horizon ($N_p = N_2 - N_1$), the control horizon ($N_u$) and the weighting factor for control increments ($\lambda$). The prediction horizon determines the number of samples ahead that are considered in the control algorithm, the control horizon determines the number of calculated samples, and the control-weighting factor affects the control effort. For the control-weighting factor, larger values generate smaller control actions. Conversely smaller values are associated with a fast system response, because the controller minimization calculation between the output and the reference, tends to overlook the control action [38, 74].

The conducted tests, presented in this section involve the variation of the prediction horizon ($N_p$) and the lambda ($\lambda$) value. For the prediction horizon, the following values were considered: $N_p = 5$, $N_p = 10$, $N_p = 15$, and $N_p = 25$. For $\lambda$, the following values were considered: $\lambda = 0.08$, $\lambda = 0.8$, $\lambda = 1.8$, $\lambda = 8$, and $\lambda = 80$. In each presented test, a set of variations in the selected variables is considered. Nevertheless, certain variables maintain their values throughout all the presented tests. The fixed values were the following: the control horizon $N_u = 1$, the time delay $d = 3$, the number of clusters $N = 4$, the polynomials $a_i(z^{-1})$, $b_i(z^{-1})$ and $d_i(z^{-1})$ order $n_a = 4$, $n_b = 3$ and $n_d = 1$, respectively, the initial values of $\varphi_i(0) = 0.1$, $\tau_i(0) = 0.01$, $\nu_i(0) = 0.1$, and $\mathbf{C}_i(0) = I_8 \times 10^5$. The reference value was set to 8. Moreover, each combination of variables considered in the following subsections encompasses two simulation times, one corresponding to 51 days and one to 127 days. These two distinct simulation times were chosen to perform an error analysis based on distinct input values, with the selected error metric being the Mean Squared Error (MSE). The 51-day simulation comprises moderate irradiance values, whereas the 127-day simulation includes the concatenation of the 51 days of moderate irradiance values plus 76 days of elevated irradiance values. These two simulation time scenarios were constructed to test the distinct behavior of the developed system for both situations, since the controller behavior is prone to be more unstable with higher irradiance values.

The following results are presented in tables and figures. The tables present the MSE error for each simulation test, in order to provide a notion of the overall system performance. On the other hand, the figures provide a visual notion of the system performance. Each figure comprises two sub-figures, illustrating parts of the results for each simulation time (51 days and 127 days), corresponding to moderate and high irradiance values.

### 5.5.1 Fixed Model Parameters Results

In this subsection, the fixed parameters approach results are presented. The tests were divided into five scenarios, according to $N_p$ and $\lambda$ values variation. In each scenario, the $\lambda$ value was fixed, whereas the predictive horizon was varied. The results for each scenario are as follows:

1. Scenario with $\lambda$ fixed at 0.08 (Figure 5.6, Table 5.1).
2. Scenario with $\lambda$ fixed at 0.8 (Figure 5.7, Table 5.2).
3. Scenario with $\lambda$ fixed at 1.8 (Figure 5.8, Table 5.3).
4. Scenario with $\lambda$ fixed at 8 (Figure 5.9, Table 5.4).

Table 5.1: MSE error for $\lambda$ equal to 0.08 with fixed parameters.

| **Time** | $N_p = 5$ | $N_p = 10$ | $N_p = 15$ | $N_p = 25$ |
|---|---|---|---|---|
| 51 days | 0.5560 | 0.4680 | 0.4310 | 0.4856 |
| 127 days | 135.5790 | 176.5540 | 169.6480 | 170.3899 |

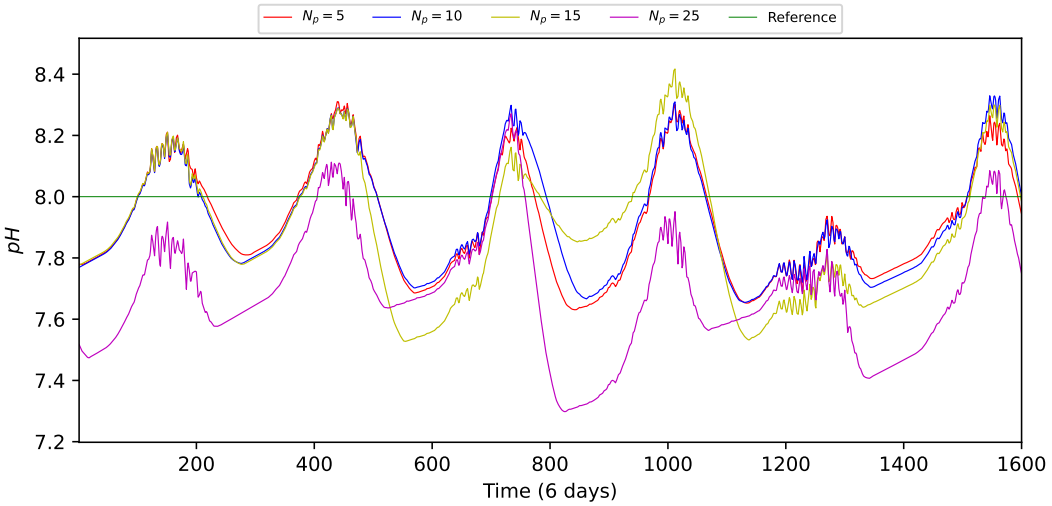


(a)

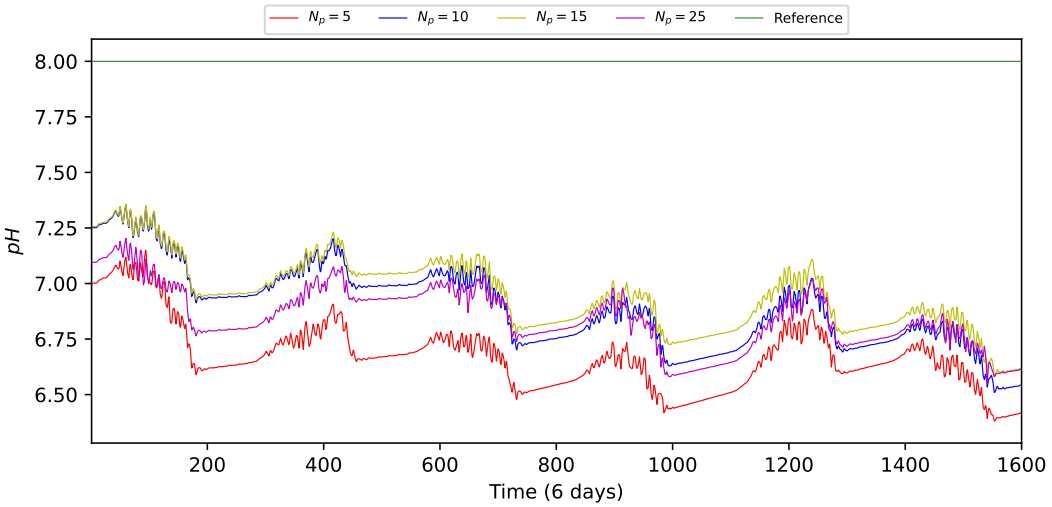


(b)

Figure 5.6: Fixed parameters results with $\lambda$ equal to 0.08, for (a) scenario with moderate irradiance values (more stable) and (b) scenario with high irradiance values (less stable).

5. Scenario with $\lambda$ fixed at 80 (Figure 5.10, Table 5.5).

Observing the first scenario results (Figure 5.6 and Table 5.1), with $\lambda$ assigned to 0.08, the general system performance is unsatisfactory. For the results with moderate irradiance (51 days) the MSE error is smaller when compared to the results with high irradiance values (127 days). This is also visible in both figures related to this scenario. In Figure 5.6a, representing the system behavior with moderate irradiance values, the pH

Table 5.2: MSE error for $\lambda$ equal to 0.8 with fixed parameters.

| **Time** | $N_p = 5$ | $N_p = 10$ | $N_p = 15$ | $N_p = 25$ |
|---|---|---|---|---|
| 51 days | 0.1032 | 0.1266 | 0.1280 | 0.1285 |
| 127 days | 0.1641 | 0.2004 | 0.2257 | 0.2273 |

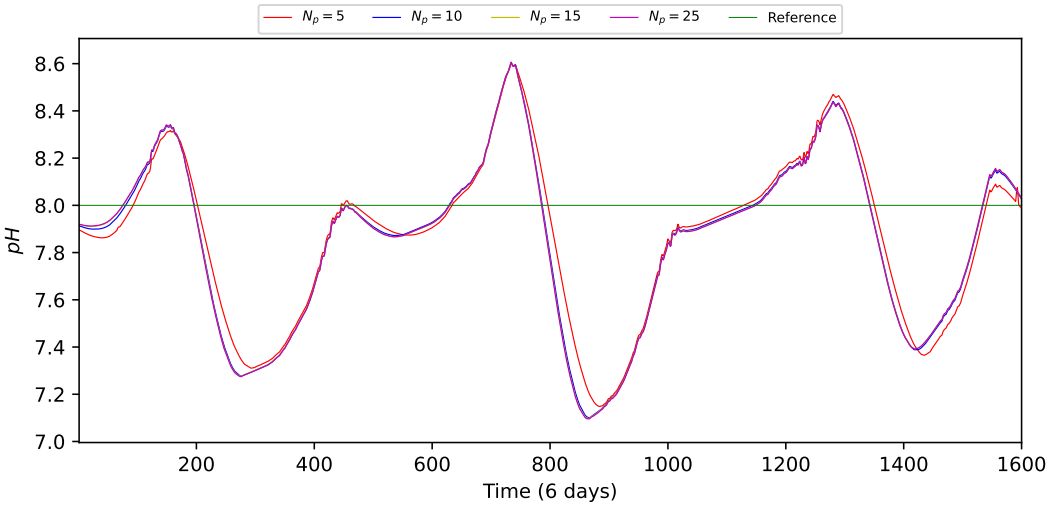


(a)

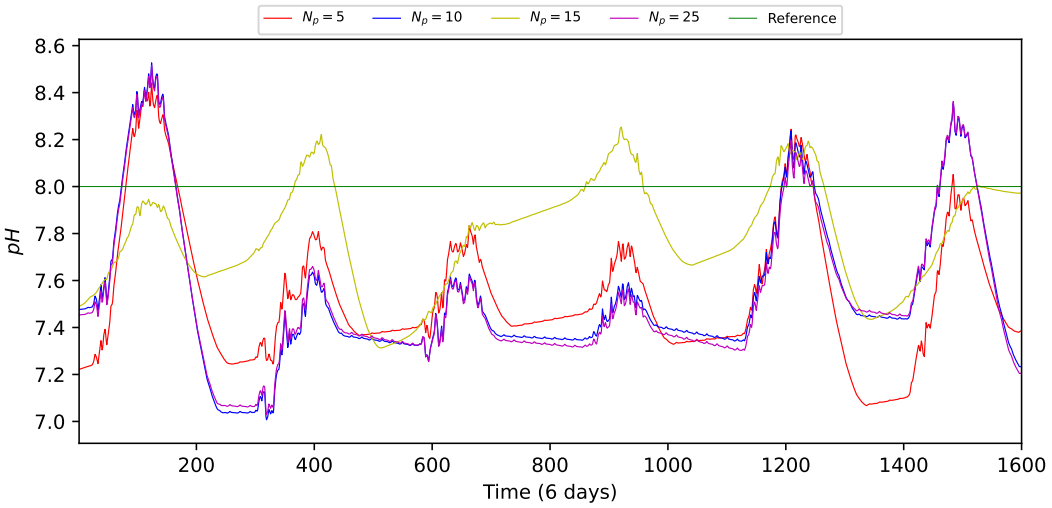


(b)

Figure 5.7: Fixed parameters results with $\lambda$ equal to 0.8, for (a) scenario with moderate irradiance values (more stable) and (b) scenario with high irradiance values (less stable).

values are maintained closer to the reference value than in Figure 5.6b, representing the system behavior with high irradiance values. This difference between both simulations means that there is an overall better performance with moderate irradiance. However, none of the results is satisfactory.

Observing the results from the second scenario (Figure 5.7 and Table 5.2), where the $\lambda$ value is set to 0.8, there is a noticeable overall improvement in the system's performance compared to the previous scenario. This improvement is evident from the significantly

Table 5.3: MSE error for $\lambda$ equal to 1.8 with fixed parameters.

| **Time** | $N_p = 5$ | $N_p = 10$ | $N_p = 15$ | $N_p = 25$ |
|---|---|---|---|---|
| 51 days | 0.0759 | 0.1085 | 0.1070 | 0.1120 |
| 127 days | 0.1870 | 0.1720 | 0.1760 | 0.1730 |

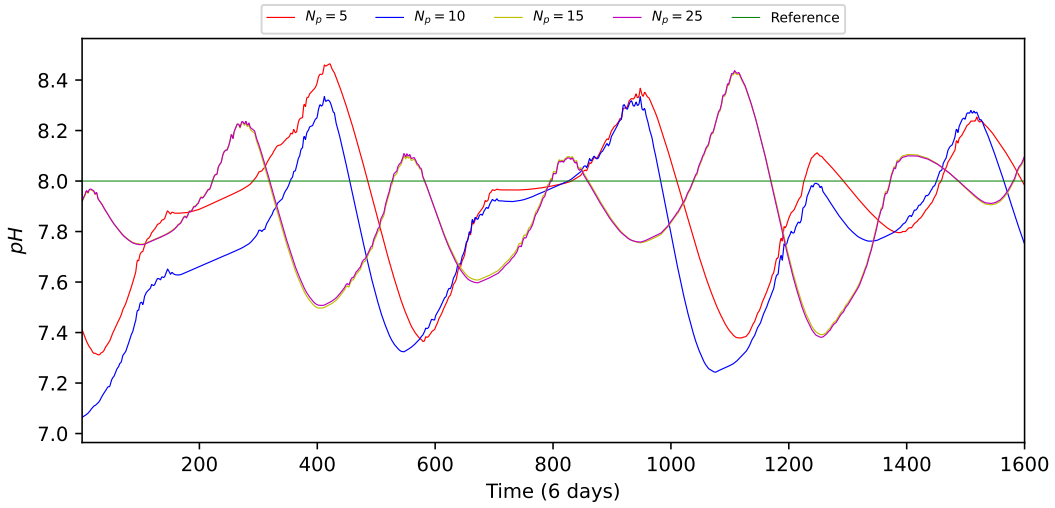


(a)

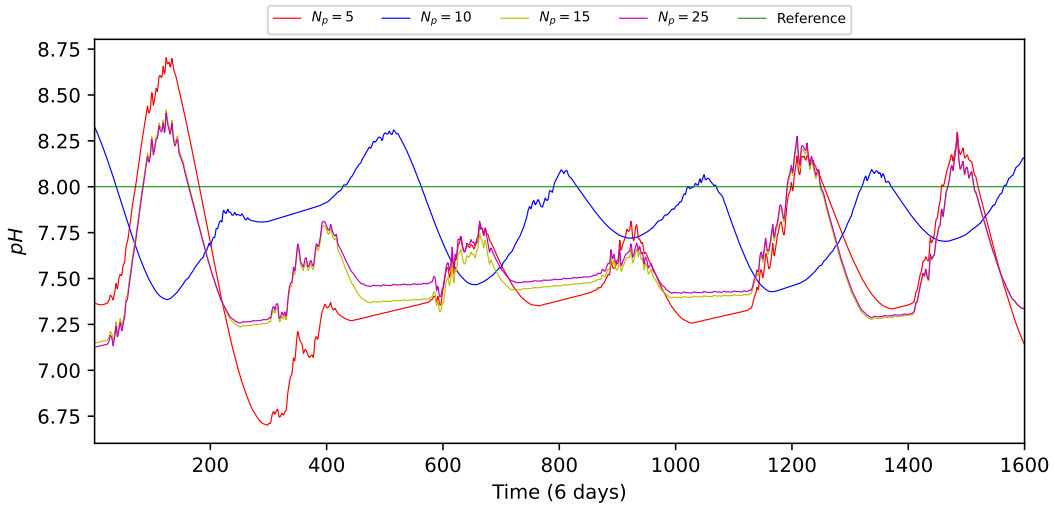


(b)

Figure 5.8: Fixed parameters results with $\lambda$ equal to 1.8, for (a) scenario with moderate irradiance values (more stable) and (b) scenario with high irradiance values (less stable).

smaller MSE error values observed for both moderate irradiance conditions (51 days) and high irradiance conditions (127 days). Between these two simulations, it is also possible to identify an error increase from the 51-day values to the 127-day values.

Observing the results from the third scenario (Figure 5.8 and Table 5.3), where the $\lambda$ is fixed at 1.8, a slight improvement in the system's performance compared to the second scenario is identified. These simulations present better results in terms of MSE error values, except for the $N_p = 5$ values in the 127-day simulation. Additionally, there is a

Table 5.4: MSE error for $\lambda$ equal to 8 with fixed parameters.

| **Time** | $N_p = 5$ | $N_p = 10$ | $N_p = 15$ | $N_p = 25$ |
|---|---|---|---|---|
| 51 days | 0.1529 | 0.0795 | 0.1258 | 0.0938 |
| 127 days | 0.1628 | 0.1828 | 0.2121 | 0.2700 |

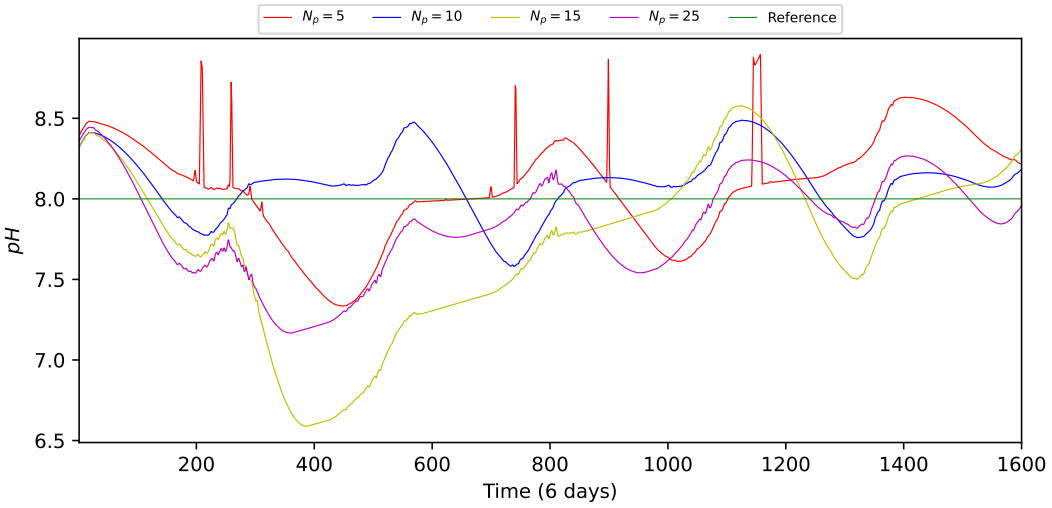


(a)

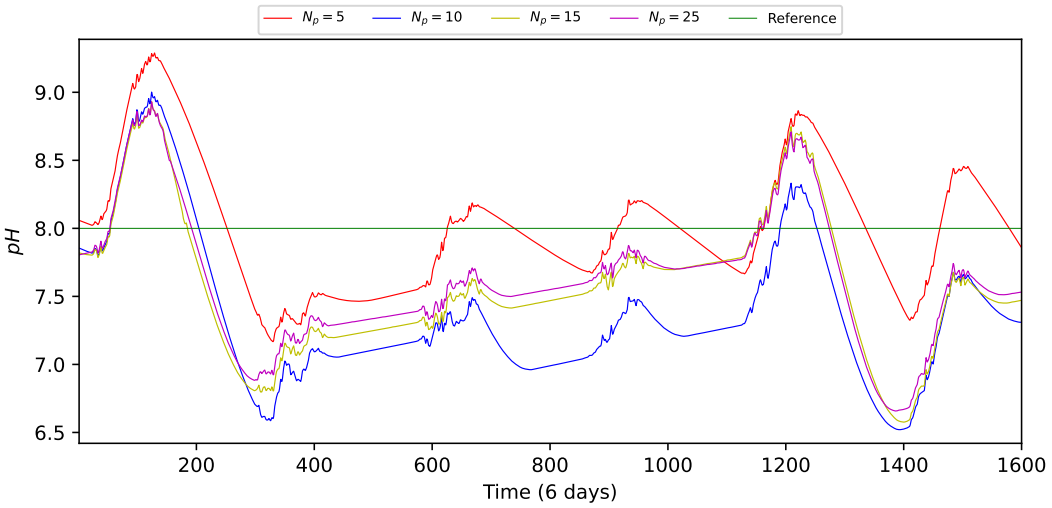


(b)

Figure 5.9: Fixed parameters results with $\lambda$ equal to 8, for (a) a scenario with moderate irradiance values (more stable) and (b) a scenario with high irradiance values (less stable).

visible degradation in error when testing with higher irradiance values.

Observing the results from the fourth scenario (Figure 5.9 and Table 5.4), where the $\lambda$ is fixed at 8, a slight general deterioration in the overall system performance is identified compared to the third scenario. From the MSE error values it is observed the expected increase between moderate irradiance and high irradiance results.

Lastly, upon observing the results from the fifth scenario (Figure 5.10 and Table 5.5) with $\lambda$ fixed at 80, a noticeable deterioration in the overall system performance is evident

Table 5.5: MSE error for $\lambda$ equal to 80 with fixed parameters.

| **Time** | $N_p = 5$ | $N_p = 10$ | $N_p = 15$ | $N_p = 25$ |
|---|---|---|---|---|
| 51 days | 0.6848 | 0.4665 | 0.5167 | 0.4478 |
| 127 days | 0.9656 | 0.7706 | 3.7259 | 3.1485 |

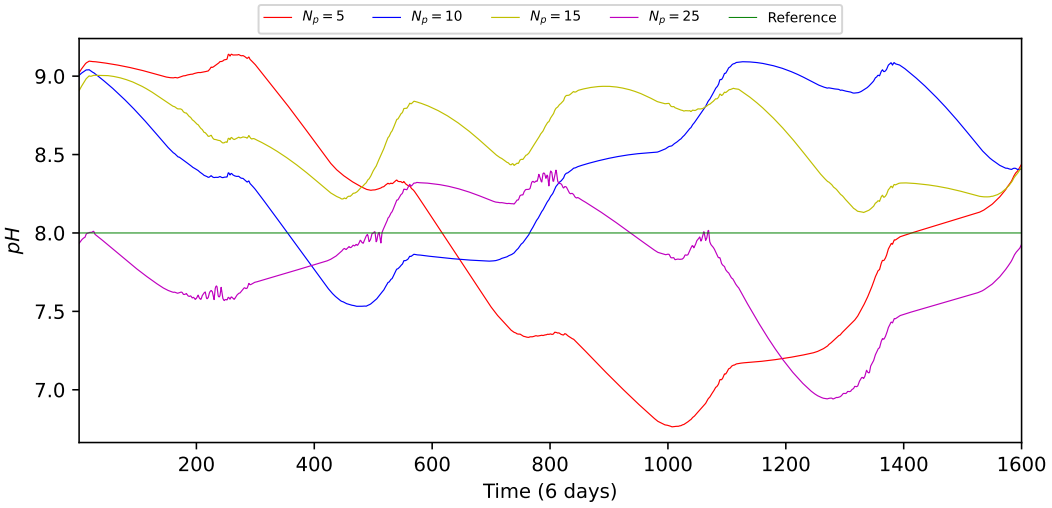


(a)

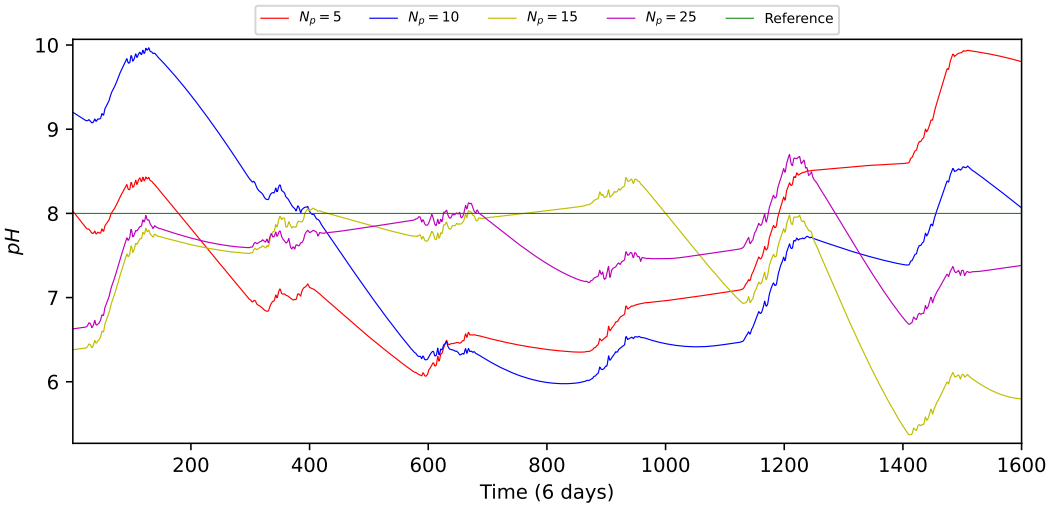


(b)

Figure 5.10: Fixed parameters results with $\lambda$ equal to 80, for (a) a scenario with moderate irradiance values (more stable) and (b) a scenario with high irradiance values (less stable).

compared to the second, third, and fourth scenarios. Additionally, worse results are also visible for the 127-day high irradiance simulation.

Analyzing the fixed parameters results presented, several consistencies can be identified. Firstly, there is a general degradation observed from the 51-day simulations to the 127-day results. Indicating a system performance decline with high irradiance values. Secondly, when comparing the results for each $\lambda$ variation, the second, third, and fourth scenarios consistently exhibit more favorable outcomes. This is evidenced by lower MSE error

Table 5.6: MSE error for $\lambda$ equal to 0.8 with adaptive parameters.

| **Time** | $N_p = 10$ | $N_p = 15$ |
|---|---|---|
| 51 days | 0.1207 | 0.1275 |
| 127 days | 0.1947 | 0.2177 |

Table 5.7: MSE error for $\lambda$ equal to 1.8 with adaptive parameters.

| **Time** | $N_p = 10$ | $N_p = 15$ |
|---|---|---|
| 51 days | 0.1081 | 0.1046 |
| 127 days | 0.1510 | 0.1533 |

values, particularly notable in the 127-day simulations. Additionally, upon analyzing the predictive horizon variations, a trend is observed where increasing the predictive horizon leads to an increase in MSE error. However, with a predictive horizon set to 5, the results tend to be inconsistent. Since the 51-day and the 127-day simulation, in some scenarios, present worse results than with higher predictive horizon values.

### 5.5.2 Adaptive Parameters Results

In this subsection, the adaptive parameters approach results are presented. For this testing phase, the fixed parameters results were considered, when selecting the variables variations. Since there were three $\lambda$ values that allowed to achieve better results, the tests performed in this subsection are relative to those three $\lambda$ values. Regarding the variations in predictive horizon, only the two best values were tested, as they presented the most favorable results. Therefore, when testing the adaptive parameters performance only $\lambda = 0.8$, $\lambda = 1.8$ and $\lambda = 8$ were considered. For the predictive horizon variations, only $N_p = 10$ and $N_p = 15$ were considered. Moreover, the calculus of adaptive parameters involves other variables. For this reason, in the following tests, the variable $\rho$ was also adjusted. This variable determines the rate at which previous data is forgotten in the iterative estimation process. Adjusting this parameter allows the algorithm to update its learning speed and responsiveness to the system dynamics. Typically, higher $\rho$ values indicate a lower forgetting rate, resulting in a stronger influence of past estimated data. Conversely, lower $\rho$ values usually imply a faster forgetting process, giving more weight to more recent data. However, the influence of this parameter can vary depending on the implementation and context [75]. Therefore, the developed tests involved variations in the prediction horizon ($N_p$), lambda ($\lambda$) value and $\rho$ value.

The results for the adaptive parameters with $\lambda$ fixed at 0.8 are presented in Figure 5.11 and Table 5.6. These outcomes were achieved with a $\rho$ value adjusted to 0.05. Comparing these results with those of the second scenario in the fixed parameters tests, we observe smaller MSE error values. Also corroborated by the figures results. Additionally, an increase in MSE is observed from the 51-day simulation to the 127-day simulation in these results.

The outcomes for the adaptive parameters with lambda set at 1.8 are presented in Figure 5.12 and Table 5.7. These results, obtained with a $\rho$ value of 0.9, show significantly reduced MSE error values compared to the third scenario in the fixed parameters tests. Additionally, an increase in MSE is observed between the 51-day simulation and the

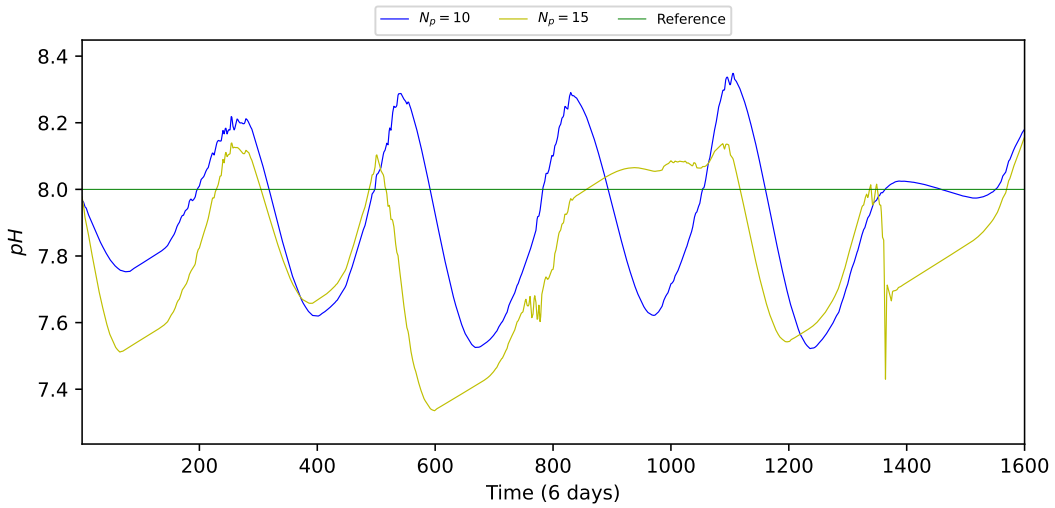


(a)

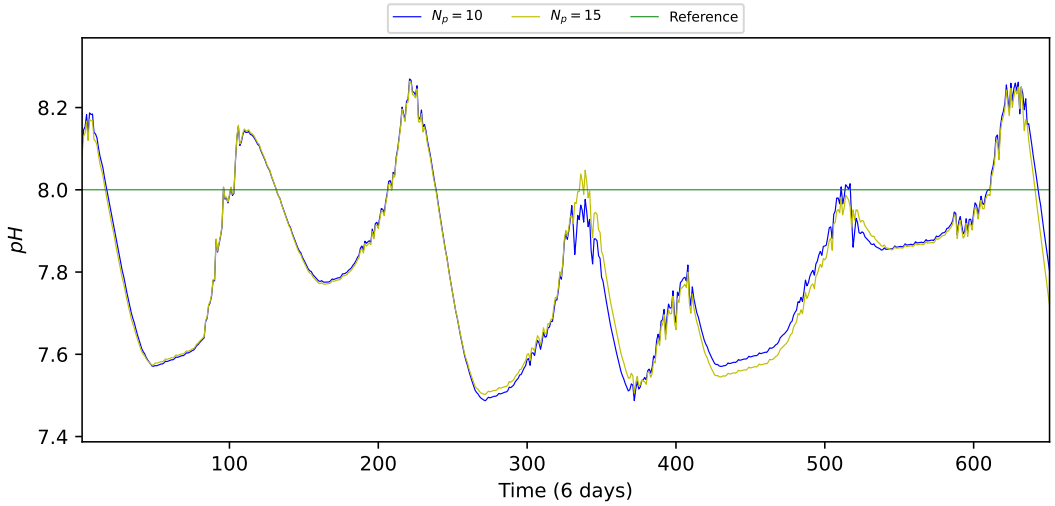


(b)

Figure 5.11: Adaptive parameters results with $\lambda$ equal to 0.8, for (a) a scenario with moderate irradiance values and (b) a scenario with high irradiance values.

127-day simulation values.

In Figure 5.13 and Table 5.8, the results for the adaptive parameters with $\lambda$ fixed at 8 are presented. For these tests, the $\rho$ value was adjusted to 0.07. Comparing these outcomes with those of the fourth scenario in the fixed parameters tests, the MSE error values are smaller. Nevertheless, its improvement is not between the prediction horizon variation. Additionally, it is once more observed an increase in MSE between the 51-day simulation and the 127-day simulation values.

To select the most appropriate combination of variables, the primary factor to explore is the MSE error values, particularly those associated with the 127-day simulation. This simulation encompasses both moderate and high irradiance values, offering insight into the system's behavior across a broader input spectrum. Nevertheless, it is also important to contemplate a small error in the 51-day simulation.

Analyzing the adaptive parameters results, three tests stand out for their favorable

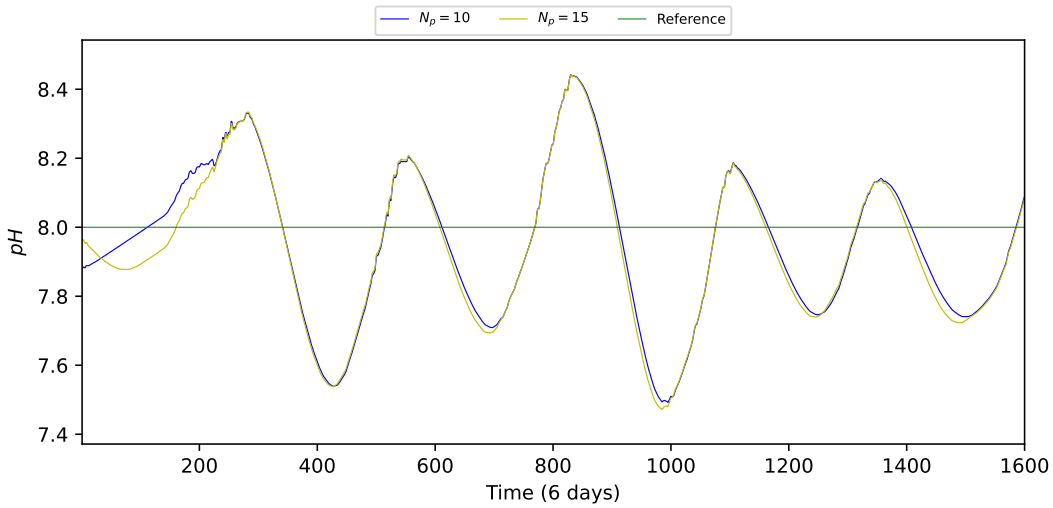


(a)

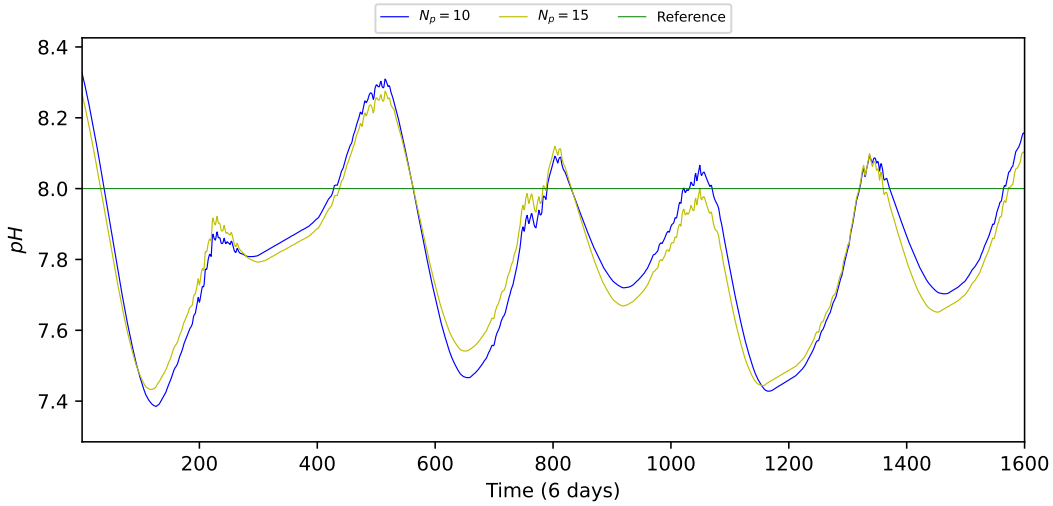


(b)

Figure 5.12: Adaptive parameters results with $\lambda$ equal to 1.8, for (a) a scenario with moderate irradiance values and (b) a scenario with high irradiance values.

outcomes. These include the results with $\lambda$ fixed to 1.8 and the test with $\lambda$ equal to 8 and $N_p = 10$. Considering these three tests and their proximate results, it is relevant to further examine the influence of $\lambda$ on the system. A noticeable difference is observed in the carbon dioxide valve aperture curve between the approach with $\lambda$ equal to 1.8 and $\lambda$ equal to 8, as illustrated in Appendix B. With a higher $\lambda$ value, the carbon dioxide valve aperture range is considerably smaller than with a smaller $\lambda$ value. Therefore, a system with $\lambda$ equal to 1.8 expresses a more suitable behavior for a broader range of situations, as it allows for a more ample and adequate response to abrupt input variations.

Moreover, comparing the results between the 51-day simulation and the 127-day simulation, with $\lambda$ set to 8 and $N_p$ equal to 10, a high degradation is observed from the 51-day results to the 127-day results. This indicates that with these parameters combination, the system reveals a greater difficulty controlling the pH levels with higher irradiance inputs than with lower ones.

Table 5.8: MSE error for $\lambda$ equal to 8 with adaptive parameters.

| **Time** | $N_p = 10$ | $N_p = 15$ |
|---|---|---|
| 51 days | 0.0767 | 0.1226 |
| 127 days | 0.1522 | 0.1892 |

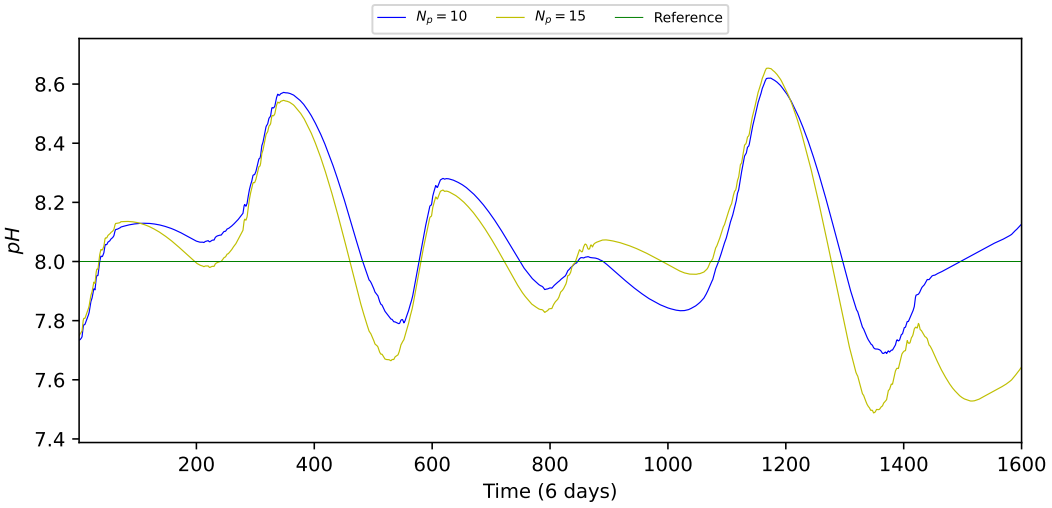


(a)

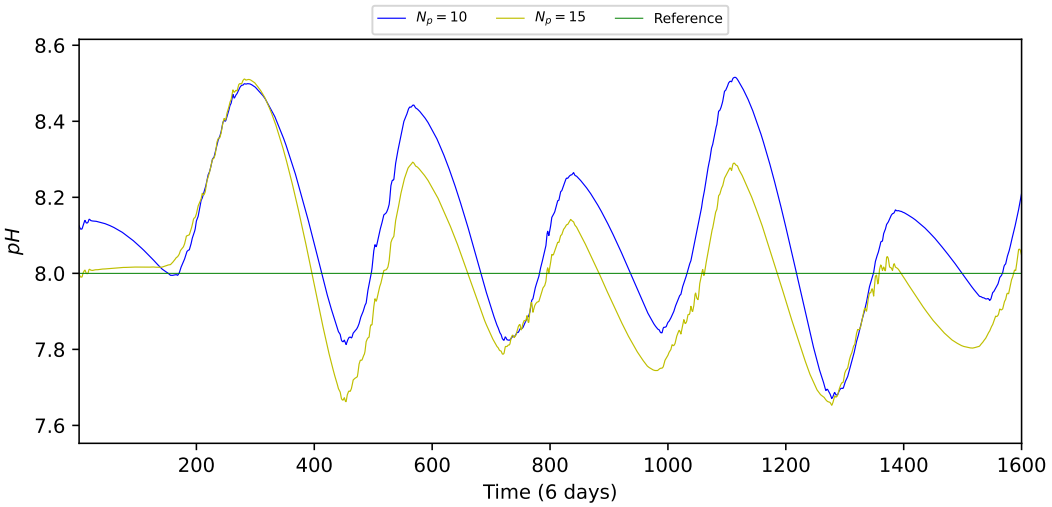


(b)

Figure 5.13: Adaptive parameters results with $\lambda$ equal to 8, for (a) a scenario with moderate irradiance values and (b) a scenario with high irradiance values.

Additionally, among the tests with lambda set to 1.8, the results with $N_p$ equal to 10 demonstrate slightly better performance, especially in the 127-day simulation.

In conclusion, the combination of variables that exhibits the most beneficial behavior for controlling pH levels in a photobioreactor is the test with $\lambda = 1.8$ and $N_p = 10$.

Contemplating the best result from the earlier three tests with adaptive parameters, a further investigation was conducted regarding the $\lambda$ variation. From this, it was observed that by slightly increasing it, there was an improvement in the 127-day simulation with a

Table 5.9: MSE error for $\lambda$ equal to 2 with adaptive parameters.

| **Time** | $N_p = 10$ |
|---|---|
| 51 days | 0.1040 |
| 127 days | 0.1411 |

$\lambda$ set to 2 and a $\rho$ value set to 0.45. In Table 5.9, the results obtained from this test are presented.

### 5.5.3 Results Analysis

After individually analyzing the fixed and the adaptive parameters results, these two approaches are discussed in this subsection.

In Subsection 5.5.1, the fixed parameters approach was studied, and it was established that the best scenarios corresponded to the tests with $\lambda = 0.8$, $\lambda = 1.8$ and $\lambda = 8$. This conclusion was drawn based on the MSE error values, particularly those obtained from the 127-day simulations. The results for $\lambda = 0.08$ showed MSE error values ranging from 135.5790 to 176.5590, indicating the worst outcomes. On the other hand, the results for $\lambda = 80$ showed MSE error values ranging from 0.7706 to 3.1485, demonstrating a significant degradation compared to the tests with $\lambda = 0.8$, $\lambda = 1.8$, and $\lambda = 8$. Conversely, the three best scenarios, with $\lambda = 0.8$, $\lambda = 1.8$, and $\lambda = 8$, presented MSE error results ranging from 0.1628 to 0.2700, indicating a smaller interval and lower values. From these three scenarios, analyzing the prediction horizon variation, the results from $N_p = 10$, $N_p = 15$ and $N_p = 25$ present a growing tendency in their MSE error values, with $N_p = 25$ presenting overall worse results. As for the results from $N_p = 5$, demonstrated inconsistent behavior, presenting worse results than some of the tests with a higher prediction horizon, which deviates from the observed trend. This behavior occur due to the small prediction horizon, that affects the control calculus and its resulting variation. Therefore, as for the predictive horizon, the best results were obtained with $N_p = 10$ and $N_p = 15$.

In Subsection 5.5.2, the adaptive parameters approach was studied, taking into consideration the results obtained from the fixed parameters approach scenarios. The adaptive parameters tests were performed considering a variation of $\lambda$ among 0.8, 1.8 and 8, and a variation of $N_p$ among 10 and 15. From these tests, the best results were obtained with the combination of $\lambda = 1.8$ with $N_p = 10$, $\lambda = 1.8$ with $N_p = 15$, and $\lambda = 8$ with $N_p = 10$, exhibiting MSE error results ranging from 0.1515 to 0.1533. Upon comparing this MSE error value interval with those from the best three scenarios of the fixed parameters approach, it is evident that the range of MSE errors were noticeably smaller in the tests with adaptive parameters. These results can be explained due to the adaptive parameters positive performance, responding to the system variations. Additionally, one further test was conducted with the adaptive parameters, focusing on the $\lambda$ variable variation starting from the test with $\lambda = 1.8$ and $N_p = 10$. In this test were performed small variations in the $\lambda$ value, and the most favorable outcomes were obtained with $\lambda = 2$, $N_p = 10$ and a further adjustment of $\rho$ to 0.45. From this test, the 51-day simulation MSE error value was similar to previous test with $\lambda = 1.8$ and $N_p = 10$; Indicating that, when responding to moderate irradiance values its response is similar. However, in the 127-day simulation, there was a decrease in the Mean Squared Error (MSE) error, indicating a general improvement in its response to high irradiance values. Furthermore, in each scenario, an adjustment

was made to the variable $\rho$. In the tests where $\lambda$ was set to 0.8 and 8, this variable was adjusted to 0.05 and 0.07, respectively. And, in the tests with $\lambda$ set to 1.8 and 2, it was adjusted to 0.9 and 0.45, respectively. This behavior indicates distinct optimal rates for parameter adaptation, dependent on the controller's performance.

From the MSE error values presented in Section 5.5 tables, it is possible to retrieve information regarding the overall performance of the system in each test scenario. However, the figures presented in this section provide insight into the output behavior of each scenario. Upon observing each figure in this section relative to the simulation results, it becomes evident that there is less oscillation from the reference value in the adaptive parameters tests.

In conclusion, balancing the results and respective analysis of both fixed and adaptive parameters approaches, it is concluded that the adaptive parameters approach permitted to obtain overall better results. This directly results from the parameters iterative update according to the system's conditions. Consequently, the adaptive parameters approach is capable of controlling the pH levels, of a photobioreactor producing microalgae, with an overall better performance than the fixed parameters approach.

# Chapter 6

# Conclusions and Future Work

## Contents



## 6.1 Conclusions

Microalgae are microscopic organisms that habit aquatic environments, when these provide proper conditions. Essentially, these conditions must include light exposure, nutrients like carbon and phosphorus, an adequate temperature and an appropriate acidity level. When the environment provides suitable conditions, these organisms have the potential to thrive. For centuries humans have used algae as a food source, mainly motivated by food shortage periods. However, it was only in more recent years that these organisms started being cultivated in special infrastructures; Which allowed to increase their production and their industry applications. Microalgae have a high biotechnological potential and have been used in numerous industries, such as pharmaceutical, animal nutrition and human supplements, cosmetics production, wastewater treatment processes, and as a new approach in clean energy sources, as a biofuel. For this reason, there has been some recent investment in photobioreactors, in order to reduce production costs and increase production rates. The developed work falls into this area, since the objective is to control the pH levels of a tubular photobioreactor producing microalgae. For this effect, the selected variable to manipulate was the carbon dioxide valve aperture. Since this variable directly influences the culture medium acidity, contra-balancing the microalgae photosynthetic process effect.

Adaptive fuzzy predictive control has been used in industrial processes, mainly in approaches that require accurate process models. This method is a control methodology that combines the principles of fuzzy logic and predictive control to regulate the behavior of dynamic systems. In this approach, a fuzzy system is used to represent the system dynamics, and predictive control techniques are employed to anticipate future system behavior and generate control actions accordingly. Their entanglement permits an iterative update of the controller parameters, which allows the controller to adapt its behavior throughout its operation. This type of system has been successfully applied in multiple fields, such as process control, automotive systems, and renewable energy systems. The objective of this work is to control the pH levels of a microalgae culture, that entails

biological reactions to light exposure and to carbon dioxide gas injections. For this characteristic nonlinear system, the selected control method was an Adaptive Fuzzy Generalized Predictive Control.

This work was initiated with the study of microalgae, from their compositions to their production process and main requirements, addressed in Chapters 1 and 2. Afterward, it was studied the state-of-the-art processes of the production of this organism, detailed in chapter 2. These first two chapters were particularly important when considering this work preparation and the system behavior understanding. Then, in Chapter 3 the main concepts around the selected control approach were studied. This chapter was divided into two main parts: predictive control notions and fuzzy systems theory. In Chapter 4, some crucial details about the implementation of the selected control method were addressed; Focused on the developed fuzzy model identification process, including its algorithms description, and in the controller's adjustment process. In Chapter 5, the results of the developed control approach were presented and analyzed; Where, the developed approach is also compared to its version without adaptive parameters. Overall, this work describes the developed process to implement an Adaptive Fuzzy Generalized Predictive Control, to control a photobioreactor producing microalgae plants.

Two control alternatives were explored: one with fixed parameters and the other with adaptive parameters, which is the approach proposed in this work. Both methods were tested under similar conditions, encompassing moderate and high irradiance values. The tests were conducted using the MATLAB simulator, utilizing the constructed blocks described in this document, as illustrated in Figure 4.1. To evaluate the fixed and adaptive parameters methods, the predictive horizon $N_p$, the $\lambda$ value, and the $\rho$ value were studied and adjusted. The $\lambda$ value adjusts the control action, the predictive horizon influences the samples considered in the control calculation, and $\rho$ influences the parameter adaptation. Each variable was studied considering a relevant interval, based on literature and similar works. The resulting combination of variables was tested for both methods and further compared. The presented results encompass the MSE error value associated with each simulation, and a corresponding graph to provide a visual notion of the system behavior. From the presented results and respective analysis, it was concluded that the fixed parameters approach permitted to achieve satisfactory outcomes in some scenarios; Maintaining the system's $pH$ value within a small interval of the reference value. Given that this approach obtained favorable results, it allowed for the conclusion that the consequent parameters estimated with the LSM were suitable. This is essential for the adaptive parameters approach, as without a suitable parameter base, the adaptation would not achieve satisfactory results. As for the adaptive parameters results, when comparing each scenario to the corresponding fixed parameters scenario, these exhibited less variation from the reference value; Which leads to the conclusion that an iterative parameters adaptation throughout the system operation is beneficial.

Furthermore, in each test analysis, the value of $\rho$ was also adjusted. It was observed that this variable had a distinct optimal value in each test, indicating that the parameter adjustment rate is crucial in each scenario and varies within each control framework. It is still possible to observe differences in the results regarding the amplitude of the carbon dioxide valve aperture, which is directly associated with the value of $\lambda$. With a lower value for $\lambda$, the variations are larger and more abrupt, while with a higher value of $\lambda$, the variation is smoother and smaller. Therefore, it is considered important to select a middle-ground scenario to avoid a system that responds too slowly or exhibits overly exaggerated responses.

Based on the presented results and respective analysis, it can be concluded that while the fixed parameters approach permitted some satisfactory results, the adaptive version achieved superior outcomes. Thus, the implemented Adaptive Fuzzy Generalized Predictive Control demonstrated the ability to effectively control the pH levels of a tubular photobioreactor, consistently maintaining its value within a small interval from the set reference.

## 6.2 Future Work

In terms of future developments, related to the implemented controller, some steps could be considered. Firstly, a practical testing of the controller in a real photobioreactor, aiming to empirically validate its functionality, could be considered. During this experimental stage, the system's performance should be rigorously evaluated under multiple conditions and testing scenarios, providing further insights into its adaptability, robustness, and overall effectiveness. Secondly, a study regarding the influence of the carbon dioxide valve aperture percentage on the operational cost of the photobioreactor could be essential. This analysis aim would be to optimize the financial implications, by examining the cost dynamics associated with the manipulated variable. Moreover, a strategic research involving energy monitoring and optimization could also be studied. This addition could further enhance the efficiency and sustainability of the system. In essence, the future trajectory of this work could involve a real-world experimentation to validate the controller's performance, a study focused on the financial aspects related to the manipulated variable, and the incorporation of energy monitoring and optimization.

# References


[1] Modestus O. Okwu et al. "Emerging Technologies of Industry 4.0: Challenges and Opportunities". In: *2022 International Conference on Artificial Intelligence, Big Data, Computing and Data Communication Systems (icABCD)*. 2022, pp. 1–13. DOI: 10.1109/icABCD54961.2022.9856002.

[2] Sarah El Hamdi, Abdellah Abouabdellah, and Mustapha Oudani. "Industry 4.0: Fundamentals and Main Challenges". In: *2019 International Colloquium on Logistics and Supply Chain Management (LOGISTIQUA)*. 2019, pp. 1–5. DOI: 10.1109/LOGISTIQUA.2019.8907280.

[3] Manuel Gonçalves et al. "Real-Time Event-Driven Learning in Highly Volatile Systems: A Case for Embedded Machine Learning for SCADA Systems". In: *IEEE Access* 10 (2022), pp. 50794–50806. DOI: 10.1109/ACCESS.2022.3173376.

[4] Pauline Spolaore et al. "Commercial applications of microalgae". In: *Journal of Bioscience and Bioengineering* 101.2 (2006), pp. 87–96. ISSN: 1389-1723. DOI: 10.1263/jbb.101.87.

[5] Worasaung Klinthong. "A Review: Microalgae and Their Applications in CO2 Capture and Renewable Energy". In: *Aerosol and Air Quality Research* 15 (Jan. 2015). DOI: 10.4209/aaqr.2014.11.0299.

[6] Yusuf Chisti. "Biodiesel from microalgae". In: *Biotechnology Advances* 25.3 (2007), pp. 294–306. ISSN: 0734-9750. DOI: 10.1016/j.biotechadv.2007.02.001.

[7] D.H. Meadows et al. *The Limits to Growth*. Universe Books, New York, 1972.

[8] Patrick Moriarty and Damon Honnery. "Earth's Resources Are Finite". In: *Rise and Fall of the Carbon Civilisation*. Springer, London, Jan. 2011. Chap. 3. ISBN: 978-1-84996-482-1. DOI: 10.1007/978-1-84996-483-8_3.

[9] Ali Maghzian, Alireza Aslani, and Rahim Zahedi. "Review on the direct air CO2 capture by microalgae: Bibliographic mapping". In: *Energy Reports* 8 (2022), pp. 3337–3349. ISSN: 2352-4847. DOI: 10.1016/j.egyr.2022.02.125.

[10] Priti Yewale et al. "Studies on Biosmotrap: A multipurpose biological air purifier to minimize indoor and outdoor air pollution". In: *Journal of Cleaner Production* 357 (2022), p. 132001. ISSN: 0959-6526. DOI: 10.1016/j.jclepro.2022.132001.

[11] F.G. Acién et al. "1 - Photobioreactors for the production of microalgae". In: *Microalgae-Based Biofuels and Bioproducts*. Ed. by Cristina Gonzalez-Fernandez and Raúl Muñoz. Woodhead Publishing Series in Energy. Woodhead Publishing, 2017, pp. 1–44. ISBN: 978-0-08-101023-5. DOI: 10.1016/B978-0-08-101023-5.00001-7.

[12] F.G. Acién et al. "Production cost of a real microalgae production plant and strategies to reduce it". In: *Biotechnology Advances* 30.6 (2012). Special issue on ACB 2011, pp. 1344–1353. ISSN: 0734-9750. DOI: 10.1016/j.biotechadv.2012.02.005.

[13] Michael A. Borowitzka. "Commercial production of microalgae: ponds, tanks, tubes and fermenters". In: *Journal of Biotechnology* 70.1 (1999). Biotechnological Aspects of Marine Sponges, pp. 313–321. ISSN: 0168-1656. DOI: 10.1016/S0168-1656(99)00083-8.

[14] OSAMU TSUKADA, TAKAYOSHI KAWAHARA, and SHIGETOH MIYACHI. "MASS CULTURE OF CHLORELLA IN ASIAN COUNTRIES". In: *Biological Solar Energy Conversion*. Ed. by AKIRA MITSUI et al. Academic Press, 1977, pp. 363–365. ISBN: 978-0-12-500650-7. DOI: 10.1016/B978-0-12-500650-7.50032-5.

[15] Otto Pulz and Wolfgang Gross. "Valuable products from biotechnology of microalgae". In: Applied Microbiology and Biotechnology, 2004, pp. 635–648. DOI: 10.1007/s00253-004-1647-x.

[16] Clemens Posten. "Design principles of photo-bioreactors for cultivation of microalgae". In: Engineering in Life Sciences, July 2009, pp. 165–177. DOI: 10.1002/elsc.200900003.

[17] John Benemann. "Microalgae for Biofuels and Animal Feeds". In: *Energies* 6.11 (2013), pp. 5869–5886. ISSN: 1996-1073. DOI: 10.3390/en6115869.

[18] V Kumar and Shri Jain. "Plants and algae species: Promising renewable energy production source". In: *Emirates Journal of Food and Agriculture* 26 (Aug. 2014). DOI: 10.9755/ejfa.v26i8.18364.

[19] Tomáš Grivalský et al. "Development of thin-layer cascades for microalgae cultivation: milestones (review)". In: *Folia Microbiol* 64 (2019), pp. 603–614. DOI: 10.1007/s12223-019-00739-7.

[20] Peter Lindblad et al. "CyanoFactory, a European consortium to develop technologies needed to advance cyanobacteria as chassis for production of chemicals and fuels". In: *Algal Research* 41 (Apr. 2019), p. 101510. DOI: 10.1016/j.algal.2019.101510.

[21] Giuseppe Torzillo and Graziella Chini Zittelli. "Tubular Photobioreactors". In: Jan. 2015, pp. 187–212. ISBN: 978-3-319-20199-3. DOI: 10.1007/978-3-319-20200-6_5.

[22] M.R. Tredici and G.C. Zittelli. "Efficiency of Sunlight Utilization: Tubular versus Flat Photobioreactors". In: *Biotechnology and Bioengineering* (1998), pp. 187–197. DOI: 10.1002/(SICI)1097-0290(19980120)57:2<187::AID-BIT7>3.0.CO;2-J.

[23] T.A. Costache et al. "Comprehensive model of microalgae photosynthesis rate as a function of culture conditions in photobioreactors". In: *Applied Microbiology and Biotechnology* (2013), pp. 7627–7637. DOI: 10.1007/s00253-013-5035-2.

[24] Giuseppe Torzillo and Graziella Chini Zittelli. "Tubular Photobioreactors". In: *Algal Biorefineries: Volume 2: Products and Refinery Design*. Ed. by Aleš Prokop, Rakesh K. Bajpai, and Mark E. Zappi. Cham: Springer International Publishing, 2015, pp. 187–212. ISBN: 978-3-319-20200-6. DOI: 10.1007/978-3-319-20200-6_5.

[25] Jack Legrand, Arnaud Artu, and Jérémy Pruvost. "A review on photobioreactor design and modelling for microalgae production". In: *Reaction Chemistry & Engineering* 6 (Jan. 2021). DOI: 10.1039/D0RE00450B.

[26] I. Fernández et al. "Modelling and Control Issues of pH in Tubular Photobioreactors". In: *IFAC Proceedings Volumes* 43.6 (2010). 11th IFAC Symposium on Computer Applications in Biotechnology, pp. 186–191. ISSN: 1474-6670. DOI: 10.3182/20100707-3-BE-2012.0046.

[27] A. Pawlowski et al. "Event-based predictive control of pH in tubular photobioreactors". In: *Computers & Chemical Engineering* 65 (2014), pp. 28–39. ISSN: 0098-1354. DOI: 10.1016/j.compchemeng.2014.03.001.

[28] F.G. Shinskey. *Control of pH. In The Control Hndbook*. CRC-IEEE Press, 1996.

[29] C. Knospe. "PID control". In: *IEEE Control Systems Magazine* 26.1 (2006), pp. 30–31. DOI: 10.1109/MCS.2006.1580151.

[30] Luís Osório et al. "A comparison of adaptive PID methodologies controlling a DC motor with a varying load". In: *2013 IEEE 18th Conference on Emerging Technologies & Factory Automation (ETFA)*. 2013, pp. 1–6. DOI: 10.1109/ETFA.2013.6648093.

[31] Kiam Heong Ang, G. Chong, and Yun Li. "PID control system analysis, design, and technology". In: *IEEE Transactions on Control Systems Technology* 13.4 (2005), pp. 559–576. DOI: 10.1109/TCST.2005.847331.

[32] Mariana Titica et al. "Simultaneous control of pH and dissolved oxygen in closed photobioreactor". In: *2018 22nd International Conference on System Theory, Control and Computing (ICSTCC)*. 2018, pp. 372–378. DOI: 10.1109/ICSTCC.2018.8540689.

[33] Tiago Matias et al. "Adaptive identification and predictive control using an improved on-line sequential extreme learning machine". In: *IECON 2014 - 40th Annual Conference of the IEEE Industrial Electronics Society*. 2014, pp. 58–64. DOI: 10.1109/IECON.2014.7048477.

[34] M. Berenguel et al. "Model predictive control of pH in tubular photobioreactors". In: *Journal of Process Control* 14.4 (2004), pp. 377–387. ISSN: 0959-1524. DOI: 10.1016/j.jprocont.2003.07.001.

[35] Jérôme Mendes, António Craveiro, and Rui Araújo. "Iterative Design of a Mamdani Fuzzy Controller". In: *2018 13th APCA International Conference on Automatic Control and Soft Computing (CONTROLO)*. 2018, pp. 85–90. DOI: 10.1109/CONTROLO.2018.8516415.

[36] Jérôme Mendes, Francisco Souza, and Rui Araújo. "Online evolving fuzzy control design: An application to a CSTR plant". In: *2017 IEEE 15th International Conference on Industrial Informatics (INDIN)*. 2017, pp. 218–225. DOI: 10.1109/INDIN.2017.8104774.

[37] Laurentiu Luca et al. "Fuzzy Control of a Microalgae GrowMh Process in Photobioreactors". In: *2018 22nd International Conference on System Theory, Control and Computing (ICSTCC)*. 2018, pp. 480–485. DOI: 10.1109/ICSTCC.2018.8540698.

[38] E.F. Camacho and C. Bordons. *Model Predictive Control*. Advanced Textbooks in Control and Signal Processing. Springer London, 2004. ISBN: 9781852336943.

[39] J. Richalet et al. "Model predictive heuristic control: Applications to industrial processes". In: *Automatica* 14.5 (1978), pp. 413–428. ISSN: 0005-1098. DOI: 10.1016/0005-1098(78)90001-8.

[40] Cutler CR and Ramaker BL. "Dynamic matrix control - a computer control algorithm". In: *Joint Automatic Control Conference* (1980).

[41] Carlos E. Garcia and Manfred Morari. "Internal model control. A unifying review and some new results". In: *Industrial & Engineering Chemistry Process Design and Development* 21.2 (1982), pp. 308–323. DOI: 10.1021/i200017a016.

[42] Peter J. Campo and Manfred Morari. "$\infty$ -norm formulation of model predictive control problems". In: *1986 American Control Conference*. 1986, pp. 339–343. DOI: 10.23919/ACC.1986.4788961.

[43] Daniel L. Laughlin and Manfred Morari. "Smith Predictor Design for Robust Performance". In: *1987 American Control Conference*. 1987, pp. 637–642. DOI: 10.23919/ACC.1987.4789395.

[44] Peter J. Campo and Manfred Morari. "Robust Model Predictive Control". In: *1987 American Control Conference*. 1987, pp. 1021–1026. DOI: 10.23919/ACC.1987.4789462.

[45] A. Zheng and M. Morari. "Stability of model predictive control with mixed constraints". In: *IEEE Transactions on Automatic Control* 40.10 (1995), pp. 1818–1823. DOI: 10.1109/9.467664.

[46] Alberto Bemporad and Manfred Morari. "Robust model predictive control: A survey". In: *Robustness in identification and control*. Ed. by A. Garulli and A. Tesi. London: Springer London, 1999, pp. 207–226. ISBN: 978-1-84628-538-7.

[47] V. Peterka. "Predictor-based self-tuning control". In: *Automatica* 20.1 (1984), pp. 39–50. ISSN: 0005-1098. DOI: 10.1016/0005-1098(84)90063-3.

[48] B.E. Ydstie. "Extended Horizon Adaptive Control". In: *IFAC Proceedings Volumes* 17.2 (1984). 9th IFAC World Congress: A Bridge Between Control Science and Technology, Budapest, Hungary, 2-6 July 1984, pp. 911–915. ISSN: 1474-6670. DOI: 10.1016/S1474-6670(17)61089-9.

[49] D.W. Clarke, C. Mohtadi, and P.S. Tuffs. "Generalized predictive control—Part I. The basic algorithm". In: *Automatica* 23.2 (1987), pp. 137–148. ISSN: 0005-1098. DOI: 10.1016/0005-1098(87)90087-2.

[50] D.W. Clarke. "Application of generalized predictive control to industrial processes". In: *IEEE Control Systems Magazine* 8.2 (1988), pp. 49–55. DOI: 10.1109/37.1874.

[51] C. Bordons and E.F. Camacho. "A generalized predictive controller for a wide class of industrial processes". In: *IEEE Transactions on Control Systems Technology* 6.3 (1998), pp. 372–387. DOI: 10.1109/87.668038.

[52] Shiwen Xie et al. "Generalized Predictive Control for Industrial Processes Based on Neuron Adaptive Splitting and Merging RBF Neural Network". In: *IEEE Transactions on Industrial Electronics* 66.2 (2019), pp. 1192–1202. DOI: 10.1109/TIE.2018.2835402.

[53] Jérôme Mendes, Nuno Sousa, and Rui Araújo. "Adaptive Predictive Control With Recurrent Fuzzy Neural Network for Industrial Processes". In: *Proc. 16th IEEE International Conference on Emerging Technologies and Factory Automation (ETFA 2011)*. Toulouse, France: IEEE, Sept. 2011, pp. 1–8. DOI: 10.1109/ETFA.2011.6059066.

[54] L.A. Zadeh. "Fuzzy sets". In: *Information and Control* 8.3 (1965), pp. 338–353. ISSN: 0019-9958. DOI: 10.1016/S0019-9958(65)90241-X.

[55] L.A. Zadeh. "Fuzzy algorithms". In: *Information and Control* 12.2 (1968), pp. 94–102. ISSN: 0019-9958. DOI: 10.1016/S0019-9958(68)90211-8.

[56] R. E. Bellman and L. A. Zadeh. "Decision-Making in a Fuzzy Environment". In: *Management Science* 17.4 (1970), B141–B164. ISSN: 00251909, 15265501.

[57] L.A. Zadeh. "Similarity relations and fuzzy orderings". In: *Information Sciences* 3.2 (Apr. 1971), pp. 177–200. DOI: 10.1016/s0020-0255(71)80005-1.

[58] Lotfi A. Zadeh. "Outline of a New Approach to the Analysis of Complex Systems and Decision Processes". In: *IEEE Transactions on Systems, Man, and Cybernetics* SMC-3.1 (1973), pp. 28–44. DOI: 10.1109/TSMC.1973.5408575.

[59] E.H. Mamdani and S. Assilian. "An experiment in linguistic synthesis with a fuzzy logic controller". In: *International Journal of Man-Machine Studies* 7.1 (1975), pp. 1–13. ISSN: 0020-7373. DOI: 10.1016/S0020-7373(75)80002-2.

[60] M. Sugeno and M. Nishida. "Fuzzy control of model car". In: *Fuzzy Sets and Systems* 16.2 (1985), pp. 103–113. ISSN: 0165-0114. DOI: 10.1016/S0165-0114(85)80011-7.

[61] L.X. Wang. *A course in fuzzy systems and control*. Prentice-Hall, 1997. ISBN: 9780135930052.

[62] Radu-Emil Precup and Hans Hellendoorn. "A survey on industrial applications of fuzzy control". In: *Computers in Industry* 62.3 (2011), pp. 213–226. ISSN: 0166-3615. DOI: 10.1016/j.compind.2010.10.001.

[63] Oscar Castillo and Patricia Melin. "A review on interval type-2 fuzzy logic applications in intelligent control". In: *Information Sciences* 279 (2014), pp. 615–631. ISSN: 0020-0255. DOI: 10.1016/j.ins.2014.04.015.

[64] Abdelwahab Hamam and Nicolas D. Georganas. "A comparison of Mamdani and Sugeno fuzzy inference systems for evaluating the quality of experience of Hapto-Audio-Visual applications". In: *2008 IEEE International Workshop on Haptic Audio visual Environments and Games*. 2008, pp. 87–92. DOI: 10.1109/HAVE.2008.4685304.

[65] Jorge S. S. Júnior et al. "Survey on Deep Fuzzy Systems in Regression Applications: A View on Interpretability". In: *International Journal of Fuzzy Systems* 25.7 (June 2023), pp. 2568–2589. DOI: 10.1007/s40815-023-01544-8.

[66] Tomohiro Takagi and Michio Sugeno. "Fuzzy identification of systems and its applications to modeling and control". In: *IEEE Transactions on Systems, Man, and Cybernetics* SMC-15.1 (1985), pp. 116–132. DOI: 10.1109/TSMC.1985.6313399.

[67] H. Ying. "General MISO Takagi-Sugeno fuzzy systems with simplified linear rule consequent as universal approximators for control and modeling applications". In: *1997 IEEE International Conference on Systems, Man, and Cybernetics. Computational Cybernetics and Simulation*. Vol. 2. 1997, 1335–1340 vol.2. DOI: 10.1109/ICSMC.1997.638158.

[68] Jérôme Mendes and Rui Araújo. "Fuzzy Model Predictive Control for Nonlinear Processes". In: *Proc. 17th IEEE International Conference on Emerging Technologies and Factory Automation (ETFA 2012)*. Kraków, Poland: IEEE, Sept. 2012, pp. 1–8. DOI: 10.1109/ETFA.2012.6489611.

[69] Jérôme Mendes, Rui Araújo, and Francisco Souza. "Adaptive Fuzzy Identification and Predictive Control for Industrial Processes". In: *Expert Systems with Applications* 40.17 (Dec. 2013), pp. 6964–6975. DOI: 10.1016/j.eswa.2013.06.057.

[70] Jérôme Mendes et al. "Iterative Learning of Multiple Univariate Zero-Order T-S Fuzzy Systems". In: *Proc. of The IEEE 45th Annual Conference of the Industrial Electronics Society (IECON 2019)*. Lisbon, Portugal: IEEE, Oct. 2019, pp. 3657–3662. DOI: 10.1109/IECON.2019.8927224.

[71] Rudolf Kulhavý. "Restricted exponential forgetting in real-time identification". In: *Automatica* 23.5 (1987), pp. 589–600. ISSN: 0005-1098. DOI: 10.1016/0005-1098(87)90054-9.

[72] Jérôme Mendes. "Computational Intelligence Methodologies for Control of Industrial Processes". PhD thesis. University of Coimbra, 2014.

[73] Inc The MathWorks. *Fuzzy Clustering*. URL: https://www.mathworks.com/help/fuzzy/fcm.html.

[74] S.B.M. Noor S. Ansarpanahi and M.H. Marhaban. "Stability Study of Model Predictive Control in Presence of Undesirable Factors". In: *Journal of Applied Sciences* 8 (2008), pp. 3683–3689.

[75] S. Thomas Alexander. *Adaptive Signal Processing: Theory and Applications*. 1st ed. Springer New York, NY, 1986.

# Appendix A

# Adaptive Fuzzy Generalized Predictive Control of pH in Tubular Photobioreactors on Microalgae Plant

Mafalda Amaro*, Jérôme Mendes†, Tiago Matias‡, and Rui Araújo*
* University of Coimbra, Institute of Systems and Robotics,
Department of Electrical and Computer Engineering, Pólo II, 3030-290 Coimbra, Portugal
Email: mafalda.amaro@isr.uc.pt, rui@isr.uc.pt
† University of Coimbra, CEMMPRE, ARISE, Department of Mechanical Engineering, Coimbra, Portugal
Email: jerome.mendes@uc.pt
‡ Oncontrol Technologies, Rua Cidade Poitiers, nº 155 – 1º Andar 3000-108 Coimbra, Portugal
Email: tiago.matias@oncontrol-tech.com

***Abstract*—Culture conditions in a photobioreactor on a microalgae plant are essential for production rates, and the pH value is one of the critical variables for a harmonizing process. However, the biological nature of microalgae growth represents a complex reaction that is arduous to model and control. This work proposes an approach of the application of adaptive identification and predictive control to regulate the pH in a photobioreactor in a microalgae production system. The proposed approach is composed of two main stages: identification and control. The identification is performed by a Takagi-Sugeno (T-S) fuzzy model, which will be learned with an offline strategy, by Fuzzy c-means, for the antecedent part, and by the Least Squares Method (LSM), for the consequent part. Then, the model is updated with an online method, the Recursive Least Squares with Adaptive Directional Forgetting (RLS-ADF) factor algorithm. The control scheme is based on a Generalized Predictive Control approach, which is a Model Predictive Controller (MPC), with the adaptive T-S fuzzy model designed in the identification stage. In this way, the model parameters from GPC are online adapted by RLS-ADF. To validate the control structure, the proposed approach was tested by using an estimated model from real data of a microalgae production process.**

***Index Terms*—Predictive fuzzy control, T-S fuzzy model, Generalized predictive control, pH control, Microalgae plant**

## I. Introduction

For a few years now, there has been a new chapter in industrial processes, the Industry 4.0 concept [1]. This movement intends to revolutionize the industrial process, both improving it's flexibility and agility, with the use of automated systems. However, the industrial systems are known to be highly complex and their development may represent a challenge [2].

A microalgae production process is one example of a complex nonlinear biological operation. The chemical reactions during this process are highly complex to describe in a mathematical equation, caused by the culture elements' biological nature, for instance, its heterogeneous light distribution [3]. Microalgae have a high biotechnological potential to produce a diversity of substances present in many valuable industries, such as the pharmaceutical industry, animal nutrition and human supplements, cosmetics production, wastewater treatment processes, and, as a new approach, in clean energy sources, called "third generation biofuels" [4]. However, there are several constraints to control the microalgae production process. The most important factor for an operating photobioreactor is light availability (sun radiation), which is essential for photosynthetic growth. Moreover, the nutrients supply is also one of the main components in a photobioreactor and indispensable for microalgae development, which when under sufficient quantity, are a limiting factor in microalgae growth. A relevant concern in microalgae production is the culture condition, that encompasses the culture's pH and temperature. The culture pH can have an optimal range value of 7.0 to 10.0, which requires an adaptation to the specific microalgae species in production [5]. The control of this variable is frequently done by managing pure carbon dioxide injections in the culture and is one of the most important variables to control since this gas injection can constitute up to 30% of production costs [6]. A photobioreactor operation dynamic is an unstable process through time due to the presented conditions fluctuations, mostly solar input, which makes it difficult to achieve an optimal point of operation, mainly during the day.

In the last couple of years, there has been a new interest in the microalgae industry due to its recent application in thriving industries. This renewed interest triggered investment in the existing high-value photobioreactors structures to transform the microalgae cultivation process more productive, by minimizing costs and maximizing microalgae harvesting. Some control approaches have been developed to control certain photobioreactor variables, with multiple approaches, such as based on Proportional-Integral (PI), Proportional-Integral-Derivative (PID), Model Predictive Control (MPC) and Fuzzy Logic Control (FLC). In [7], it is studied a conventional linear feedback PID [8] and a PID with a feed-forward compensation for pH and dissolved oxygen control in the photobioreactor, by manipulating the carbon dioxide and nitrogen injections. In 2004 [9] and 2014 [10], two distinct MPC approaches were proposed. In the first one, the aim is to control the pH and minimize $CO_2$ losses in a photobioreactor to improve the

This research was co-financed by the European Regional Development Fund, through Centro Regional Operational Program 2014/2020 (Centro2020), of Portugal 2020 by the Project InGestAlgae (CENTRO-01-0247-FEDER-046983). This work has been partially supported by the FCT project UIDB/00048/2020.

production of high-value algal products. In the second one, the control process objective is to maintain a more stable pH level variation to improve microalgae production and to minimize the $CO_2$ losses, where the control strategy is based on a Generalized Predictive Control (GPC) with an event detector, which serves as an enabler for a new control signal. In [11], it is proposed to apply a fuzzy control algorithm to simultaneously control the algal biomass concentration, the culture pH, and the average irradiance inside the photobioreactor (laboratory setup).

This paper proposes an approach to model and control the pH in a photobioreactor on a microalgae plant, based on online identification and predictive control. The identification of a Takagi-Sugeno (T-S) fuzzy model is initially performed in an offline way, where Fuzzy c-means is used to design the antecedent part, and the Least Squares Method to design the consequent part. Then, due to the uncertainty of the process and time-varying behaviour through the seasons, the T-S fuzzy model parameters are updated using Recursive Least Squares with Adaptive Directional Forgetting (RLS-ADF) factor algorithm. This T-S fuzzy model is used as the predictive model on the model predictive controller, the Generalized Predictive Controller (GPC). In this way, the GPC parameters, which depend on the model, are updated online. The proposed approach was validated by using an estimated model from real data of a microalgae production process.

This paper is organized as follows. Section II briefly overviews the microalgae production process. In Section III, the concepts of a T-S fuzzy model are presented. Section IV presents the proposed fuzzy model for pH. In Section V, it is presented the control approach. In Section VI, the results are presented. And in Section VII, the conclusions are presented.

## II. Microalgae Production Process

Microalgae are microscopic eukaryotic organisms or prokaryotic (cyanobacteria) that can be found in seawater and freshwater. Regarding industrial production, there are two major categories of photobioreactors structures [3]: open and closed. The most elementary type of structures is the open photobioreactors due to their operation simplicity, where the culture has direct contact with the environment, such as artificial ponds, raceways, tanks, and thin-layer. These systems are not considered in this work. The closed photobioreactors systems are characterized by the absence of contact between the culture and the environment, frequently represented by tubular loops, flat-panels, or bubble columns. In this system, it's possible to produce mono-cultures and to grow more sensitive strains due to their controlled environment and higher contamination protection.

To obtain high levels of production, it is required to maintain some culture conditions at optimal values. One of the fundamental variables to regulate is the pH value, which measures the culture acid/base levels. The photosynthesis process, in which irradiance is the motor, is responsible for the microalgae growth; however, this process produces a decrease in the carbon dioxide concentration levels, resulting in an increase in pH level. Therefore, the pH variable regulation can be accomplished by controlling carbon dioxide injections ($CO_2$) in the system, that result in a pH levels decrease. As a result, the model is usually simplified as represented in Fig. 1 [9], [10], three inputs (past $pH$ values, carbon dioxide valve aperture percentage $CO_2$, and the last measured irradiance values $Irr$,), and one output (the pH value).

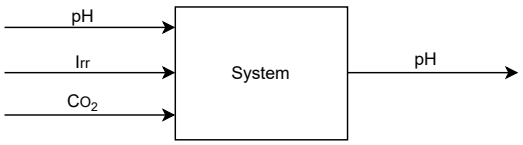


Fig. 1: Black box diagram of the pH model.

## III. Fuzzy Model Concepts

Takagi-Sugeno (T-S) fuzzy systems are characterized by their consequent parameters that are defined by mathematical functions instead of fuzzy sets, being more feasible for the identification of dynamic systems [12]. In general, a T-S fuzzy model can be defined by a set of rules with the following structure [13]:

$$\begin{aligned} R_i : \text{IF } x_1(k) \text{ is } A_1^i, \text{ and } \ldots \text{ and } x_n(k) \text{ is } A_n^i \\ \text{THEN } y_i(k) \;=\; a_i(z^{-1})y(k-1) + \\ b_i(z^{-1})u(k-d-1) + \zeta(k), \end{aligned} \tag{1}$$

where $R_i$ represents the $i$-th rule, $\mathbf{x}(k) = [x_1(k), \ldots, x_n(k)]^\intercal$ and $x_j(k)$ $(j = 1, \ldots, n)$ represents the system inputs of instant $k$, $n$ is the total number of inputs of the fuzzy system, and $N$ is the total number of rules. $y(k)$ represents the system output of instant $k$. The $A_j^i$ is the respective symbol for the linguistic term, with $i = 1, ..., N$ and $j = 1, ..., n$, characterized by the fuzzy membership function, $\mu_{A_j^i}(x_j)$ [14]. The $u(k)$ represent the control output, $d$ is the delay of the system, and $a_i$ and $b_i$ are polynomials defined by:

$$\begin{aligned} a_i(z^{-1}) &= a_{1i} + a_{2i}z^{-1} + \ldots + a_{n_y i}z^{-(n_y-1)}, \\ b_i(z^{-1}) &= b_{1i} + b_{2i}z^{-1} + \ldots + b_{n_u i}z^{-(n_u-1)}. \end{aligned} \tag{2}$$

Considering Gaussian membership functions (MFs), the fuzzy membership function is given by

$$\mu_{A_j^i}(x_j(k)) \;=\; \exp\left[\frac{(x_j(k) - v_{ij})^2}{\sigma_{ij}}\right], \tag{3}$$

where $v_{ij}$ and $\sigma_{ij}$ correspond, respectively, to the center and width of the defined MFs (antecedent parameters to be learned). The system output $y[\mathbf{x}(k)]$ of the T-S fuzzy model is calculated by the following equation [13]:

$$y[\mathbf{x}(k)] = \sum_{i=1}^{N} \bar{\omega}_i[\mathbf{x}(k)]\mathbf{x}^\intercal(k)\boldsymbol{\theta}_i, \tag{4}$$

where:

$$\bar{\omega}_i[\mathbf{x}(k)] = \frac{\prod_{j=1}^{n} \mu_{A_j^i}(x_j(k))}{\sum_{p=1}^{N} \prod_{j=1}^{n} \mu_{A_j^p}(x_j(k))}, \quad (5)$$

$$\boldsymbol{\theta}_i = [a_{1i}, \ldots, a_{n_y}, b_{1i}, \ldots, b_{n_u i}]^\intercal. \quad (6)$$

$\boldsymbol{\theta}_i$ contains the model (consequent) parameters to be learned.

## IV. Fuzzy Model for pH

This section presents the approach to model the pH in tubular photobioreactors by a T-S fuzzy model with the structure of (1). The presented approach is composed of two main steps: 1) the learning of the antecedent part by obtaining the MFs parameters ($v_{ij}$ and $\sigma_{ij}$) (Subsection IV-A), and then, 2) the offline learning of the consequent part $\theta_{ij}$ (Subsection IV-B) and by an online procedure ( Subsection IV-C).

### A. Antecedents Learning: Fuzzy c-means

The fuzzy c-means (FCM) clustering method [15] allows a multidimensional data organization into clusters and, in this case, it is used to obtain the antecedent parameters ($\mathbf{v}_i$ and $\boldsymbol{\sigma}_i$ (3)) of the T-S fuzzy model (1). The learning process initializes with the data-set division into $N$ clusters and the definition of its centers. The following step encompasses the calculus of each data-set point level of membership to the different clusters. To evaluate the correspondent belonging degree of each point to the clusters, it is performed a calculus dependent on its distance to every cluster center. For example, a data set point close to a cluster center will have a high membership value to that cluster, however, if the point is located far from the cluster center, the point will have a low level of membership related to that cluster.

Considering the data-set values

$$\boldsymbol{X} = \begin{bmatrix} x_1(1) & x_2(1) & \ldots & x_n(1) \\ x_1(2) & x_2(2) & \ldots & x_n(2) \\ \vdots & \vdots & \vdots & \vdots \\ x_1(K) & x_2(K) & \ldots & x_n(K) \end{bmatrix}, \quad (7)$$

where $N$ is the predefined number of clusters (corresponding to the number of fuzzy rules), $n$ is the number of inputs, and $K$ is the total number of samples, the fuzzy partition of the set $\boldsymbol{X}$ into $N$ clusters, is a family of fuzzy subsets defined as $\mu_i(k) = \mu_{A_j^i}(x_j(k)) \in [0,1]$ [15]. The membership values originate a partition matrix $\mathbf{U} = [\mu_i(k)] \in \mathbb{R}^{N \times K}$, where the $i$-th row of this matrix corresponds to the $i$-th sample membership values. The sum of all membership values of a sample is one, $\sum_{i=1}^{K} \mu_i(k) = 1$.

The FCM objective function depends on the clusters centers, the distance between a given sample and a cluster center, and a fuzziness parameter $\eta$, that controls the membership degree computation [15]. With a higher $\eta$ the clusters are more fuzzier and each point belongs to more clusters, with similar belonging values. The FCM objective function, that is to be minimized, is given by:

$$\mathbf{J}(\mathbf{X}, \mathbf{U}, \mathbf{V}) = \sum_{i=1}^{N} \sum_{k=1}^{K} \mu_i(k)^\eta d_i(k)^2, \quad (8)$$

where $\mathbf{v}_i = [v_{i1}, ..., v_{in}]^\intercal$ is the vector containing the center of the $i$-th cluster and $\mathbf{V} = [\mathbf{v}_1, \ldots, \mathbf{v}_N]^\intercal \in \mathbb{R}^{N \times n}$ is a matrix composed of all the clusters centers. Furthermore, $d_i(k)$ represents the norm of the difference between $\mathbf{x}(k)$ and a cluster centroids vector $\mathbf{v}_i$, given by the Euclidean distance:

$$d_i(k)^2 = (\mathbf{x}(k) - \mathbf{v}_i)^\intercal (\mathbf{x}(k) - \mathbf{v}_i), \quad (9)$$

where

$$\mathbf{v}_i = \frac{\sum_{k=1}^{K} \mu_i(k)^\eta \mathbf{x}(k)}{\sum_{k=1}^{K} \mu_i^\eta(k)}. \quad (10)$$

Then, $\sigma_{ij}$, the width of Gaussian MFs, is obtained using the $\mathbf{U}$ matrix values [15]:

$$\sigma_{ij} = \sqrt{\frac{2 \sum_{k=1}^{K} \mu_i(k)(x_j(k) - v_{ij})^2}{\sum_{k=1}^{K} \mu_i(k)}}. \quad (11)$$

### B. Offline Consequent Learning: Least-Squares Method

The least squares method has been widely used to determine the rule consequent parameters ($\theta_{ij}$) [15]. Considering $\mathbf{y}_d$ a vector containing the target output values:

$$\mathbf{y}_d = [y_d(\mathbf{x}(1)), \ldots, y_d(\mathbf{x}(K))]^\intercal, \quad (12)$$

$\boldsymbol{\Theta}$ that contains the consequent parameters of all rules

$$\boldsymbol{\Theta} = [\boldsymbol{\theta}_1^\intercal, \ldots, \boldsymbol{\theta}_N^\intercal]^\intercal, \quad (13)$$

and according to (1), the T-S fuzzy model can be given by

$$\mathbf{y}_d = \boldsymbol{\Psi}\boldsymbol{\Theta}, \quad (14)$$

where

$$\boldsymbol{\Psi} = [\boldsymbol{\psi}(\mathbf{x}(1)), \ldots, \boldsymbol{\psi}(\mathbf{x}(K))]^\intercal, \quad (15)$$

$$\boldsymbol{\psi}[\mathbf{x}(k)] = [\bar{\omega}_1 \mathbf{x}^\intercal(k), \ldots, \bar{\omega}_N \mathbf{x}^\intercal(k)]^\intercal. \quad (16)$$

Using the pseudo-inverse in (14), the optimal values of the consequent parameters, $\boldsymbol{\Theta}^*$, are obtained throughout:

$$\boldsymbol{\Theta}^* = (\boldsymbol{\Psi}^\intercal \boldsymbol{\Psi})^{-1} \boldsymbol{\Psi}^\intercal \mathbf{y}_d. \quad (17)$$

### C. Online Consequent Learning: RLS-ADF

At this point of the process, using the Least Square method, it was calculated an optimal set of the consequent parameters values. Although computed with a large sample of data, the limited data set may not provide adequate accuracy, considering a nonlinear system and its time-varying characteristics. As such, an adaptive algorithm generally represents a favourable alternative to solve this limitation. In this way, the Recursive

Least Squares with Adaptive Directional Forgetting (RLS-ADF) is a combination of Recursive Least Squares (RLS) algorithm, centered in a constant forgetting factor, and an Adaptive Directional Forgetting (ADF) factor algorithm. This approach is presented in [16] and used in [15] to recursively update the consequent parameter values of a T-S fuzzy model.

Using the RLS-ADF, the consequent parameters are updated at each sample time $k$ by

$$\boldsymbol{\theta}_i(k) = \boldsymbol{\theta}_i(k-1) + \frac{\mathbf{C}_i(k-1)\boldsymbol{\psi}_i^{\intercal}}{1+\xi_i}[y_i(k) - \boldsymbol{\psi}_i\boldsymbol{\theta}_i(k-1)], \quad (18)$$

where $\boldsymbol{\psi}_i = \bar{\omega}_i[\mathbf{x}(k)]\mathbf{x}^{\intercal}(k)$, $\xi_i = \boldsymbol{\psi}_i\mathbf{C}_i(k-1)\boldsymbol{\psi}_i^{\intercal}$, $y_i(k) = \bar{\omega}_i[\mathbf{x}(k)]y(k)$, and $\mathbf{C}_i(k)$ is the $i$-th rule covariance matrix given by

$$\mathbf{C}_i(k) = \mathbf{C}_i(k-1) - \frac{\mathbf{C}_i(k-1)\boldsymbol{\psi}_i^{\intercal}\mathbf{C}_i(k-1)}{\varepsilon_i^{-1} + \xi_i}, \quad (19)$$

where

$$\varepsilon_i = \varphi_i(k-1) - \frac{1-\varphi_i(k-1)}{\xi_i}, \quad (20)$$

being $\varphi_i(k-1)$ the last iteration forgetting factor, for the $i$-th rule. The forgetting factor is given iteratively by:

$$\varphi_i(k) = \frac{1}{1+(1+\rho)\left(\ln(1+\xi_i) + \left[\frac{(\nu_i(k)+1)\gamma_i}{1+\xi_i+\gamma_i} - 1\right]\frac{\xi_i}{1+\xi_i}\right)}, \quad (21)$$

where $\nu_i(k) = \varphi_i(k-1)(\nu_i(k-1)+1)$,

$$\gamma_i = \frac{(y_i(k) - \boldsymbol{\psi}_i\boldsymbol{\theta}_i(k-1))^2}{\tau_i(k)}, \quad (22)$$

$$\tau_i(k) = \varphi_i(k-1)\left[\tau_i(k-1) + \frac{(y_i(k) - \boldsymbol{\psi}_i\boldsymbol{\theta}_i(k-1))^2}{1+\xi_i}\right], \quad (23)$$

and $\rho$ is a positive constant. The initialization of these parameters, $\varphi_i(0)$, $\tau_i(0)$ and $\nu_i(0)$, should be between zero and one. The covariance matrix must be initialized to an identity matrix multiplied by a large number, for example, $10^5$.

## V. Adaptive fuzzy generalized predictive control

This section presents the control algorithm to control the pH. The controller is based on the well-known classic generalized predictive control (GPC), where the model is an adaptive T-S fuzzy model (Section IV-C). Selected for their easy adaptation of the control parameters, by updating the model. The controller, the Adaptive Fuzzy Generalized Predictive Control (AFGPC) is represented in the diagram of Fig. 2. In Fig. 2, it is possible to identify three different components: the plant to be controlled; the GPC controller, which is a type of Model Predictive Control (MPC), that naturally uses a predictive model; and the predictive model represents an adaptive T-S fuzzy model, that allows an iterative adaptation of the GPC parameters.

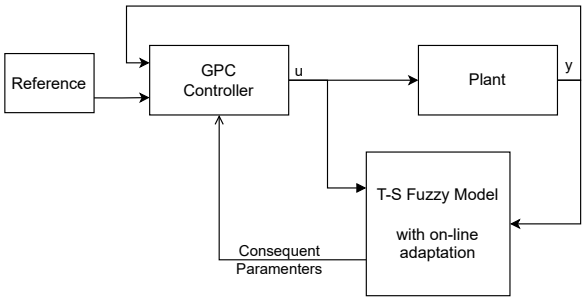


Fig. 2: Diagram of the AFGPC controller.

### A. Predictive Control Law

The GPC controller uses the following cost function

$$J(k) = \sum_{p=d+1}^{N_p}[\hat{y}(k+p|k) - r(k+p)]^2 + \sum_{p=d+1}^{d+N_u}[\lambda(z^{-1})\Delta u(k+p-d-1|k)]^2, \quad (24)$$

that is to be minimized, using the output values over the prediction horizon $N_p$, and the control values over the control horizon $N_u$ [14], where $r(k+p)$ is the next $p$ reference value, $\hat{y}(k+p|k)$ is the $p$-ahead prediction value of the system, and $\lambda$ is a control action weighting factor.

Furthermore, considering a series of Diophantine equations presented in [14], [17], the best prediction of $y(k+p|k)$ can be obtained by:

$$\mathbf{y}(k) = \mathbf{G}\mathbf{u}(k) + \mathbf{F}(z^{-1})y(k) + \mathbf{L}(z^{-1}), \quad (25)$$

where

$$\mathbf{y}(k) = \begin{bmatrix} \hat{y}(k+d+1) \\ \hat{y}(k+d+2) \\ \vdots \\ \hat{y}(k+d+N_p) \end{bmatrix}. \quad (26)$$

$\mathbf{G}$, $\mathbf{F}$ and $\mathbf{L}$ are defined in [14], and the control signal variation $\Delta u(k)$ at every iteration is given by [14]:

$$\Delta u(k) = \mathbf{K}[\mathbf{R} - \mathbf{F}y(k) - \mathbf{L}], \quad (27)$$

where $\mathbf{K}$ is the first row of $(\mathbf{G}^{\intercal}\mathbf{G} + \lambda I)^{-1}\mathbf{G}^{\intercal}$, $\mathbf{R}$ is a vector with the future reference values, and $\lambda(z^{-1})$ is considered to be a constant ($\lambda > 0$) [14].

### B. Algorithm

Algorithm 1 presents the proposed approach to control the pH in photobioreactors on microalgae plants. The first part is to organize a data set with a defined structure to the system, considering the adequate inputs. The second part is the offline model learning, where the antecedent parameters, $v_{ij}$ and $\sigma_{ij}$, are calculated based on FCM algorithm, and the consequent parameters, $\theta_{ij}$, through LSM algorithm. At this point, with all

**Algorithm 1** Control approach for pH control.

1: **Input**:
2: Data set $D = \{CO_2, I_{rr}, pH\}$.
3: Identification parameters: the time delay $d$, the number of clusters $N$, and the parameters for RLS-ADF: $\rho$, $\varphi_i$, $\tau_i$, $\nu_i$, $\mathbf{C}_i$, $n_y$ and $n_u$.
4: Controller parameters: prediction horizons $N_p$ and $N_u$, and the control action weighting factor $\lambda$.
5: **Offline:** Design the T-S fuzzy model (1) using data set $D$.
6: Obtain the antecedent part using FCM (Subsection IV-A): the parameters $v_{ij}$ (10) and $\sigma_{ij}$ (11).
7: Obtain the consequent part using LSM (Subsection IV-B): the parameters $\theta_{ij}$ (17).
8: **Online:**
9: **while** Controller turned on **do**
10: Read the input variables $CO_2$, $I_{rr}$ and $pH$.
11: Update the T-S fuzzy model, using RLS-ADF (18).
12: Obtain the new values of model polynomials $a(z^{-1})$ and $b(z^{-1})$.
13: Apply the control signal from GPC using (27).
14: **end while**

the identification and control parameters defined, the third part is the online algorithm part, where the consequent parameters adaptation is performed with the RLS-ADF algorithm, and the control signal is applied.

## VI. Results

This section describes the real data set used to estimate the pH on a photobioreactor and to create a model to test the control approach. Afterwards, the results are presented.

### A. Data set

The data set used was formed through the collected data of an operational photobioreactor. The selected variables, according to the plant description in Section II, were carbon dioxide ($x_1$), irradiance ($x_2$), and culture pH ($y$). The data set comprises roughly five months, some spring and fall months, and all summer periods, with a five minutes sample period. Furthermore, the data set was divided so the estimation data used for the simulation model to test the controller (Subsection VI-B) is distinct from the one used to learn the T-S fuzzy model (Subsection VI-C).

### B. Simulation Model to Test the Controller

For control simulation purposes, it was used a discrete-time estimated model of ARX type (28),

$$A(z)y(t) = B_1(z)u_1(t) + B_2(z)u_2(t) + e(t), \qquad (28)$$

Using the part of the collected data, the model (28) was learned by the "arx" MATLAB function. Note that the selected data to learn the model was not used to test the proposed control approach, as explained before. The resulted model (28) was $A(z) = 1 - 0.3707z^{-1} - 0.2609z^{-2} - 0.2008z^{-3} - 0.1684z^{-4}$, $B_1(z) = 0.00126 - 0.000909z^{-1} - 0.004927z^{-2}$ and $B_2(z) = 0.0001459$. The Mean Square Error (MSE) of the learned model is 0.0259 for the training data. In Fig. 3 the estimated model output is compared with the real output data.

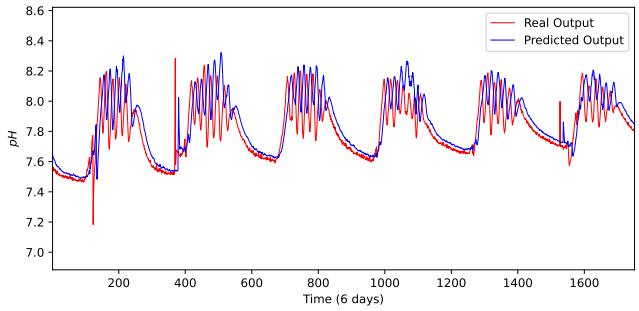


Fig. 3: Results of the simulation model to test the controller: estimated and real outputs.

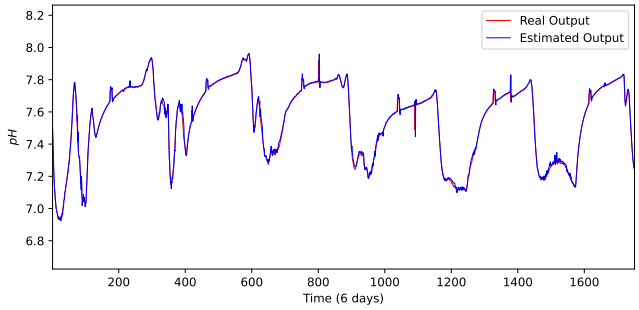


Fig. 4: Results of the offline fuzzy model training: estimated and real outputs.

### C. Results Analysis

The offline training and testing results of the fuzzy model (Algorithm 1, Step 5) are presented in Figs. 4, 5 and 6. The first one, refers to the training part, and the second and third to different segments of the testing parts, using four clusters.

Furthermore, this section also presents the control simulation results of the Generalized Predictive Control (GPC) using fixed parameters (offline model) and parameters adaptation (online model). The reference value of pH was defined equal to 8. The controller parameters were: the control weighting factor adjusted to $\lambda = 0.8$, the control horizon to $N_u = 1$, the prediction horizon to $N_p = 10$ min, and a $d = 3$. The identification parameters were: $\rho = 43$, $\varphi_i = 0.1$, $\tau_i = 0.01$, $\nu_i = 0.1$, $n_y = 4$, $n_u = [3, 1]$, and $\mathbf{C}_i = I_8 \times 10^5$. Fig. 7 presents a graphic with both approaches in order to compare them. The efficiency of the adaptive parameters control (blue line) is visible, compared to the system with fixed parameters (red line) that presents higher oscillations from the set reference value. Thus, with adaptive parameters, it is possible to maintain a more steady pH value.

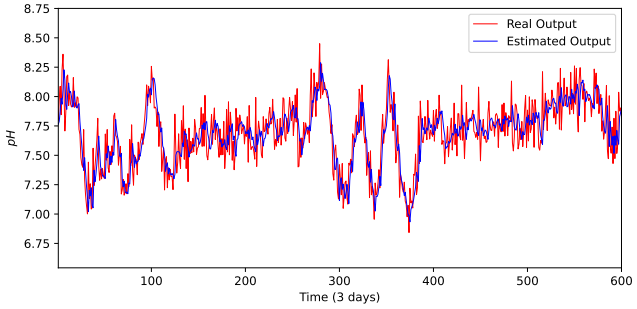


Fig. 5: Tests results of the offline fuzzy model.

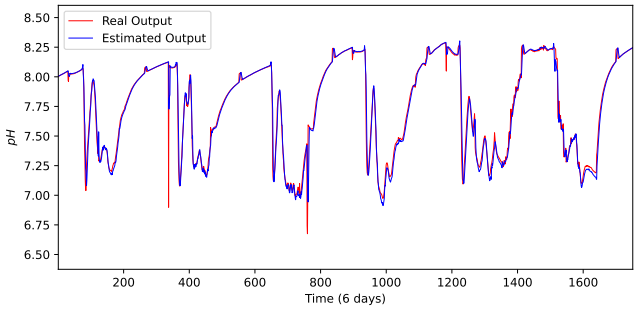


Fig. 6: Tests results of the offline fuzzy model.

## VII. Conclusions

This work has shown the improvements obtained when implementing an adaptive predictive control approach to control a photobioreactor pH when compared to a similar scheme with fixed parameters. Considering dynamic environmental conditions, the proposed design adapts the controller by updating the consequent parameters of the fuzzy model. In this particular application, an adaptive control approach allows an iterative rearrangement to new conditions due to a large spectrum of environmental conditions, possibly out of the scope of the collected data set.

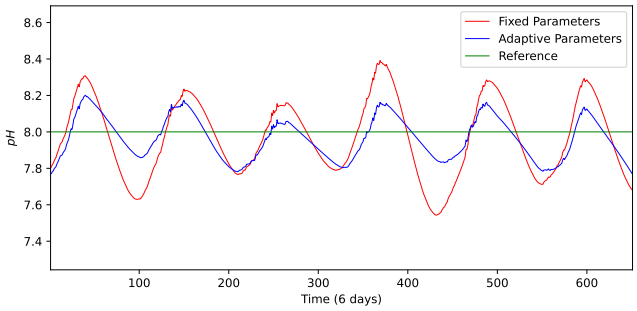


Fig. 7: pH simulation with adaptive parameters and fixed parameters control, during 6 days.

## References


[1] M. O. Okwu, L. K. Tartibu, C. Maware, D. R. Enarevba, J. O. Afenogho, and A. Essien, "Emerging technologies of industry 4.0: Challenges and opportunities," in *2022 International Conference on Artificial Intelligence, Big Data, Computing and Data Communication Systems (icABCD)*, 2022, pp. 1–13.

[2] S. El Hamdi, A. Abouabdellah, and M. Oudani, "Industry 4.0: Fundamentals and main challenges," in *2019 International Colloquium on Logistics and Supply Chain Management (LOGISTIQUA)*, 2019, pp. 1–5.

[3] I. Fernández, J. L. Guzmán, M. Berenguel, and F. G. Acién, *Dynamic Modeling of Microalgal Production in Photobioreactors*. Singapore: Springer Singapore, 2017, pp. 49–87.

[4] I. Fernández, F. G. Acién, M. Berenguel, and J. L. Guzmán, "First principles model of a tubular photobioreactor for microalgal production," *Industrial & Engineering Chemistry Research*, vol. 53, no. 27, pp. 11 121–11 136, 2014.

[5] F. Acién, E. Molina, A. Reis, G. Torzillo, G. Zittelli, C. Sepúlveda, and J. Masojídek, "1 - photobioreactors for the production of microalgae," in *Microalgae-Based Biofuels and Bioproducts*, ser. Woodhead Publishing Series in Energy, C. Gonzalez-Fernandez and R. Muñoz, Eds. Woodhead Publishing, 2017, pp. 1–44.

[6] F. Acién, J. Fernández, J. Magán, and E. Molina, "Production cost of a real microalgae production plant and strategies to reduce it," *Biotechnology Advances*, vol. 30, no. 6, pp. 1344–1353, 2012, special issue on ACB 2011.

[7] M. Titica, A. Kazbar, H. Marec, J. Pruvost, G. Ifrim, M. Barbu, and S. Caraman, "Simultaneous control of ph and dissolved oxygen in closed photobioreactor," in *2018 22nd International Conference on System Theory, Control and Computing (ICSTCC)*, 2018, pp. 372–378.

[8] L. Osório, J. Mendes, R. Araújo, and T. Matias, "A comparison of adaptive pid methodologies controlling a dc motor with a varying load," in *Proc. 18th IEEE International Conference on Emerging Technologies and Factory Automation (ETFA 2013)*, Cagliari, Italy, September 10-13 2013, pp. 1–8.

[9] M. Berenguel, F. Rodrıíguez, F. Acién, and J. García, "Model predictive control of ph in tubular photobioreactors," *Journal of Process Control*, vol. 14, no. 4, pp. 377–387, 2004.

[10] A. Pawlowski, I. Fernández, J. Guzmán, M. Berenguel, F. Acién, and J. Normey-Rico, "Event-based predictive control of ph in tubular photobioreactors," *Computers & Chemical Engineering*, vol. 65, pp. 28–39, 2014.

[11] L. Luca, M. Barbu, G. Ifrim, E. Ceanga, M. Miron, and S. Caraman, "Fuzzy control of a microalgae growmh process in photobioreactors," in *2018 22nd International Conference on System Theory, Control and Computing (ICSTCC)*, 2018, pp. 480–485.

[12] J. S. S. Júnior, J. Mendes, F. Souza, and C. Premebida, "Survey on deep fuzzy systems in regression applications: A view on interpretability," *International Journal of Fuzzy Systems*, vol. 25, no. 7, p. 2568–2589, June 2023.

[13] J. Mendes and R. Araújo, "Fuzzy model predictive control for nonlinear processes," in *Proc. 17th IEEE International Conference on Emerging Technologies and Factory Automation (ETFA 2012)*, Kraków, Poland, September 17-21 2012, pp. 1–8.

[14] J. Mendes, N. Sousa, and R. Araújo, "Adaptive predictive control with recurrent fuzzy neural network for industrial processes," in *Proc. 16th IEEE International Conference on Emerging Technologies and Factory Automation (ETFA 2011)*, Toulouse, France, September 5-9 2011, pp. 1–8.

[15] J. Mendes, R. Araújo, and F. Souza, "Adaptive fuzzy identification and predictive control for industrial processes," *Expert Systems with Applications*, vol. 40, no. 17, pp. 6964–6975, December 2013.

[16] R. Kulhavý, "Restricted exponential forgetting in real-time identification," *Automatica*, vol. 23, no. 5, pp. 589–600, 1987.

[17] E. Camacho and C. Bordons, *Model Predictive Control*, ser. Advanced Textbooks in Control and Signal Processing. Springer London, 2004.

# Appendix B

In this appendix, graphs illustrating the variation of carbon dioxide valve aperture percentage across different lambda values are presented. For the following tests, the prediction horizon is set to 10 or 15, while the lambda value is varied between 0.8, 1.8, and 8.

In Figures B.1 and B.2, where $N_p$ is fixed at 10, three curves representing the variations associated with the lambda variable are presented. Similarly, in Figures B.3 and B.4, where $N_p$ is fixed at 15, three curves are presented, each representing one lambda variations. From these four graphs, a trend in the CO2 valve aperture percentage is observed, with higher values associated with smaller lambda values. This effect is attributed to lambda's influence on the control behavior.

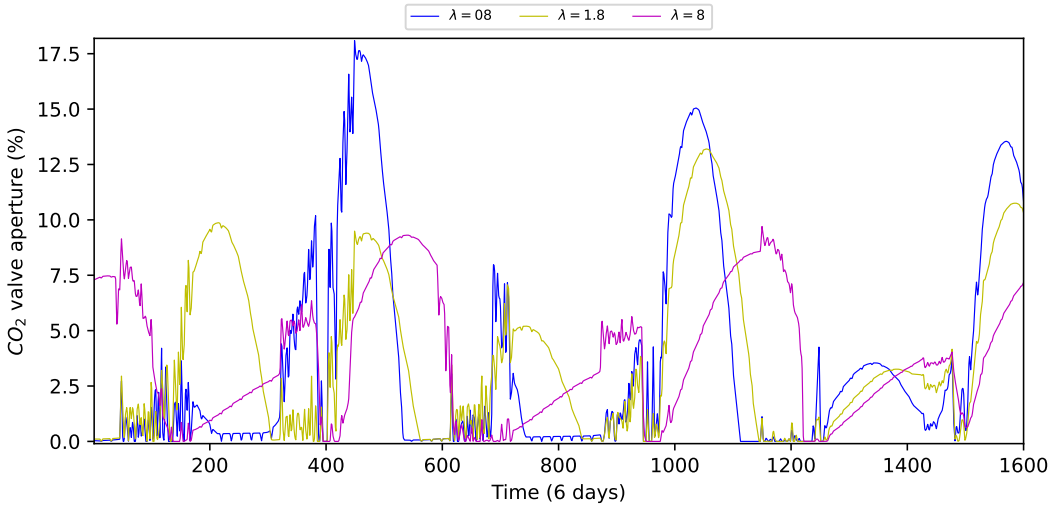


Figure B.1: Adaptive parameters $CO_2$ valve aperture percentage results, with moderate irradiance values, for $\lambda = 0.8$, $\lambda = 1.8$ and $\lambda = 8$. With a predictive horizon set to 10.

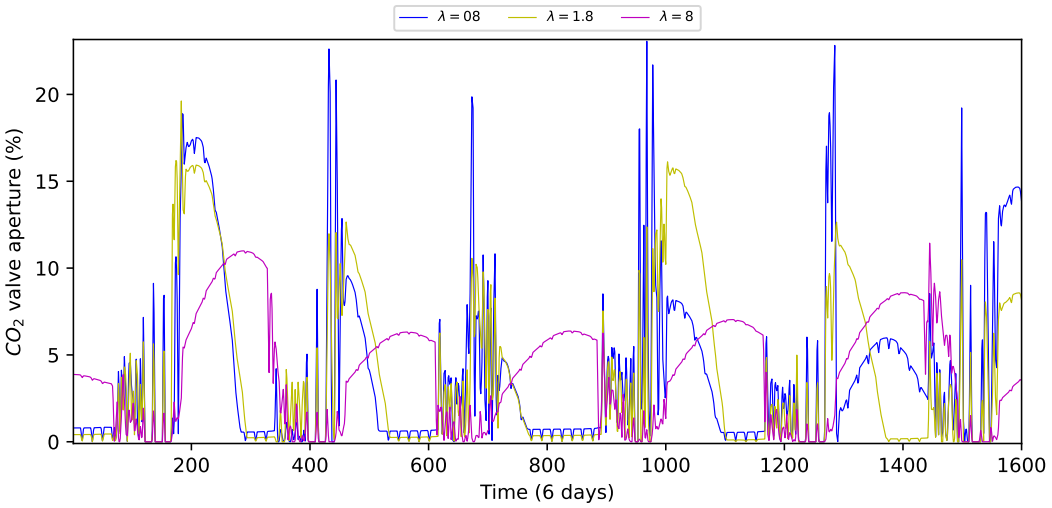


Figure B.2: Adaptive parameters $CO_2$ valve aperture percentage results, with high irradiance values, for $\lambda = 0.8$, $\lambda = 1.8$ and $\lambda = 8$. With a predictive horizon set to 10.

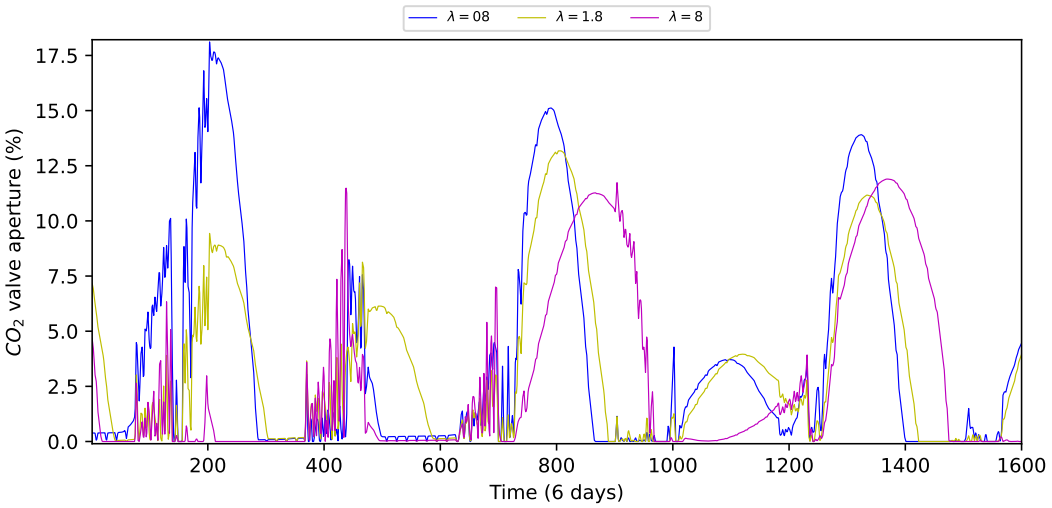


Figure B.3: Adaptive parameters $CO_2$ valve aperture percentage results, with moderate irradiance values, for $\lambda = 0.8$, $\lambda = 1.8$ and $\lambda = 8$. With a predictive horizon set to 15.

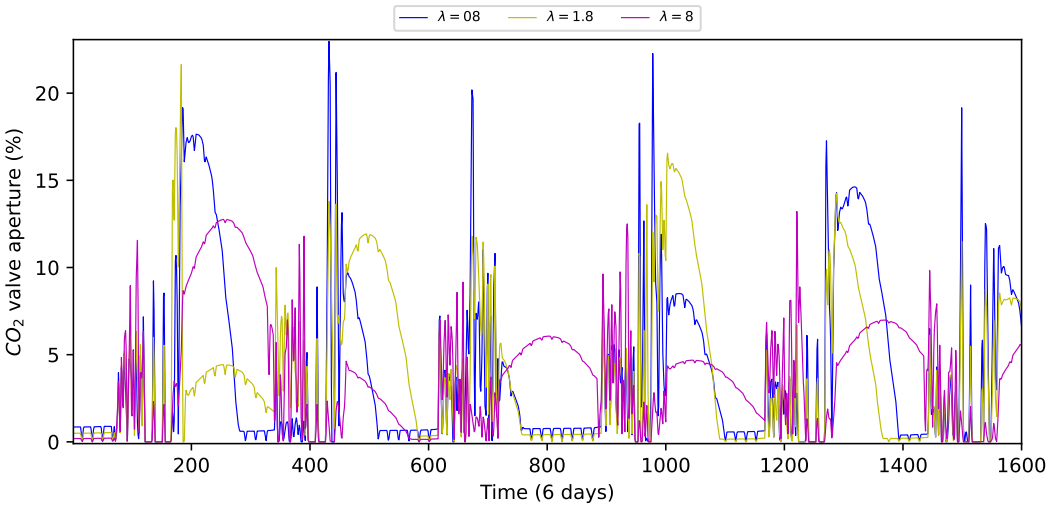


Figure B.4: Adaptive parameters $CO_2$ valve aperture percentage results, with high irradiance values, for $\lambda = 0.8$, $\lambda = 1.8$ and $\lambda = 8$. With a predictive horizon set to 15.